STUDIES ON INORGANIC COATINGS ON METALS AND ALLOYS

SUMMARY

THESIS SUBMITTED FOR THE DEGREE OF

DOCTOR OF PHILOSOPHY

IN

CHEMISTRY

SHARIF AHMAD

M. Sc., M. Phil. (Alig.)

2400

DEPARTMENT OF CHEMISTRY

ALIGARH MUSLIM UNIVERSITY

ALIGARH.

Oct. 1981

SUMMARY

The use of coatings for protection against corrosion has been an area of active investigations ever since the materials were first used for engineering and technological purposes. Painting, galvanising, metal plating, aluminising, chromising etc. were employed for corrosion protection as well as decoration purposes for quite some time. The polymer coatings e.g., polyvinyl, epoxy, silicones, are some of the recent additions to a long list of coatings which are currently used in industry. These coatings act as suitable barrier against corrosion at ambient to moderately high temperatures. In recent years interest has been developed to produce coatings for metals and alloys, providing satisfactory protection against high temperature oxidation and corrosion under severe environments. This is largely due to the development of new high temperature corrosion resistance materials for applications in Aerospace and Marine Industries and high efficiency power generating units, working on low grade fossil fuels and coal gasification plants. Aluminide, boride, silicide, carbide, nitride and refractory oxide are some of the base materials which proved promising as corrosion resistant coatings on heat resistant or high temperature alloys.

The main objective of the investigations which are described in this thesis is to study the high temperature performance of some inorganic coatings and to explore the possibility of application of some of the coatings on high temperature materials to improve corrosion resistance. AISI 303 steel, which is 18 Cr:8.5 Ni austenitic steel and mild steel (0.3% C) have been chosen as materials for these investigations.

The work described in this thesis deals with the corrosion behaviour of AISI 303 steel and mild steel in presence of inorganic coatings. The alloys have been coated with phosphate, silicate, borate, oxide, chromate and carbide coatings. The corrosion behaviour has been studied at ambient temperature in aqueous medium using electrochemical techniques. The high temperature oxidation behaviour has been studied in air and in presence of ionic salts (e.g. Na_2SO_4, NaCl, Na_2CO_3 and their mixtures in the temperature range 400 - 1000°C. Oxidation kinetics, metallography, scanning electronmicroscopy and X-ray diffraction are the main tools on which high temperature corrosion studies are based.

Chapter I presents a critical survey of the coating materials with especial emphasis on the coating materials and coating techniques introduced during the last 20 years or so. Some of the recent techniques include pack cementation, ion

implantation, gas phase chemical vapour deposition, electro-plating plus pack cementation and electrophoresis.

Chapter II deals with the preparation, properties and mechanism of formation of coatings which have actually been used in the work and described in the following chapters. The coatings include phosphate, chromate, carbide, oxide, borate and silicate. The first 4 coatings have been applied on polished alloy specimen surfaces using a coating slurry, where as the other two viz., borate and silicate are formed on alloy surfaces by diffusion technique. The composition of the coating materials or the constituents present in the coatings have been determined on the basis of X-ray diffraction analysis and analysis of the scanning electron micrographs of the coated surfaces. The following are the main constituents identified in the coating materials.

Phosphate [a]	Silicate[a]	Chromate[a]	Borate[a]	Oxide[a]
$FePO_4$	F_2SiO_4	$NiCr_2O_4$	Fe_3BO_6	ZrO_2
	Al_2SiO_5	$ZnCr_2O_4$	Fe_2B,NiB	

Borate[b]	Chromate[b]	Carbide[b]
Fe_3BO_6	$FeCr_2O_4$	SiC
ZnB_2O_4		

a = coatings on AISI 303 steel; b = coatings on mild steel

Chapter III describes electrochemical studies on the corrosion behaviour of coated 303 steel in presence of mineral acids (e.g., HCl, H_2SO_4 and HNO_3). The corrosion potential/time plots indicate that in H_2SO_4 medium oxide, phosphate and chromate coatings are stable where as other coatings show the tendency of dissolution in HNO_3. Corrosion potential for coated alloy specimens initially shifted in the cathodic direction which is followed by no or little variation in potential for the rest of the period. In HCl, phosphate and borate coated alloy specimens show better corrosion performance than the uncoated alloy steel. The scanning electronmicrographs of the coating surfaces (after treatment with acids) show features typical of passivated coating metal/reacted metal/detached coating/undetached coating. For example, phosphate (H_2SO_4 and HCl) and oxide (H_2SO_4 and HNO_3) show nearly uniform coatings with close resemblence to untreated coatings. Where as in HCl the SEM pictures indicate some features typical of acidic corrosion.

Chapter IV contains oxidation studies of phosphate, silicate, borate, oxide and chromate coated 303 steel alloy in air at temperatures ranging from 400 to 1000°C. In the temperatures range 400 to 800°C, the kinetic curves (wt.gain/time) show parabolic behaviour. Above 800°C, however, most of the coatings show deviation from the parabolic rate law. Chromate, phosphate

and oxide coatings show better corrosion resistance than uncoated alloy in the temperature range 400 - 600°C. At 800°C, only chromate coating has better corrosion resistance than the uncoated steel. At 1000°C, phosphate coated alloy has superior corrosion resistance than the uncoated alloy. It has been concluded that phosphate and chromate coatings are the promising materials for high temperature corrosion resistance purposes in environments containing air or oxygen.

In Chapter V, the high temperature oxidation behaviour of phosphate, borate, silicate, oxide and chromate coated 303 steel, has been discussed in presence of ionic salts. The hot corrosion studies have been carried out at four different temperatures viz., 700, 800, 850 and 1000°C, in air.

In general, the corrosion rates of the coated alloys in presence of NaCl are much higher (at least one order of magnitude) than in presence of Na_2SO_4 or Na_2CO_3. Moreover, the addition of NaCl to Na_2SO_4 or Na_2CO_3 increases the corrosion rates appreciably in nearly all the cases. This indicates the pivotal role of NaCl in enhancing the corrosion attack in all the coated alloys as well as in the uncoated alloy. The phosphate coated alloy has lower corrosion rates than the uncoated alloy in presence of Na_2SO_4 and 1:1 mixture of Na_2SO_4 and NaCl. Like uncoated steel none of the five coatings is

capable of withstanding severe attack of corrosion in presence of ionic salts.

The morphological studies of the corroded alloys indicate similarities in the scale structures. Multilayered scales are usually formed. In presence of Na_2SO_4, a sulfide spinel ($FeS.Cr_2S_3$) is invariably present as the inner most layer followed by a sulfur rich layer predominantly containing FeS., the penultimate layer contains oxide(s) and the coating materials form the outer most layer. $FePO_4$, Al_2SiO_3, $CrBO_3$, Fe_2SiO_4 and ZrO_2 present initially in phosphate, silicate, borate, chromate and oxide coatings, respectively, remain unattacked during hot corrosion and appear in the form of outer layer in the scale. During hot corrosion, Na_2SO_4 penetrated through coating pores and attack the alloy at coating/metal interface, a sulfur induced degradation mode is operative . This is perhaps produced by a fluxing mode involving reprecipitation of oxide near the coating interface. The coated alloys corroded in presence of NaCl show penetration of the salt through grain boundaries and in some cases is accompanied by fragmentation of the alloy surface. The oxide scales are discontinuous and porous and chloride phase is presumably accumulated at the alloy interface. The Na_2SO_4 - NaCl corroded alloys show extensive sulfidation, though the nature of the sulfide scalesis similar to that observed in case of Na_2SO_4 alone but they are thicker and more porous. The alloy

matrix of the corroded alloy shows evidence of internal sulfidation in some cases (uncoated, silicate and chromate whereas in other cases the alloy is fragmented extensively.

Chapter VI presents the results of high temperature oxidation and hot corrosion studies carried out on chromate borate and carbide coated mild steel.

The high temperature oxidation studies have been carried out in air in the temperature range 400 - 800°C. The coated mild steel alloys usually, follow a parabolic rate law in the temperature range 400 - 800 C, however, the mild steel shows a linear rate law at 800°C. In general, all the three coatings offer better oxidation resistance than the mild steel. The oxidation resistance of different coatings follows the sequence : Borate > Carbide > Chromate > mild steel.

The hot corrosion studies carried out on borate, carbide and chromate coated mild steel under thin films of Na_2SO_4 of varying concentrations (0.4 to 8.0 mg/cm^2) at 5 different temperatures. Concentration of Na_2SO_4/wt gain and concentration of Na_2SO_4/temperature plots indicate that at a particular temperature there is a critical concentration of Na_2SO_4 at which corrosion rate is maximum. This critical amount of Na_2SO_4 decreases with increasing temperature. For example, the chromate, borate and mild steel require 3.8-4.4

and 0.4 to 0.5 mg/cm^2 of Na_2SO_4 at 800 and 850°C, respectively for achieving maximum corrosion rate.

The scale morphology of the coated alloys is similar to that of mild steel. Invariably all the coatings show a thick sulfide layer of FeS adjacent to the alloy followed by a oxide or a duplex oxide scale which is porous, and the outer scale usually comprising of coating material. The Na_2SO_4 penetrates through the coating pores and attacks the alloy at the coating/alloy interface. The corrosion proceeds by sulfidation in which carbon (from the solid solution phase in the alloy) and cementite (Fe_3C) react with sodium sulfate to give S and Na_2S respectively. The removal of cementite from the alloy is indicated by the absence or depletion of the pearlite phase in the matrix of the corroded alloy.

STUDIES ON INORGANIC COATINGS ON METALS AND ALLOYS

THESIS SUBMITTED FOR THE DEGREE OF

DOCTOR OF PHILOSOPHY

IN

CHEMISTRY

SHARIF AHMAD

M. Sc., M. Phil. (Alig.)

DEPARTMENT OF CHEMISTRY

ALIGARH MUSLIM UNIVERSITY

ALIGARH.

Oct. 1981

A. U. Malik
M.Sc., Ph.D. (Alig.), Ph.D. (Liverpool)
D.Sc. (Alig.)
Reader in Materials Science

CHEMISTRY SECTION
Zakir Husain College of
Engg. & Technology
Aligarh Muslim University
ALIGARH-202001 INDIA

Dated..October..23, 1981

CERTIFICATE

This is to certify that the work presented in this thesis entitled, 'Studies on Inorganic Coatings on Metals and Alloys', submitted by Mr. Sharif Ahmad, is the original piece of research carried out by him under my supervision, and has not been submitted earlier for the award of any other degree or diploma.

A. U. Malik

(A. U. Malik).

ACKNOWLEDGMENT

The author wishes to express his thanks to Dr. A. U. Malik, Ph.D. (Alig.), Ph.D. (Liverpool), D.Sc.(Alig.), Reader in Materials Science, Faculty of Engineering & Technology, for the general supervision and his able guidance during the course of this work.

He is also indebted to Professor Mohsin Kuroshi, Ph.D. (Louisiana), Head, Chemistry Section for providing laboratory facilities.

The author is also thankful to Prof. M. L. Mehta, Head, Metallurgical Engg. Department, University of Roorkee, Roorkee (U.P.), India for providing facilities during electrochemical measurements and useful discussions he has had with him.

Last but not the least, the author thanks Mr. M. Abdul Kadir for his technical help and laboratory colleagues for their cooperation and understanding.

The financial assistance from C.S.I.R. is also gratefully acknowledged.

Sharif Ahmad

Sharif Ahmad.

C O N T E N T S

LIST OF PUBLICATIONS

i) A. U. Malik and Sharif Ahmad,
High temperature oxidation and Hot corrosion Behaviour of some Inorganic coated 18 Cr - 8.5Ni steel.
Ind. J. Tech. 17, 4 (1979) 156-157.

ii) A. U. Malik, Sultan Ahmad and Sharif Ahmad,
Corrosion Behaviour of Stainless Steels coated with Coal Ash Deposits at 800 - 1000°C.
Ind. J. Tech. 18 (1980) 221-224.

iii) A. U. Malik and Sharif Ahmad
Hot Corrosion Behaviour of Some Inorganic Coated 18 Cr - 8.5 Ni steel in presence of Na_2SO_4.
Practical Metallography (1981).

iv) A. U. Malik, M. Ishaq and Sharif Ahmad,
Influence of Carbon on the hot corrosion Behaviour of iron-base alloys.
Communicated.

v) A. U. Malik and Sharif Ahmad,
High temperature oxidation and Hot Corrosion Behaviour of Mild steel in presence of some Inorganic coatings.
Communicated.

vi) A. U. Malik, Sharif Ahmad and B. L. Mehta,
Hot Corrosion Behaviour of Inorganic Coated 18:8.5 CrNi steel in Mineral Acids.
Communicated.

LIST OF TABLES

LIST OF FIGURES

LIST OF PHOTOMICROGRAPHS

Fig. 2.8(b) Cross-sectional view of chromate coating on mild steel (SEM) 500 x.

3.1(a) SEM picture of 303 steel corroded in 1N HCl showing voids on the surface 900 x.

3.1(b) SEM picture of phosphate coating corroded in 1N HCl showing pits and microcracks on the surface 800 x.

3.1(c) SEM picture of chromate coating corroded in 1N HCl showing pits and voids on the surface 800 x.

3.1(d) SEM picture of oxide coating corroded in 1N HCl showing voids and pits on the surface 400 x.

3.2(a) SEM picture of phosphate coating corroded in 1N HNO_3 showing microcracks and pits on the surface 400 x.

3.2(b) SEM picture of phosphate coating corroded in 1N HNO_3 showing microcracks and pits on the surface 1600 x.

3.2(c) SEM picture of chromate coating corroded in 1N HNO_3 showing fine pits and pores on the surface 1600 x.

3.2(d) SEM picture of borate coating corroded in 1N HNO_3 showing hexagonal pellets of iron borate along with flacks of Cr_2O_3 on the surface 400 x.

3.2(e) SEM picture of borate coating corroded in 1N HNO_3 showing hexagonal pellets of Fe_3BO_6 and flacks of Cr_2O_3 on the surface 1600 x.

3.2(f) SEM picture of borate coating corroded in 1N HNO_3 showing hexagonal pellets of Fe_3BO_6 and flacks of Cr_2O_3 on the surface 1600 x.

3.2(g) SEM picture of oxide coating corroded in 1N HNO_3 showing micropores and cracks along the grain boundaries 400 x.

CHAPTER - I

GENERAL INTRODUCTION

CHAPTER - 1

GENERAL INTRODUCTION

1.1 Introduction:

The development of coating materials has been a subject of intensive research for atleast three decades, but the concept of using a coating for decorating as well as corrosion resistance purposes has been employed ever since materials were first used. From metallurgical point of view the main objective behind coating development has been to achieve a combination of properties not conceivable by the metal or alloy acting alone. Inorganic and organic coatings have long been used to protect metals from atmospheric corrosion and from corrosion produced by the oxidising environments. Inorganic coatings have also been applied to high temperature materials for protection against corrosion. Infact the development of this type of coatings has been an area of extensive research during the last two decades. The high temperature materials such as super alloys have wide applicability ranging from nuclear reactors to gas turbines and to the components used in power generating units. The application of some special coatings on these alloys undoubtedly produced beneficial effects as far as their high temperature corrosion resistance is concerned. Taking a specific example of a gas turbine, the aerofoil section, in particular of turbine rotor blades and nozzle guide vanes, requires protection

against the hot gas environment in which it has to operate. Environmental aspects are complex and depend upon the application for which the engine is used. The environmental aspects may include a high velocity oxidising gas-stream, a marked non-uniformity of temperature, impurities in the fuel, sea water (ingested by marine engines), carbonous particles in the combustor gas stream and fuel ash deposits.

The premature failure of the metal of alloy due to the corrosion could be controlled by the careful selection from a large number of coatings known for quite some time. These coatings include metal or oxide particulate, phosphate, chromate, silicate, aluminide etc. The recent additions are those of carbide, boride, nitride, silicide, phosphide etc., which can withstand severe operating conditions at which materials have to function.

Non-metallic coating (as applied to the metal) is defined as the coating of metals with thin layers of non-metallic substances, which protect the substrate from the action of surrounding medium, and should also have a decorative effect. Non-metallic coating can be classified into two main groups: Organic and Inorganic. The chief constituent of an organic coating may include an organic compound (usually of higher molecular weight)/dye/rubber/plastic or a combination of two or more aforesaid materials and a carrier (usually a mineral oil).

Inorganic coatings include metal itself (Cr, Al, Zn and Sn are the typical examples) and compounds such as phosphates, chromates or oxides formed in situ on the surface of metals or coatings based on silicate or borate enamels and may contain simple silicates or simple borates or complex boro-silicates or alumino silicates. The hard refractory materials such as carbides, silicides, borides, nitrides etc., have indeed promising future as coatings for specialized applications in aero-space industry. The final selection of the coating material and the technology involved during coating process depend on prior knowledge about the nature of the component and its performance in environments existing under operating conditions. While choosing a material for coating, the following broad property requirements must be considered[1].

1. High degree of oxidation/corrosion resistence depending upon the temperature and service environment.

2. Adequate plasticity to withstand changes in substrate dimensions without cracking.

3. Compatibility with the base alloy in terms of constitution and thermal expansion.

4. Low rate of coating/substrate interdiffusion.

5. Ease of application to the base alloy.

6. Low cost.

The protective properties of coatings[2] are dependent on two extremely important factors:

i) The mechanical and chemical properties of the film itself.

and ii) adhesion, the bond between the film and the surface it covers.

The first factor is independent of the surface to be covered and is entirely determined by the properties of the film former and other constituent of the film. The second factor is determined by the physical and chemical properties of the surfaces of the coating and the substrate, and by the forces acting between the surfaces. The adhesion factor plays an important role in coating technology.

1.2 Coating Methods:

A number of processes are available for depositing protective coatings on the surface of the substrate. These methods range from the traditional paint, dip and electro-plating through chemical vapour - deposition to the more recently developed physical - vapour deposition methods. The latter includes plasma - spraying ion plating, sputter ion plating, ion-implantation, and electron beam evaporation. Some of these recently discovered techniques have reached commercial status, whilst others are still in the research and development stage. Combinations of various above mentioned methods could

be employed for depositing multilayer complex coatings, depending upon the requirements.

1.2.1 Pack cementation: This is the most widely used commercial method for depositing aluminide and chromised coatings. Pack cementation is essentially a chemical vapour deposition process in which components are embedded in a retort containing a powder pack composed of metal(s) required to be deposited (Al, Cr, Si etc.), a halide energiser (Cl, Br, Fe and I) and in some cases an inert diluent. The retort is heated under inert or reducing conditions in the temperature range of 750°C to 1050°C for periods of time usually in excess of one hour. Using aluminising as an illustration, the superalloy components are immersed in a mixture of finely divided powders of alumina/aluminum/aluminum alloy containing compounds of Ni, Cr, Si, B etc; a small amount of halide is then added in order to provide easy passage for vapour phase transport of aluminium, from the pack mixture to the surface of the substrate to be protected. Details of the various reactions which occur are conjectural, but the most important step involves the formation of an aluminium monohalide gas, which is transported to the nickel or cobalt base super alloy component, which on decomposition leaves a surface deposit of aluminium. At the elevated temperatures of pack cementation process the aluminium reacts with substrate to form essentially nickel or cobalt aluminide. The coating deposition rate is dependent on the process temperature, time of exposure

and pack constitution. Most of the existing industrial aluminising processes are proprietory, and the thickness, microstructure, morphology and over all composition depend on the detailed process technology and the composition of the substrate alloy. Pichoir[3] has shown that the morphology and composition of aluminide coatings and the subsequent corrosion behaviour is determined to a large extent on whether the nickel or cobalt diffuse outwards to react with the aluminium, or vice versa. With certain aluminising operations, a layer of the brittle and low melting point Ni_2Al_3 phase is produced and the coating requires further heat treatment to convert the coating to nickel aluminide NiAl[4,5]. Fortunately, the heat treatment schedule is often arranged to coincide with that required to restore the mechanical properties of the substrate. The protection afforded by these coatings is based on their ability to form and replenish protective scales of alumina. Thus the aluminium acts as a reservoir for replenishing the scale where loss or mechanical rupture of the Alumina skin occurs . Detailed description of the mechanisms occurring during aluminising and effects of subsequent heat treatments can be found in literature.

1.2.2 Gas-phase-chemical-vapour-deposition: Strictly, this is an essential part of the pack-cementation process but, a distinction can be made that for cementation, the active coating

vapours are generated by reactions occurring inside the retort, whereas in the gas-phase CVD process, the coating material is introduced as a gas or liquid phase from a source outside the coating chamber. Thermal decomposition of a volatile metal compound at the hot surface of the component deposits the metal coating, and the spent products of the reaction are exhausted from the chamber. Both metals and semiconductors can be deposited by CVD. CVD falls into four groups: i) thermal decomposition e.g., Al-triisobutyl to produce Al. The coatings of Ru, Pd, Pt, Au, Bi, Sb and Zr can also be thermally deposited, ii) reduction of a halide by H_2 results in depositions of Os, Rh, W, V and Nb (iii) reaction of a halide to give a refractory compound of a metal like, carbide or nitride or oxide of titanium, and iv) disproportionation reactions e.g., AlCl giving Al and $AlCl_3$. In CVD, bonding between the coating materials and substrate takes place by inter diffusion process. CVD can form both strongly binded coatings or thick poorly bonded surface which can be separated to give free standing shapes. CVD can form wear resistant layers and high temperature coatings[6].

1.2.3 <u>Electroplating plus pack cementation:</u> A combination of electroplating and cementation processes for sequential deposition of metal coatings has been explored for some considerable time. The most significant advance in recent years was made

by TRW, who are accredited with the first development of a Pt modified aluminide coating, designated LDC$_2$. The method involves the electrodeposition of a thin layer (upto 10 μm) of Pt followed by a pack aluminising treatment during which the Al and Pt interdiffuse with each other and with the substrate alloy[1]. The effectiveness of these coating appears to depend on the initial cleanliness of the substrate surface, coupled with the quality of the precious metal deposit and the aluminising approach used.

1.2.4 Slurry coatings: Typically this involves the low temperature spray application of the coating powder mixture on a component surface, followed by a heat treatment sufficient to obtain the desired coating diffusion. In many instances, halide carriers are employed in the heat treatment chamber to provide vapour transport of the coating elements to the surface of the component. This type of process has been employed on a commercial basis for aluminising turbine components. Slurry technique has successfully been used for the preparation of inorganic coatings on austenitic (AISI 303) and mild steels as referred in the various chapters of this thesis. The inorganic coatings include: phosphate, borate, silicate, chromate, oxide carbide etc. The inorganic coating materials were mixed with a pigment or surfactant or both (such as citric acid, TiO_2, ZnO_2 boric acid etc.) to promote the surface adhesion. The

slurries were prepared by admixing the materials with water or alkali or acid solutions. The slurry was then applied to the substrate material followed by sintering at high temperatures (700 - 900°C) for different periodsof time depending upon the nature of the coating.

Precious metal aluminide coatings and silicon modified slurry coatings for super alloys have recently been developed. A slurry coating designated SERMALOY is commercially available[7] which employs silicon and aluminium for the protection of turbine components.

1.2.5 Fused salt electrolysis: This is a high temperature process in which Al is deposited from a molten salt bath on to a nickle-base alloy cathode and then diffuses inward to form a nickel aluminide coating. A significant amount of research has already been done on this process, but it is expensive, partly due to the exacting control required for handling fused - salt technology. Much work in this field was pioneered in U.S.A. many years ago and this process offers a unique method for depositing some elements on the substrate[1].

1.2.6 Electrophoresis: Electrophoretic deposition (fig. 1) is a coating process in which finely divided particles of coating materials are suspended in a liquid dielectric medium, and migrate under the influence of an electrostatic field and deposit on an electrode. The migration occurs because the

particles are electrically charged, either positively or negatively, depending on the composition of the system. Advantages claimed for this method include very high rates of deposition, combined with good control of thickness, good "throwing power" for irregularly shaped components, and its applicability for a variety of materials (both metallic and ceramic)[8]. The major disadvantage is that some coatings are easily damaged on handling, so a separate heat treatment is required for sintering and densification.

1.2.7 Electron-beam evaporation: The deposition of metallic coatings on substrate is achieved by thermal evaporation of a metal source, followed by condensation of the vapour on to the component. The basic methods of evaporation are resistance heating, using heat or filamentory sources, and electron beam evaporation. The only method that has reached full scale production status for depositing the overlay type MCrAlY coatings on turbine components uses electron-beam evaporation[9,10]. In the process (fig. 1b) blades and vanes with suitably cleaned surfaces are mounted in jigs, inserted into a load lock rotating shafts and then moved through a vacuum lock into a preheating position in the main chamber. After preheating they are positioned directly over the molten pool of coating material, which is produced by high-voltage, electron-beam heating. They are then rotated in the vapor cloud at an elevated temperature for sufficient time to achieve the desired thickness of condensed

coating. The components are then withdrawn, cooled in vacuum and removed from the equipment.

1.2.8 Soft vacuum vapour deposition process: This method may also be described as sputtering ion plating process and operates at pressure of the order of 10^{-2} torr. This process may be physical or chemical in nature and employs gas discharges to influence both chemical and physical effects, e.g., to generate vapour by sputtering and to cause chemical reactions amongst the vapour species in order to improve deposit adhesion and morphology.

In the simple sputtering process, inert ions (usually argon) from a plasma (glow) discharge in a low pressure chamber are accelerated under a high voltage to a surface of target (cathode) made up of the alloy to be coated. Momentum interchange in the surface atomic layers of the target, where the binding energy is lowest, causes sputtering of atoms or atom clusters of the coating material some of which may be ionised (fig. 1. c), these are deposited on the substrate to be coated, which is suitably positioned to achieve maximum collection efficiency. A schematic outline of the process is described in fig. 1.c. Mattox[11] has done pioneering working on soft vacuum vapour deposition process. Very recently, Bunett et al[12,13,14] used ion-implantation technique in studying the high temperature oxidation studies. They produced ion implanted coating of Y, Ce

Si, Al, Li, Ti and Cs on titanium, zirconium, chromium, iron, nickel and copper metals and their alloys. The oxidation studies indicate beneficial effects of Co, Y and Si ion implanted coatings on Fe-Cr alloy in the temperature range 700 - 1000°C, for the period varying from 700 to 5000 h. The scales formed on the ion-implanted metals are protective in nature whereas the scales formed on the uncoated metals are porous in nature though the coated and uncoated alloys exhibited similar oxidation behaviour.

1.2.9 Flame spray process:

A novel development in the conventional flame - spraying process is made by Union Carbide[15]. Known as "Detonation Gun" which is employed for depositing wear - resistant coatings and is claimed to offer some more advantages than the convention thermal spray process. Briefly, the D. Gun, which resembles a large - calibre machine gun, employs the detonation in a firing chamber of measured quantities of oxygen, acetylene and particles of coating materials. This creates a hot high-speed gas steam which heats the particles to a plastic state (Plastic properties are developed in the particles) and accelerates them at a supersonic velocity from the gun barrel. The near molten particles impinge on the surface of the work piece and produce a tenacious mechanical bond. Although, as in other thermospray processes, temperature

above 3200°C is reached inside the gun, the work piece temperature remains comparatively low to minimize distortion and retain the metallurgical properties of the base material. Flame spraying is not employed as a method for depositing oxidation and corrosion resistant coatings to turbine rotor blades, because of its limitations in providing thickness control, surface finish, porosity and adhesion.

1.3 Inorganic Coatings:

Amongst the various types of coatings considered for corrosion resistance purposes, phosphate, oxide, silicate chromate and borate coatings have been found suitable for applications in less severe corrosive environments and at moderate temperatures. On the other hand, aluminide, boride, silicide, carbide and nitride coatings have been found satisfactory at high temperatures and in relatively more severe corrosive environments.

In the proceeding pages a critical survey of the various type of inorganic coatings is given. The survey includes important work carried out during the last three decades. The survey contains the recent work concerning with the preparation of coatings, mechanism of the formation of coatings and their applications.

1.3.1 Aluminide coatings: The most widely used and best established coating as high temperature oxidation and corrosion resistant, which was introduced into service in the late 1950's, is based on Aluminide compounds. These coatings have been used on Ni- and Co base super alloys where nickel and cobalt aluminides are formed respectively. Aluminide coatings are effective at moderate temperatures and/or where the environments is not too severe. In more severe or highly corrosive environments, diffusion coatings based on the addition of noble metal (Pt, Rh) to aluminide, e.g., noble metal enriched aluminide coatings have been used to protect super alloy components (made of IN 792, IN 738 and MM 509) in the hot section of RB211 engines installed on oil rig in the north sea in 1980. These components will be operating in a highly "sulfidating" environment. MCrAlY (where M = Fe, Co, Or Ni base) coatings have also been designed to produce an Alumina or chromia scale depending on the engine environment. The yttrium additions are made to improve scale adherence[12].

Brennflock et al[16] reported the preparation of a hot corrosion resistant Aluminide coating within the borings of turbine blades at deposition temperature $>1000^{o}C$. They have given special emphasis to optimisation of the temperature profile in the tubular deposition reactor to obtain a uniform coating. The authors have discussed the influence of pressure, gas composition and flow conditions on the deposition rate and

uniformity of the coatings. Orcn and Lernor[17] reported the formation of aluminium film of 5 μm thickness on Cr - Mo air craft steels. High deposition rates were achieved by employing the high power electron-beam-gun for surface evaporation. The effect of temperature on the relevent properties of the film mainly adhesion and corrosion resistance were studied. The properties of film improve with increasing substrate temperature.

Levendal and Henry[18] have prepared corrosion resistant aluminide coatings on Fe - and Ni base alloys. The fused slurry of nickel containing coatings having 55-65% Al and 5-10% Si was deposited on mild steel and inconel 600 substrates. Phase composition and distribution in the coating were controlled by adjustment of the reciprocal activities of Al and Ni in the reactive liquid generated during fusion. Slurries with balanced Al - Ni concentrations produce single phase coatings. The coating forms a thin adherent protective scale on inconel 600 within the first 125 h of cyclic air exposure at 1100°. The coating is degraded either by the loss of Al or enrichment in Ni or Fe by interdiffusion with the substrate. The γ-NiAl, a transformation product of β NiAl, retains enough Si in solution to maintain unchanged oxidation kinetics. The coating has performance superior to that of common aluminide coatings and is promising for use in gas turbine.

1.3.2 Phosphate coatings: Among the conventional inorganic coatings the phosphate coatings have most extensively been used and innumerable references[19-24] are available concerning with their preparation properties and uses.

Phosphate coatings[2] are primarily produced by treating metals and alloys with phosphoric acid or solutions of primary phosphates of Mn, Fe, Zn, Al or Cd. The basic properties of phosphate coatings depend on the surface preparation, the solution composition and operating conditions. Although the phosphate coatings are unstable in acids and alkalies, their most valuable property is to adsorb oil. Phosphate coatings greatly improve the adhesion of paints on metals and retard the process of corrosion under the paint film, even in those regions where the paint has been damaged. Thus the phosphate coatings have beneficial effects on the durability of paint coatings.

Three main types of phosphating processes have been envolved viz., i) phosphating under normal conditions, ii) accelerating phosphating and iii) cold phosphating. Some of the newer type of phosphate coatings worth mentioning are those of boron phosphate[25,26], prepared by mixing equimolar amounts of P_2O_5 and B_2O_3 at 600-650°C. Conversion coatings[27] for Al have been prepared by using Zn, Cr and Ni phosphates. In these

coatings the crystalline and amorphous phosphates are present in the form of 54 $Zn_3(PO_4)_2$. 11 $AlPO_4$. $Ni_3(PO_4)_2$. 114 H_2O. and $Cr(OH)_2$. 11 CrO_4. $Al(OH)_3$. $2H_2O$ respectively. These coatings are suitable for the construction of containers and applications in aerospace industry. Inorganic paint compositions[28] based on metallic oxides, water soluble silicates and polyphosphates have been prepared by heating oxides and hydrides of Zn, Mg, Al, Zr, Ti and Ca with silicates of Na, K, and/or Li followed by mixing with phosphates of Al, K, or Mg, a pigment and a filler to give inorganic coating compound. A white crystalline inorganic coating has recently been described by the reaction of $AlCl_3$ and H_3PO_4 in presence of C_2H_5OH and HCl.

Ved et al[29] have recently prepared mechanically stable, heat resistant and high speed gas flow resistant phosphate coating by the addition of Al_2O_3 15-20%, B_2O_3 1-4%, CaO 1-3% and BaO 1.5-3.5% to a composition containing SiO_2 10-30%, $Al(OH)_3$ 3-15% and a Al phosphate binder. A corrosion resistant glassy coating of phosphate[30] on the ferrous alloy was obtained by mixing ZnO:54% P_2O_5:45.6% and Al_2O_3: 0.5% and an oxide of group II A or III A metal ($>$1.0%).

Bogi and Mc Millan[31] recently reported a two stage phosphating process for coating on steels. X-ray diffraction, electron probe micro analysis and differential thermal analysis were used to evaluate the mechanism of coating. According to

the authors the electrochemical attack of the metal surface immersed in the phosphoric acid medium results in the formation of a soluble primary metal phosphate:

$$Me^{+} + 2H_3PO_4 \longrightarrow Me(H_2PO_4)_2 + H_2\uparrow$$

any surface oxide will also be dissolved

$$MeO + 2H_3PO_4 \longrightarrow Me(H_2PO_4)_2 + H_2O$$

the corresponding pH change can cause an equilibrium shift to the more insoluble phosphate

$$Me(H_2PO_4)_2 \rightleftharpoons MeHPO_4 + H_3PO_4$$

Further depletion of hydrogen ion causes a dissociation to the insoluble tertiary phosphate:

$$3MeHPO_4 \rightleftharpoons Me_3(PO_4)_2 + H_3PO_4$$

The zinc phosphate in solution is behaving as a typical anodic inhibitor by precipitating itself as mixed zinc-iron phosphate at the anodic site. Uniform crystalline coatings of manganese iron phosphates are deposited at the cathode site due to the change of pH at the metal solution interface. The authors proposed that the difficulties in controlling the size and distribution of the crystalline coating, can however, be overcome by the use of a 2-stage phosphating process, namely, by initially deposition at cathodic regions and subsequent precipitation of a zinc phosphate coating which will deposit on the

steel. This will leave anodic regions exposed by the incomplete primary coat. Excellent protection could be provided to the ferrous metal in this manner. The coated specimens (b) had been stored for a year without any visible sign of corrosion.

1.3.3 Silicate coating: A large number of references[32-36] are available on silicate coatings. The basic constituent is an alkali or alkaline earth silicate. The silicate coatings are suitable for aluminium or steel and provide excellent high temperature corrosion resistance in air, H_2S and cathodic protection of underground metal structures[33]. A relatively recent addition in silicate coatings is the introduction of complex silicates of the glass compositions[37]. Ibpev and Appen[38] made coatings from glass of systematically variable compositions: $16Na_2O.20M_mO_n.64SiO_2$ (mole %) where M_mO_n is CuO, BeO, CaO, SnO, BaO, ZnO, CdO, B_2O_3, CeO_2, TiO_2, Cr_2O_3, Fe_2O_3 CoO, NiO and MnO_2. The thickness of the coating varies from 95 to 100 μ. The specimens were heated in air at 800°C and it was found that nearly all the coatings protected iron against oxidation at varying degrees. The exception was the sodium borosilicate glass coating which rapidly becomes saturated with iron oxides thereby loosing its protective properties. The strongest protection was conferred by enamel containing NiO and CaO.

Very recently some Si based[39-41] ceramic coatings have been developed for heat resistant Ni -, Co - and Fe base alloys The substrate matrix contains embedded particles, which are capable to form protective oxides. After coating, the coated substrates are heated 1-4 h at 1000-1250°C, the coating is found suitable for gas turbine parts. Kaumanati et al[42] have prepared a fire proof, heat resistant and vibration damping silicate coating for steel sliding boards. Inorganic coatings of phosphate, borate, silicate etc. are frequently used as inorganic inhibitors and sacrificial coatings[40] to prevent the service corrosion caused by the stray currents, differences in stress through structure and the differences in soil conditions. The mechanism for the oxidation of iron under a thin layer of silicate melt in air is believed to involve the following stages: diffusion of oxygen through the enamel layer, its chemical interaction with iron and dissolution of interaction products in the coating.

1.3.4 Borate coatings: Surprisingly, only a limited amount of work has been carried out on borate coatings. Coatings of orthoboric acid[43,44] on high purity iron were found to decrease the oxidation rate in oxygen between 700°C and 1100°C. When in contact with the heated iron surface, the B_2O_3 powder melts and dissolves any residual or reformed scale. It has been proposed that the oxygen dissolves in the melt and is transported to the melt/iron interface. At the interface, solution of iron and

oxygen ions continues until a complex iron-oxide-boron oxide complex is precipitated. The complex oxide is iron borroferrite, 4 FeO Fe_2O_3.B_2O_3 (Vonsenite).

1.3.5 Carbide coatings: Extensive amount of work has been reported on carbide coatings[45-52] during the last two decades. Carbide coatings have an edge over other coatings due to their hardness and strength, durability and superior heat resistance and oxidation resistance properties. Silicon carbide, boron carbide and the transition metal refractory carbides have been used as coating materials. The phenomenal advances in the technology of carbide coatings owe to their applications in nuclear reactors and other high temperature assemblies working in corrosive environments. The most convenient method[53] to deposit carbide is thermally decomposing the halide vapours and diffusing carbon simultaneously. Another method consists of mixing oxide of metals with graphite and Al powder and igniting the product in a crucible containing metal which has to be coated. Uranium and thorium carbides[54] have been deposited by using CH_4 and C_2H_4 in fluidised beds of Al_2O_3, UO_2 or ThO_2. Heat resistant coating of chromium carbide[55] on steel has been obtained by using a mixture of low alkali boro silicate glass and chromium carbide powder. The coating operation was carried out in an atmosphere of argon and thickness of the resulting coating was 0.15-0.28 mm. The rate determining step in the

coating is the interaction of boro silicate glass with oxide films on carbide grains. The carbide grains interacted with the steel whereby the non-porous compact and well adhering blisters of chromium carbide are formed on the surface of the steel. The carbide coating showed good adhesion and protection against high temperature corrosion. Titanium carbide[56] was deposited on the substrate by gas phase reaction between $TiCl_4$ C_6H_6 and Ti at 1000-1100°C. The coating of group VB carbides on iron or iron base alloys[29] has been reported by cathodic treatment in a B_2O_3 melt containing the respective element. Thus for vanadium carbide coating, a crucible containing $Na_2B_4O_7$ was heated to 930 - 950°C. Ferrovanadium was added and a test piece of steel was immersed in the melt and finally treated cathodically for 10 minutes with a current density: 3-5 A/cm^2. Recently titanium carbide[57] coatings of 3-26 μ thickness have been obtained at 950-1050°C on the external surface of the alloy steel (20, 45, uBA and u12A). $(TiFe)_{cx}$ was identified on the surface and transitional layer comprises of (α + TiC + Fe_3C). The coating has good corrosion resistance and hard wear resistance properties. TiC coating is commonly applied to iron base alloy (steel) used in navy in order to overcome the marine corrosion. Beahm et al[58] found TiC - 99 film is insoluble in sea water up to 90°C.

1.3.6 Boride coatings: A limited number of references are available on boride coatings. The general method[59] of depositing

boride coating is to carry out gas plating according to the reaction:

$$TiCl_4 + 2BCl_3 + 5H_2 \longrightarrow TiB_2 + 10HCl.$$

TiB_2 coating is formed at temperatures higher than 600°C and deposition takes place at 700 - 950°C with a coating thickness of $\gtrsim 3\,\mu$. Boronizing[60] of steel has been carried out by heating steel at 850°C for 3h in a mixture containing B_4C, Ferroboron and Al_2O_3 with addition of alkali metal fluoride as accelerators when a boride layer of 130 μ thickness is obtained. Recently Moskowitz et al[61] have obtained boride coatings by spray and fuse self fluxing process. Powdered Ni or Co base alloys containing chromium were mixed with elemental boron sprayed on the substrate surface and fused. self-fluxing alloy powder was precipitated from a viscous melt of the alloy and forms a hard coating of chromium boride or chromium carbide. The properties of boride coatings[62] on Ti, Zr, Mo, W and Ta metals have been studied. The coatings are deposited in the form of TiB_2, ZrB, NbB_2, Mo_2B, Mo_2B_5, W_2B and W_2B_5 respectively. The order of the sinterability of the various boride coatings follows the sequence: $ZrB > TiB_2 > NbB_2 > W_2B_5 > Mo_2B$.

1.3.7. Silicide coatings: Silicide coatings[63-64] have been used on Nb, W, Ta, Mo and other refractory materials as heat resistant coatings for protection against high temperature oxidation. The usual method is to deposit silicon on metal

surface by passing mixture of H_2 and silicon halides over the metal surface.

A silicide coating[65] has been prepared from a flame spray powder mixture, it consists of agglomerates of a metal silicide mixed with a coating metal powder. The metal silicide being at least one selected from the group consisting of disilicides of Ti, Zr, Hf, V, Nb, Ta, Cr, Mo, W, Mn, Co, B and Ng. The silicide agglomerates are made up of fine particles of average size $\leq 20\,\mu m$ bonded together in a matrix of a binder.

Recently Bernard et al[66] have produced a thin film of transition metal silicides by the static and flow pyrolysis system. The pyrolysis of $[Co(CO)_4(SiH_3)]$, $[Fe(CO)_4(SiH_3)]$ and $[Mn(CO)_5(SiH_3)]$ at 773°K in a flow system results in the formation of the transition metal silicides CoSiB - $FeSi_2$, and MnSi - Mn_5Si_3 respectively. Static pyrolysis of $[Mn(Co)_5(SiH_3)]$ gives only amorphous solid products, which contain, in addition to metal and silicon, appreciable quantities of C, H, and O. The coatings have high thermal stability and are corrosion resistant.

1.3.8 Nitride coatings: Although first nitride coating on metallic surface was reported 20 years ago, only a very limited amount of work has been carried out since then.

The nitride coatings possess excellent adhesion, and

high temperature corrosion resistance properties. NH_3 is the usual nitriding agent and is admixed with the vapours of metal halide and passed over the substrate to give a fine nitride coating. Thus a titanium nitride coating[67] has been preprared by the reaction of $TiCl_4$ and NH_3 in the temperature range of 900 - 1200°C in a nitride coated steel or in a quartz reaction vessel.

Recently ZrN coating[68] has been used in nuclear reactor for protection against molten Pb or Pb - Bi and Pb - Bi - Sn coolant corrosion. The inner metallic surface (stainless steel) of the reactor coolant system was coated with a 1 μ ZrN layer by immersion in a solution of 0.1% Zr in molten Pb or Pb alloys at 850 - 1000°C for 24 h. The Pb was drawn off leaving a thin film of ZrN on the inner wall of the reactor. If this coated wall comes into full contact with Pb or Pb - Bi or Pb - Bi - Sn eutectics at 800 - 850°C no corrosion occurs during 4 weeks heating.

The coating of BN[69] on Cu, Ni, W, Mo metals and steels have been deposited by a simple method. The nitride films of 0.35 μm thickness were deposited by using high frequency heating in N_2 at 450°C and 0.03 torr. I.R. spectroscopy and X-ray diffraction techniques were used to characterise the film compatability temperature, which follows the order: Ni > steel > Mo > Co > W. The adhesion of BN coating was superior to those

of SiO_2 and Al_2O_3 coatings. BN coating was found suitable as a diffusion barrier in fibre reinforced metals.

Seal resistant coating of BN on steel has been reported[70]. The coating was prepared from a dispersion containing BN powder, powdered silica, $Al(PO_4)$, Aerosil and water. The dispersion was coated on a steel sheet, dried in air for 2 h followed by 60 min. baking at 300°C to give a 0.03 mm adherent film.

1.3.9 Miscellaneous coatings: A large number of hard wear-resistant coatings have been developed for gas turbine engine. The coatings were tested under gasturbine simulated conditions which consists of exposure of the coated alloys in an oven for 300 h at the maximum temperature (540 or 650°C) and ten temperature cycles from room temperature to the maximum service temperature. On the basis of these static oven screening tests, the following coatings have been recommended as future wear-resistant coating materials: TiC, Cr_2O_3, SiN_4 (sputtered), CdO and graphite (fused)[71].

Motojima and coworkers[72] have fabricated boron phosphide coatings on Molybdenum by CVD process. They have studied deposit structure, microhardness, oxidation resistance and B/P ratio. The structure of the coating consisted of two layers BP and MoP (10 mm) formed in the first 5 mm reaction time. After this the BP layer formed at a rate that varied linearly

with deposition time.

1.4 Oxidation of Coated Materials:

A limited number of references are available in literature relating to the oxidation or corrosion behaviour of coated metals or alloys.

An oxidation study has been reported[73] consisting of kinetics measurements and microscopic investigations on Cu and Ti metals coated with different vitreous enamel. The oxidation was carried out at 600, 700 and 750°C in air. The experimental results were found to be in good agreement with the calculated values based upon a theory developed for high temperature gas corrosion of metals beneath coatings.

Cyclic oxidation of aluminide coated cobalt base super alloys was carried out[74] in furnace air and in high velocity combustion gas environments at 1900 - 2100°F, cyclic frequencies varied from 1-100h in furnace tests. At all exposure temperatures, increased cyclic frequencies accelerated coating degradation because the protective Al_2O_3 scale spalled during cooling. Spalling depleted the coating of Al and permitted less protective oxide to form in high velocity tests. Coating life decreased from 300h at 1900°F to 12h at 2100°F.

1.5 Statement of the Problem, Aims and Objectives:

The work described in this thesis deals with the studies on inorganic coatings. The work covers the corrosion and oxidation behaviour of iron base alloys (steels) in presence of inorganic coatings. The main objective of the work is to explore the feasibility of developing some new coatings for steels which would show better corrosion resistance performance than the uncoated steels.

The inorganic coatings employed in the work include phosphate, silicate, borate, oxide, chromate and carbide. The corrosion behaviour of the coated steels has been investigated in presence of acids at ambient temperatures. The corrosion potential and potentiostatic polarisation techniques, have been utilised to determine the corrosion resistance performance of the coatings. High temperature oxidation and hot corrosion behaviour of the coated alloys have been investigated by measuring the corrosion rates. A detailed morphology of the corroded alloys has been carried out using optical microscopy, scanning electron microscopy and X-ray diffraction analysis.

The work described in this thesis has been presented in the form of 7 chapters:

Chapter I presents General Introduction which contains literature review, coating methods, types and kinds of coatings.

Chapter II deals with the preparation of different coatings viz., phosphate, silicate, borate, oxide, chromate and carbide. This is followed by the detailed descriptions of experimental methods, procedures, techniques employed in this work and mechanism of the coatings. In chapter III, the behaviour of coated steel in acids and alkalies at ambient temperature has been discussed and the results of the corrosion potential and polarization behaviour of the coated steel using potentiostatic technique are presented. The chapter IV described the results of high temperature oxidation kinetics studies of coated 18:8.5 Cr : Ni steel. Subsequently the hot corrosion behaviour of coated austenitic (18:8.5 Cr:Ni) steel in ionic salt environments has been discussed in Chapter V. In chapter VI high temperature oxidation and hot corrosion behaviour of borate chromate and carbide coated mild steel has been discribed. Finally in chapter VII, the summary of the work and the suggestions for the future work are given.

CHAPTER - II

COATING PREPARATIONS

CHAPTER - II

COATING PREPARATIONS

2.1 Introduction:

From the corrosion protection point of view, inorganic protective coatings on iron base alloys (alloy steels) constitute the object of numerous and comprehensive investigations. Inorganic protective coatings are very varied in chemical composition, structure, mechanism of formation and methods of preparation.

Preparation of inorganic coatings is a complex technological process. A coating should primarily have good substrate adherence and a certain thermal shock resistance, the protective layer should also have appropriate mechanical properties and thermal expansion coefficient close to that of the substrate, as well as appropriate hardness and capacity of reflective thermal radiation; optimum properties are obtained by frequently extended selection of appropriate technological conditions.

Coating properties are largely dependent on the method of its application. The most compact layers are obtained by burning enamel. High temperature enamels differ from the ordinary ones primarily by a higher softening point. On alloy steels, enamel coatings are used which have melting points

higher than 700°C. The burning temperature of such enamels is in the range of 1100 - 1200°C. Materials used for protective coatings on metal and alloy surfaces may be distinguished into the following groups:

1. Metals or alloys forming oxidation products on their surfaces which are resistant to scaling under aggressive environments: Al, Cr, Si etc.

2. Compounds of the type of silicides, carbides, borides, nitrides, phosphides etc.

3. Ceramic and glass coatings: silicate, borates, oxides etc.

4. Noble metals, in operational conditions forming no compounds with the aggressive atmosphere components: Au, Pt, Rh, In, etc.

The coatings belonging to first two groups when grew on the metal or alloy surfaces act as protective films. While the coatings of the other types mechanically prevent a direct contact between the material and the ambient atmosphere[75-78].

Before giving the details of preparation of various types of coatings, it is worthwhile to explain the techniques adopted for the preparation of coatings. Various coating methods have already been discussed in the general introduction.

Among those only slurry and diffusion techniques are found relevent to the preparation of the type of the coatings, which have been used in the present studies.

SLURRY COATINGS:

As the name implies, this type of coating involves various kind of slurries which could be applied on the surface of the substrate for protection purposes. For example, the preparation of silicate, borate type coating requires a vitreous mass, which is usually obtained by high temperature melting of a mixture of natural materials like sand, clay, feldspar etc. and fluxes such as soda potash, fluoride etc. (used to lower the melting point of the same materials). The vitreous materials is then mixed with a pigment or surfactant or both to promote the surfece adhesion and to increase thermal and mechanical stabilities of the coating, and a slurry is prepared by admixing with water or alkali or acid solutions. The slurry is then applied to the substrate material, followed by sintering at temperatures ranging from 800 to 900^{o}C[2].

DIFFUSION TECHNIQUE:

Diffusion coatings are deposited on substrate surface at high temperatures; due to instantaneous interdiffusion between coating and substrate materials. The nature of such coatings dependsupon several factors: composition of the

substrate and coating material, nature of the phases present in the substrate e.g., solid solution, intermetallic etc, and the temperature. The temperature at which diffusion coating is deposited is frequently high. Carbides borides, and nitrides and silicides are the common coating prepared by diffusion process: CO_2/CO and graphite or charcoal, boron hydrides or alkali borides or boron halides, N_2 and NH_3 and SiH_4 or SiO_2 or alkali silicides are respectively the common coating agents.

2.2 Experimental:

2.2.1 Alloys used: Standard austenitic steel AISI303 (Cr:18, Ni:8.5, Si:2.0, Mn:4.0, C:0.15, Fe - balace) and Mild steel (C:0.30, Si:0.15, S:0.03, Fe - balance) were used as substrate materials for coating purposes. Austenitic steel and mild steel strips of 20 x 8 x 1 mm size were cut from sheets. The austenitic steel strips were homogenised for 4 h in an evacuated quartz glass tube (Pressure: 1×10^{-4} torr, temperature: 900°C) whereas mild steel strips were homogenised for 2 h in an evacuated pyrex glass tube (Pressure 1×10^{-4} torr, temperature: 750°C).

2.2.2 Specimen preparation: The annealed specimens were abraded with 180, 320 and 500 grade SiC papers, respectively using a motor driven disc polisher. The abraded specimens were

then washed with distilled water and alcohol, and finally degreased with CCl_4.

2.3 Preparation and Mechanism of Coatings:

2.3.1 Phosphate coating:

Reagents used: $CaCO_3$, $Na_2H PO_4$, citric acid and H_3PO_4 (Analytical grade B.D.H. Products) were used in the preparation of phosphate coating.

PROCEDURE:

A slurry was prepared by mixing $CaCO_3$:2.5g, Na_2PO_4:1.0g, and citric acid 0.125 g in 25 ml of 12 % H_3PO_4. The steel specimens were uniformly coated with a thin layer of slurry and dried in air. The coated specimens were then placed in a silica boat, heated in a muffle furnace at 700°C for 3 h and finally cooled in the furnace. A thin dark coating was formed on the steel specimens which has excellent adhesion. The X-ray diffraction analysis of the film indicates the presence of calcium and ferric phosphates(Table - 2.1).

MECHANISM:

Electrochemical attack of the metal surface on immersion in the phosphoric acid medium containing Na_2HPO_4 results in the formation of a soluble metal phosphate

$$1)\quad Fe + 3H_3PO_4 \longrightarrow Fe(H_2PO_4)_3 + 3/2\ H_2$$

the pH decrease causes an equilibrium shift to the more insoluble secondary phosphate

ii) $2\,Fe(H_2PO_4)_3 \rightleftharpoons Fe_2(HPO_4)_3 + 3H_3PO_4$

Further depletion of hydrogen ions causes dissociation to the insoluble tertiary phosphate.

iii) $Fe_2(HPO_4)_3 \rightleftharpoons Fe_3PO_4 + H_3PO_4$

During phosphating process some tricalcium phosphate will also be formed.

iv) $3CaCO_3 + 2H_3PO_4 \longrightarrow Ca_3(PO_4)_2 + 3H_2O + 3CO_2$

As the reactions are taken place at the metal surface continuous dissolution of the substrate (acting as anode) occurs till a uniform coating of mixed phosphates is formed on the surface which prevents further dissolution of the metal. On heating the coating at 700°C some dehydration reactions take place and oxides of iron and chromium are formed at the metal/coating interface.

Figure 2.1a and 2.1b show SEM picture of phosphate coated steel and represent cross sectional and surface views respectively. The cross sectional picture of phosphate coating indicates a nearly uniform coating which is slightly distorted at the resin/coating interface. The coating seems to be reasonably adhered to the alloy surface and most likely consists

of a single phase (iron phosphate). The surface micrograph also indicates a uniform layer of the coating on the alloy surface, however, there are small pits and pores scattered evenly through out the surface of the coating.

2.3.2 Silicate coating:

Reagents used: Analytical grade $(NH_4)_2CO_3$, CdO, $Al_2(SiO_3)_3$ and Cr_2O_3 (B. D. H.) were employed for the preparation of coatings.

PROCEDURE:

Polished specimens of 20 x 8 x 1 mm size were kept completely covered in beds of homogeneous mixture containing 15% $(NH_4)_2CO_3$; 25% CdO, 20% Cr_2O_3 and 40% $Al_2(SiO_3)_3$ in silica boats. The boats were heated in a muffle furnace at 800°C for 9h followed by cooling in the furnace. An extremely adhered strong greenish black film of the silicate is formed on the steel specimens.

MECHANISM:

Complex silicates of Cr, Fe and Al are presumably formed by the interaction of Aluminium silicate with Cr_2O_3 and Fe_2O_3. At high temperature (800°C) aluminium silicate reacts with Fe, Cr and Ni to give mixed silicates of the glass composition with an additional protective coating of Al_2O_3.

At 800°C, the steel oxidises to form Cr_2O_3 and probably a spinel $FeO.Cr_2O_3$ (inner layer) and Fe_2O_3 as an outer layer. The coating materials primarily Aluminum silicate react with Fe_2O_3 to give iron silicate whereas Cr_2O_3 presumably remain unreacted. Thus the coating consists of iron silicate admixed with Cr_2O_3 with spinal $FeO.Cr_2O_3$ at the coating/alloy interface. During the reaction some Al_2O_3 is also formed which is also present in the coating.

v) $Al_2(SiO_3)_3 + Fe_2O_3 \longrightarrow Fe_2(SiO_3)_3 + Al_2O_3$

vi) $Fe_2(SiO_3)_3 \longrightarrow Fe_2SiO_4 + 2SiO_2 + O$

vii) $Al_2(SiO_3)_3 + O \longrightarrow SiO_2.Al_2O_3 + 2SiO_2$

The function of CdO is to promote adhesion between coating and the alloy surface.

Figure 2.2 shows SEM picture of a cross section of silicate coated alloy. The film contains large number of voids and micro pores. It is also not properly adhered to the alloy surface, in fact it is detached from the alloy surface. The coating appears to be consisted of only one phase e.g., iron silicate. The X-ray analysis confirms the presence of iron silicate (Table - 2.1).

2.3.3 Chromate coating:

Reagents used: CdO, ZnO, Borax, $Al_2(SiO_3)_3$, Al_2O_3,

MgO and MnO_2 were all analytical grade reagents.

PROCEDURE:

A slurry was obtained by mixing powdered chemicals in the following proportions (by weight %) in minimum amount of water. bC: 14.45%; ZnO:43.55%; Borax:14.45%; $Al_2(SiO_3)_3$:11.63%; Al_2O_3:8.64%; MgO:5.8% and MnO_2:1.45%. The steel specimens were coated with thin layers of the slurry and dried at room temperature in air. The coated specimens were put in the silica boats, and then transferred to a muffle furnace. The specimens were baked at 800°C for 2h and subsequently cooled in the furnace itself. A thin film of brown colour was obtained with a reasonably good adhesion.

MECHANISM:

The coating on the alloy is formed after a series of chemical reactions involving oxides of Mn, Mg, Al, Zn and Sb. Borax and Aluminum silicate provide B_2O_3, Al_2O_3 and SiO_2. Steel specimens on heating may provide oxides of Fe, Cr and Ni namely Fe_2O_3, Cr_2O_3, NiO and $FeO.Cr_2O_3$. These oxides involve in a variety of reactions with coating materials. Some typical reactions may be represented as follows:

viii) $Fe_2O_3 + SiO_2 \longrightarrow Fe_2SiO_4$

ix) $ZnO + Cr_2O_3 \longrightarrow ZnCr_2O_4$

x) $NiO + Cr_2O_3 \longrightarrow NiCr_2O_4$

xi) $MnO + 2Fe_2O_3 \longrightarrow MnFe_4O_7$

The coating obtained after baking in the furnace is composed of a mixture of chromates, silicates and oxides. MgO, MnO_2 and borax have been used as surfactants, to promote adhesion between the coating and the alloy surface. The X-ray diffraction analysis (Table - 2.1) of the coating confirms the formation of the chromates and silicate as indicated by reactions (viii) to (xi).

Figures 2.3a and 2.3b represent scanning electron micrographs of the cross-sectional and surface portions of the chromate coated alloy. The micrograph of the surface indicates a nearly uniform coating of the chromate with no visible presence of pores or pits. The cross-sectional view indicates a thick layer of coating strongly adhered to the alloy surface. The coating seems to contain at least two phases probably consisting of chromate and silicate.

2.3.4 Borate coating:

Reagents used: $Na_2B_4O_7.10H_2O$, $KMnO_4$ and $MgSO_4$ were all analytical grade reagents, whereas $K_2[TiO(C_2O_4)_2].2H_2O$ was a reagent grade product. Araldite resin was a ciba Geigy product.

PROCEDURE:

A powdered mixture containing $Na_2B_4O_7$:47.5%; $KMnO_4$: 19.2%; $MgSO_4$:14.3% and $K_2[TiO(C_2O_4)_2].2H_2O$:19% was sprinkled along with a thin layer of Araldite resin on the surface of the alloy specimens. Araldite resin was used for providing initial adhesion between coating mixture and the alloy specimen surface. The specimens were left overnight for drying. The dried specimens were then placed in silica boats and heated in a muffle furnace at 800°C for 2h followed by slow cooling. A black coloured coating with good adhesion is formed on the alloy.

MECHANISM:

Complex borate coating consisting of metal boroferrites such as Fe_3BO_6, is expected to be formed by the interaction of iron and chromium oxides (from the alloy) with borax in presence of $KMnO_4$. However, X-ray diffraction analysis data indicate the presence of borides of Fe and Ni and iron borate. The formation of the above constituents may be explained on the basis of the following reactions:

xii) $Na_2B_4O_7 \longrightarrow 2B_2O_3 + Na_2O$

xiii) $Na_2O + TiO_2 \longrightarrow Na_2TiO_3$

xiv) $9Fe + 2B_2O_3 \longrightarrow 3Fe_2B + Fe_3BO_6$

xv) $6Ni + 2B_2O_3 \longrightarrow 3NiB + Ni_3BO_6$.

xvi) $2KMnO_4 + [TiO(C_2O_4)_2]^{--} \longrightarrow 2MnO_4 + K_2TiO_3 + 2CO_2 + O^{--}$

xvii) $4Cr + 3O_2 \longrightarrow 2Cr_2O_3$

Figure 2.4a and 2.4b show SEM pictures of borate coated alloy under cross sectional and surface views, respectively. The cross-section indicates two layered coating. The top layer is relatively uniform and probably consists of borides of iron. The inner layer which is adjacent to the alloy is in the form of stratified layer and may consist of Cr_2O_3, FeO Cr_2O_3 and Fe_2O_3 some of the oxide particles are also incorporated with the outer layer. It appears that in borate coated alloy, the film is not adhered to the alloy surface in the strict sense, though the inner most portion of the coating is not detached from the alloy surface but is joined by a oxide rich discontinuous layer. The scanning micrograph of the coated alloy surface is reasonably uniform though the presence of some pits and pores could easily be visualised.

2.3.5 Oxide coating:

Reagents used: Zirconyl Nitrate, Cadmium Nitrate, Ammonium carbonate, Zinc phosphate, Citric acid, Borax and phosphoric acid (Reagent grade chemicals) were used.

PROCEDURE:

A slurry was prepared by mixing $ZrO(NO_3)_2$:2.0g; $Cd(NO_3)_2$: 1.0g; $(NH_4)_2CO_3$:1.0g; $Zn_3(PO4)_2$: 1.0g; citric acid:0.5g and

$Na_2B_4O_7$:0.1g. in 5 ml of 50% H_3PO_4. The steel specimens were uniformly coated with thin layers of the slurry and dried in air at room temperature. The dried specimens were placed in silica boats, and heated in a muffle furnace at 850°C. for 2h and then cooled in the furnace. A thin green coloured coating was formed on the specimens with excellent adhesion.

MECHANISM:

During heating $ZrO(NO_3)_2$ decomposes to give ZrO_2 and oxides of nitrogen.

xviii) $ZrO(NO_3)_2 \longrightarrow ZrO_2 + NO + NO_2 + O_2$

the oxygen thus liberated oxidizes iron, chromium and nickel (from the alloy) to form oxides of these metals.

xix) $2Fe + 3O_2 \longrightarrow Fe_2O_3$

xx) $4Cr + 3O_2 \longrightarrow 2Cr_2O_3$

xxi) $2Ni + O_2 \longrightarrow 2NiO$

xxii) $NiO + Cr_2O_3 \longrightarrow NiCr_2O_4$, and

xxiii) $Cr_2O_3 + 2FeO \longrightarrow (Cr, Fe)_2O_3 + O_2$

The coating is thus composed of mixture of oxides with zirconia in predominent concentration. The X-ray diffraction data support the presence of above oxide constituents (reactions xix to xxiii) in the coating.

Besides the presence of the phosphate of Zn there is also a possibility for the formation of Zr, Fe and Cd phosphates. Although X-ray diffraction analysis fails to identify the presence of phosphates or borates in the coating (Table - 2.1).

Cross-sectional and surface views of the oxide coated alloy are shown in Fig. 2.5a and 2.5b. The scanning micrograph of the surface indicates a nearly uniform coating with crystallites of zircone spread all over the surface. The electron micrograph of the cross-section shows coating in the form of disturbed layers of ZrO_2 probably with some inclusions of other oxides.

2.4 Coatings on Mild Steel.

2.4.1 Borate coating:

Reagent used: Reagent grade $Na_2B_4O_7$, ZnO; TiO_2; Fe_2O_3, CdO and Al_2O_3 were used. Kevalin clay was obtained from Khurja, U.P.

PROCEDURE:

A red coloured slurry was obtained on mixing $Na_2B_4O_7$: 0.7 g; Kevalin clay: 0.4g; ZnO; 0.2 g; TiO_2: 0.3g; Fe_2O_3:0.1g; Al_2O_3:0.1g; CdO:0.1g; and 0.05g Cr_2O_3 in 5 ml of 12N NaOH.

The polished mild steel specimens were uniformly coated with thin layers of slurry. The coated specimens were dried

in air at room temperature, and were then kept in silica boats. The dried coated specimens were subsequently heated in a muffle furnace at 800°C for 45 min. followed by cooling in the furnace. A brown coloured coating was obtained with a reasonable surface adhesion.

MECHANISM:

Borax ($Na_2B_4O_7$) on heating gives boron oxides which reacts with Fe_2O_3 and ZnO to form iron and zinc borate respectively.

xxiv) $3Fe_2O_3 + B_2O_3 \longrightarrow 2Fe_3BO_6$

xxv) $3ZnO + B_2O_3 \longrightarrow 3ZnB_2O_4$

oxides of Al and Si presumably remain unreacted and form the part of the coating. Kevalin clay which has been used as a surfactant, is an alumino silicates. Although X-ray diffraction data do not provide any evidence for the presence of alumino silicates, the coating probably contains iron borate and zinc borate (from reactions xxiv and xxv). Al_2O_3 and TiO_2 as of predominant constituents with silicate of Fe and Al in smaller concentration. The constituents present in the coating as identified by the X-ray diffraction analysis are listed in the Table - 2.2.

The SEM picture (Fig. 2.6a) of the surface of borate coated alloy shows a nearly uniform coating with pores at some

sites. There appear to be at least two phases present in coating: a needle shaped constituent and the second constituent which is trapped in between the needles. The needle shape constituent is probably iron-borate with Al_2O_3 and TiO_2 forming the second phase (Fig. 2.6a). The scanning micrograph (Fig.2.6b) of the cross section indicate a nearly adherent coating. The coating consists of two layers the outer layer is porous and the inner layer which is adjacent to the alloy is relatively compact. The outer layer presumably contains iron borate and the inner layer contains oxides of Fe, Cr, and Ti.

2.4.2 Carbide coating:

Reagents used: SiC, Cr_2O_3, $KMnO_4$, MgO, CaO, CuO and $Zr(NO_3)_2$ used for the preperation of coating, were all reagent grade products.

PROCEDURE:

A slurry was prepared by mixing powdered chemicals in the following amounts: SiC:0.6g; Cr_2O_3:0.4g; $KMnO_4$:0.1g; MgO:0.2g; $Zr(NO_3)_2$:0.8g; CaO:0.2g; and CuO:0.1g with minimal quantity of water.

The specimens were uniformly coated with slurry and dried in air. The coated specimens were then placed in silica boats and were heated in a muffle furnace for 1.5h at 850°C, followed

by slow cooling in the furnace. A greenish black thin film was formed on the specimen with good adhesion.

MECHANISM:

Zirconyl Nitrate decomposes into ZrO_2 and oxides of nitrogen

$$ZrO(NO_3)_2 \longrightarrow ZrO_2 + NO_2 + NO + O_2$$

The evolved oxygen reacts with alloy to form oxides of iron and Cr e.g., Cr_2O_3 and Fe_2O_3. SiC present in the slurry remains unaffected. Thus the coating constitutes SiC matrix in which ZrO_2 and Fe_2O_3 are dispersed. The results of the X-ray diffraction analysis (given in Table - 2.2) confirm the presence of above mentioned constituents in the coating.

Figures 2.7a and 2.7b show scanning electron micrographs of carbide coated alloy. The micrograph of the surface shows needle crystalloids of zirconia and micro crystals of silicon carbide. The coating seems to be uniform with a few voids. The cross-sectional view shows a thick coating with pits and pores, and is nearly adhered to the alloy surface (Fig. 2.7b). The coating film presumably contains ZrO_2 dispersed in carbide matrix.

2.4.3 Chromate coating:

Reagents used: Cr_2O_3, $Al_2(SiO_3)_3$, CaO, NaF, $PbCrO_4$ and boric acid, used for the preparation of coating.

were all reagent grade chemicals.

PROCEDURE:

A yellow coloured slurry is obtained on mixing powdered materials with minimal amount of water. The materials were mixed in the following proportions: Cr_2O_3:23.7%; $Al_2(SiO_3)_3$: 38.46%; $PbCrO_4$:15.4%; CaO:11.85%; NaF:7.7%; Boric acid: 3.86%.

The specimens were covered with thin layers of slurry and dried in air. The dried specimens were kept in silica boats and were heated at 850°C for 2h in a muffle furnace. The heated specimens were then allowed to cool slowly in furnace.

MECHANISM:

At 850°C, the alloy oxidizes to give mainly FeO and Fe_2O_3 with very small amounts of Fe_3O_4. The Cr_2O_3 present in the coating material reacts with oxides of iron to form iron chromates.

xxvi) $FeO + Cr_2O_3 \longrightarrow FeCr_2O_4$

xxvii) $2FeO + SiO_2 \longrightarrow Fe_2SiO_4$

xxviii) $Fe_2O_3 + Cr_2O_3 \longrightarrow Fe_2Cr_2O_6$

Aluminum silicate present in the coating may undergo double decomposition reaction to give iron silicate

xxix) $Al_2(SiO_3) + 2FeO \longrightarrow Fe_2SiO_4 + Al_2O_3$

Thus the coating contains chromate and silicate of iron as major constituents with Fe_2O_3, Cr_2O_3, Al_2O_3 and PbO as minor constituents.

The X-ray diffraction analysis data of the coated specimens (Table - 2.2) indicate the presence of most of the constituents inferred from the above reaction(xxvi to xxix).

Figures 2.8a and 2.8b show SEM pictures of the surface and cross section of the chromate coated mild steel. The coating seems to be highly uniform and most likely contains iron chromate and alumina. The cross-sectional view shows two well defined layers, a nearly uniform outer layer which is porous in nature and probably contains iron chromate. The inner layer which is uniform and compact presumably contains FeO, Cr_2O_3 and Al_2O_3.

CHAPTER - III

WET CORROSION BEHAVIOUR OF INORGANIC COATED 18:8,5 STEEL

CHAPTER - III

WET CORROSION BEHAVIOUR OF INORGANIC COATED 18:8:5 STEEL.

3.1 Introduction:

Steels are coated for variety of reasons including corrosion resistance, wear resistance, lubrication and aesthetic appearance. Electrochemical methods may be used as tools to monitor coating performance, to provide accelerated laboratory tests, to determine the quality of coatings and to investigate the mechanism of corrosion protection.

Open-circuit potential measurements indicate the break down of noble metal coatings on a steel substrate whereas in case of organic coatings such measurements explain rapid and homogenous absorption of water, electrochemical and chemical reactions with pigments, primer and steel substrate[79].

The mechanism of coating break down is investigated with electrochemical techniques. Anodic and cathodic polarisation curves can be used to identify the controlling parameters of dissolution processes. The morphology of attack of steel coated with duplex nickel and a topcoat of chromium was studied by a combination of anodic polarisation

and metallographic examination[80]. Coating deterioration occurred by pit initiation in nickel and microcracks in the chromium topcoat. The attack under cathodic control was decelerated by anodic polarization.

Recently a study[81] has been conducted on the wet corrosion of coated alloys by measuring the rate corrosion of plastic and bitumastic coated pipe section immersed in water, under various conditions of salt concentration, oxygen content and type of metal ion. At the site of coating rupture the rate of corrosion is controlled by the rate of hydrogen ion formation in a cathodic electrochemical reaction.

The dissolution kinetics of zinc alum coated steels have been studied[82] in presence of pthalate buffered sodium chloride solution (pH 5.3). The buffered salt is (about 10 times) more aggressive than the unbuffered salt solution though the same type of attack occurs on coating. The corrosion potential is initially active around 1050 mV vs SCE, which is a characteristic of Zn. After 50 hours a potential transition occurs quite rapidly to values $\sim$ 870 mV which are maintained upto 400 hours when tests were terminated. The present chapter deals with the studies on the electrochemical behaviour of the phosphate, borate, chromate and oxide coated 18:8.5 Cr - Ni steel in presence of aqueous

solutions of mineral acids e.g. HCl, HNO_3 and H_2SO_4.

3.2 Experimental:

The 18:8.5 Cr:Ni steel specimens were annealed, polished and coated with phosphate, borate, chromate and oxide coatings. The details are given in Chapter - II.

The coated and uncoated specimens were immersed in one molar solution of HCl, HNO_3 and H_2SO_4. The corrosion potential experiments were carried out using a wenking potentio state Model ST 72. The cell consisted of Pt counter electrode and S.C.E. as reference. The specimen was mounted in a teflon holder and attached to a stainless steel rod. The electrode were interconnected through a suitable salt bridge.

Corrosion Potential:

The coated and uncoated alloy specimens were immersed in one molar solutions of HCl, HNO_3 and H_2SO_4, for times varying from 120 to 170 hours. The corrosion potentials were recorded at the interval of 30 minutes in the first few hours and later on with the intervals of 2 hours upto 12 hours followed by increasing intervals ranging from 4 to 24 hours upto the end of the corrosion run.

SEM Studies:

The topography of the coated specimens(untreated and treated with acidic solutions) was carried out by scanning Electron Microscopy. The specimens were coated with colloidal silver emulsion and their structures were examined by Cambridge Scanning Electron Microscope Model S_4-10.

3.2.1 General Behaviour of Coatings in the Different Solvents:

The general behaviour of phosphate, borate, oxide and chromate coated as well as uncoated alloy specimens was studied in water, acids, alkalies and organic solvents at ambient temperature. The specimens were completely immersed in liquid for 24 hours and weight gain or loss were recorded The results of 24 hours immersion tests are summarised in table 3.1. The test were also carried out in boiling liquid using 10 minutes time, no loss or gain in weight was observed.

3.3 RESULTS

3.3.1 Corrosion Potential Measurements in HCl:

Potential/time curves for phosphate, borate, oxide and chromate coated alloy as well as uncoated alloy are shown in Fig. 3.1.

In the uncoated alloy, initially for a period of about 12 hours the corrosion potential shifted to a noble direction with a change in potential from 550 to 600 mV. followed by small variation in potentials upto the end of 170 hours. The SEM picture fig. 3.1a showed pits and voids on the surface.

The phosphate coated steel immersed in HCl showed an initial noble shift in corrosion potential followed by a shift in the cathodic direction for a period upto 72 hours. Afterwards the corrosion potential moves toward the more positive direction upto 100 hours and finally a region of constant potential appears for the rest of 144 hours run. From the usual observation and SEM picture fig. 3.1b the coating seemed to remain intact the alloy surface, though some pits and microscopic cracks are found on the coating surface.

Initially, the borate coated alloy in HCl showed a shift in the corrosion potential towards the noble direction followed by shifting to a less noble direction upto a period of 72 hours. Afterwards there was no change in potential during the rest of 120 hours run. The visual examination of the corroded coating indicated the presence of uniform

coating on the surface of the alloy and which appeared to be quite adhered to the alloy surface.

The chromate and oxide coated alloy show little or no change in their corrosion potential. Oxide coated alloy showed a gradual shift in the noble direction after an initial period of 24 hours with a change in potential of the order of 150 mV upto 96 hours followed by the shift to a less noble direction until approaching to the value of initial corrosion potential (550 mV.) at the end of 154 hours run. The SEM pictures (fig. 3.1c & 3.1d) show the presence of pits and voids on the surface of the alloys.

3.3.2 Corrosion potential measurements in HNO_3:

Potential/time curves for uncoated alloy (fig.3.2) exhibits, initially, a small shift in the corrosion potential towards the noble direction for a period of 3 hours followed by a small but sharp shift to the cathodic direction. After 6 hours little or no variation in potential is observed.

Corrosion potential for phosphate, borate, oxide and chromate coated alloy specimens initially shifted in the cathodic direction for the period ranging from 4 to 12 hours. This is followed by no or little variation in potential for rest of the duration of run.

The scanning Electron Micrographs of the surface of HNO_3 - corroded phosphate, chromate and borate coated steel specimens are shown in fig. 3.2a to 3.2f. The phosphate coated steel shows nearly uniform surface with occasional microcracks and pits. The chromate coated alloy indicates the presence of fine pits, and pores on the surface of the coating. The surface micrographs of the borate coated alloy show the presence of 2 phases : hexagonal pellets of iron borates and flake like dispersion of Cr_2O_3.

The oxide coated alloy indicates a shift in initial corrosion potential in the noble direction upto a period of 8 hours followed by a steep fall in potential towards cathodic direction, during a relatively short period of 4 hours. The plot then showed a gradual increase in potential upto a period of 48 hours followed by a sharp increase in potential upto the end of 72 hours. The shape of the curve indicates that a large immersion run would terminate the potential to a value approaching to initial corrosion potential. The topography of the HNO_3- corroded oxide coated alloy shows micropores and cracks along the grain boundaries fig. 3.2g and 3.2h.

3.3.3 Corrosion Potential Measurements in H_2SO_4:

Potential/time plots for coated as well as uncoated alloys are given in fig. 33. The potential/time

plot for the uncoated alloy in H_2SO_4 shows a sharp decrease in potential (to the cathodic direction), during initial period of 12 hours, for the next 72 hours there is little or no change in potential upto 96 hours. The potential then starts increasing till the end of 120 hours run. The scanning electron micrographs of the uncoated alloy fig.3.3a and 3.3b show cracking along the grain boundaries, these channels perhaps provide passage for the acid to further attack the alloys. Potential/time plots for the phosphate, borate and chromate coated alloy specimens show almost no variation in corrosion potential during the period extending from the initial immersion time to the end of 120 hours run. This behaviour anticipates protective nature of phosphate, borate and chromate coatings.

The visual examination of the corroded phosphate, borate and chromate coated alloy indicates uniform coatings with no sign of distortions. However, the S.E.M. fig.3.3c of the borate coated alloy shows crystallites of metallic borate with cracking channels at certain regions of the micrograph, the origin of these cracks on the surface may be attributed to mechanical shocks. Also the possibility of intergranular corrosion can not be ruled out. The chromate coated alloy on the other hand, shows microcracks along the grain boundaries and the surface is covered with pores and

voids (fig. 3.3d and 3.3e).

The oxide coated alloy shows a shift to cathodic direction from the initial stages, these are periods of varying degrees of decrease in potentials upto a period of 120 hours. At the end of run a potential decrease of 450 mV (from 475 mV to 25 mV) is observed. The chromate coated alloy on the other hand, shows microcracks along the grain boundaries and the surface is covered with pores and voids.

3.4 Discussion:

In HCl and HNO_3 solution there is a noble shift in potential followed by a constant potential in HNO_3, but in H_2SO_4 there are small variation in potential (fig. 3.3). It appears that the uncoated alloy forms a film of Cr_2O_3 which becomes passive in HNO_3. Whereas in HCl the Cr_2O_3 film is partially dissolves, in the mean time, uncoated alloy gets oxidized by the dissolved oxygen of the acid and a thin film of Cr_2O_3 is again formed on the alloy surface. This process of dissolution and formation of the film is continuous and an equilibrium is probably never achieved. In H_2SO_4 solution, the uncoated alloy shows an initial cathodic shift followed by periods of constant potential, decreasing and increasing potentials. When the alloy comes

into contact with H_2SO_4 solution in the initial stages, protective Cr_2O_3 partially dissolves and the exposed alloy then reacts with H_2SO_4 to form $FeSO_4$ which is then oxidised to $Fe_2(SO_4)_3$ and goes into solution. Meanwhile the chromium in the alloy is again oxidised to form Cr_2O_3 and the protective film is healed up. This process goes on continuously upto the end of 120 hours run.

The weight loss data and the visual observations given in table 3.2 support the above view point.

The phosphate coated alloy shows protection against H_2SO_4 as indicated by no variation in potential/time plot. In HNO_3 solution, after initial shifting of the potential to the cathodic direction, very small changes in potential are observed though a state of protection is never achieved even after 84 hours immersion. In this case, the initial step involves reduction of HNO_3.

$$HNO_3 \rightleftharpoons HNO_2 + O$$

Subsequently oxygen and the acid penetrates through the phosphate pores and the following reactions are possible at alloy coating interface.

$$4Fe + 3O_3 \longrightarrow 2Fe_2O_3 \text{(I)}$$

$$2Cr + 3O \longrightarrow Cr_2O_3 \text{ (II)}$$

$$Fe_2O_3 + HNO_3 \longrightarrow 2FeO + HNO_3 \quad (III)$$

Once the reaction I, II and III are completed a protective oxide film is formed. However, such a condition is never achieved due to slow dissolution of FeO and Ferric phosphate in HNO_3 which is indicated by small variation in potential.

In HCl, the phosphate coating achieves protection after a relatively long period of about 100 hours. This may be explained on the basis of the following reactions:

$$FeRO_4 \text{ (from coating)} + 3HCl \rightleftharpoons FeCl_3 + H_3RO_4 \quad (IV)$$

$$Fe_2O_3 + 2H_3RO_4 \longrightarrow FeRO_4 + 3H_2O \quad (V)$$

Reaction IV and V help in healing the pores of phosphate film and thus prevent the penetration of HCl through the film which may otherwise dissolve the protective film Cr_2O_3 on the alloy.

The S.E.M. picture of the phosphate coated alloy after 154 hours immersion in HCl shows microcrystals of phosphate on the coating surface.

The borate coating on steel in H_2SO_4 medium seems to be fairly protective as indicated by the nearly horizontal nature of potential/time plot. Table 3.2 shows a weight loss

of 0.3×10^{-3} g/cm^2 in a 120 hours run corresponding to 2.4×10^{-3} g/cm^2 in case of uncoated steel. In HNO_3, the borate coating seems to be disrupted and spalled at a few places, during initial period of immersion. In such a situation the alloy is exposed to the acid and state of passivity is achieved within a relatively short period of 3 hours. The time/potential plot shows a cathodic shift during the time interval of 3 hours followed by a constant potential upto the end of 72 hours run. The changes in potential justify the above mechanism. The S.E.M. picture of borate coated alloy after 72 hours immersion indicates a nearly uniform coating of the iron borate.

The potential/time plot for the borate coated alloy in HCl shows initially a shift in the noble direction upto a period of 12 hours followed by decrease in potential upto 72 hours and finally there is a region of constant Potential upto the end of 120 hours run.

In the initial stages 2 processes take place simultaneously.

(i) dissolution of the borate film in which some of the constituents e.g. Fe_3BO_6 Fe_2O_3 and Cr_2O_3 react with HCl.

CHAPTER - IV

HIGH TEMPERATURE OXIDATION BEHAVIOUR OF INORGANIC COATED 18 Cr - 8.5 Ni STEEL

$$Fe_3BO_6 + 6\ HCl \longrightarrow FeCl_3 + H_3BO_3 + 3\ O \qquad (VI)$$

$$Fe_2O_3 + 6\ HCl \longrightarrow 2FeCl_3 + 3\ H_2O \qquad (VII)$$

HCl penetrates through borate film and reacts with Fe_2O_3 and Cr_2O_3 to form $FeCl_3$ and probably $CrCl_3$. In the second stage the O_2 evolved in reaction VI oxidises the alloy to form protective film and also the borate film is cured by some unknown mechanism. When the reaction in the second stage are completed the borate film provides protection against HCl.

The chromate coating seems to be fairly protective in acid solutions. The curves indicate constant potential almost from the beginning of immersion run in case of HCl and H_2SO_4. The S.E.M. picture of coated alloy after immersion in HCl indicates the presence of a nearly uniform coating of iron silicate which is broken at a few place and underneath crystals of Cr_2O_3 are visible. The 154 hours immersion tests indicate relatively heavy weight losses (13.2×10^{-3} g/cm^2) in HCl corresponding to 4.0×10^{-3} g/cm^2 in H_2SO_4. In HCl, in the initial stages lasting for about 12 hours the $MnCr_2O_4$, $NiCr_2O_4$ and Fe_2O_3 dissolve (from coating) in acid and the acid penetrates through Fe_2SiO_4 film and attacks the alloy, the alloy is also oxidised to Cr_2O_3 from the oxygen present in the acid. It appears that when dissolution of chromate

is completed the coating is automatically healed and becomes protective. The dissolution of chromates and Fe_2O_3 and Fe_2O_3 is also confirmed by the presence of $CrCl_3$ and $FeCl_3$ in the acidic solution analysed after immersion run. In H_2SO_4 solution, though the reaction occurs in similar fashion but is much less severe therefore the weight losses are comperatively very small.

In HNO_3 after dissolution of the coating during the initial period of 12 hours, the acid makes the alloy passive as indicated by the horizontal shape of the potential/time plot. The scanning micrograph indicates a uniform coating of Fe_2SiO_4 particulates on the alloy surface.

The oxide coating does not seem to be protective in acid as indicated by the variations in potential/time plots. In HCl, during first 24 hours the coating is protective as indicated by a constant potential then it shows a shift to noble direction. The same coating in HNO_3 and H_2SO_4 shows regions of increasing and decreasing potentials.

The Fe_2O_3 and $(FeCr)_2O_3$ constituents of the coating dissolve in acid whereas ZrO_2 remains intact. The exposed surface is then attacked by the acid. The slow dissolution of the alloy is also accompanied by simultaneous oxidation of the alloy to form Cr_2O_3 film. The two processes provide variations

in potential.

The S.E.M. picture of the surface of the coated alloy after long immersion in HCl and H_2SO_4 solutions are shown in fig. 3.1a and 3.3f. In HCl the coated alloy show crystals of ZrO_2, the packing of the crystals is not compact and fairly large number of voids are visible. Figure 3.3f shows a S.E.M. picture of high magnification, but showing the same features. The oxide coated alloy in H_2SO_4 shows similar structure as that in HCl, ZrO_2 crystals in the form of needles and clusters can be seen with reasonable distribution of voids.

Thus the S.E.M. studies confirm the findings obtained from potential/time plots and weight loss measurements.

From the corrosion/potential studies following conclusions may be drawn:

i) In HCl, the phosphate coating shows best protection in comparison to uncoated alloy, which has a very poor protection against acid corrosion. The borate coating though much interior to phosphate but is slightly better than uncoated alloy.

ii) Among the coatings, the borate coating offers best protection in H_2SO_4 and its corrosion resistance performance is much better than uncoated steel. Chromate and phosphate coatings though better then steel but are inferior to borate

coating.

iii) In HNO_3, all the coatings are protective to much lesser degrees than the uncoated alloy itself. The uncoated steel attains passivity almost immediately after immersion in the acid.

iv) The chromate coating though shows relatively heavy weight losses in acids but seems to have better protective properties in service conditions involving long periods (say weeks or months) of immersions.

CHAPTER - IV

HIGH TEMPERATURE OXIDATION BEHAVIOUR OF INORGANIC COATED / 8 Cr-8.5Ni STEEL.

4.1 Introduction:

The chromium steels exhibit excellent corrosion resistance in common corrosive environments and also found to have satisfactory performance at moderately high temperatures. However, these alloys do not work satisfactorily at temperatures above 800°C. due to the absence of mechanically strong, uniform and compact protective scales. The scales which are otherwise protective are disrupted due to the decarborisation and uninterrupted growth of wustite (FeO) at high temperatures. The arrest of carbon in the form of metallic carbide, by the addition of carbide forming elements, is a probable means to decrease oxidation rates. The growth of wustite can also be restricted by the formation of spinels such as $FeO.Cr_2O_3$ or $FeO.Al_2O_3$ [37-38].

An interesting aspect of oxidation chemistry of iron-base alloys which is hitherto not yet been explored is the study of the oxidation behaviour in presence of inorganic coatings. The studies on some inorganic coatings on steel, which have been described in chapter III, indicate better corrosion resistance of coated alloy in mineral acids.

This chapter deals with the studies on the oxidation behaviour of some inorganic coated steel. 18 Cr - 8.5 Ni steel (AISI303) was coated with phosphate, silicate, borate, chromate, and oxide, and its oxidation behaviour was studied in air at temperatures ranging from 400 - 1000°C.

4.2 Experimental:

AISI 303 Steel (18Cr - 8.5 Ni) was coated with thin films of phosphate, silicate, borate, chromate and oxide. The preparation of these coatings and the methods of their application on surfaces of the alloy are described in detail in chapter II. The oxidation behaviour of inorganic coated and uncoated specimens was studied at 4 different temperatures viz., 400, 600, 800 and 1000°C in a limited supply of air.

The kinetics measurements were carried out by using a laboratory fabricated thermal balance with a sensitivity of ± 0.5 mg (Fig. 4.1). In case of phosphate, silicate, and borate coated alloy oxidation runs of 4 h durations were carried out whereas in case of oxide and chromate coated alloy the duration of the runs was 8h. Parallel runs were carried out with the uncoated alloy specimens under identical conditions.

4.3 Results:

The high temperature oxidation studies of the phosphate, silicate, borate, oxides and chromate coated alloy

were carried out in the temperature range of 400 - 1000°C in a limited supply of air. The oxidation runs were usually of 4 to 8h durations.

4.3.1 Phosphate coating: Figures 4.2a to 4.2d present weight gain vs time plots for the oxidation of phosphate coated steel at 400, 600, 800 and 1000°C respectively. The plots for the uncoated specimens oxidised under similar conditions are also given. In the temperature range 400 - 800°C, the weight gain/time plots seems to follow a parabolic rate law in both the uncoated and coated conditions. In this temperature range, the phosphate coated alloy has slightly lower oxidation rates than the uncoated alloy. At 1000°C, the coated alloy shows an approximately parabolic behaviour, although in case of uncoated alloy a loss in weight is observed which may be attributed to spalling. The weight gain^2 /time plots for coated and uncoated alloys are given in Fig. 4.3a to 4.3c. The plots for the temperatures: 400°, 600° and 800°C are nearly linear. The values of parabolic rate constants for phosphate coated and uncoated alloys at these temperatures are listed in Table-4.1. The activation energies of the oxidation are 2.80 x 10^3 cal/mole and 2.84 x 10^3 cal/mole. for phosphate coated and uncoated alloys, respectively.

4.3.2 Silicate coating: The weight gain vs. time plots for the oxidation of silicate coated and uncoated alloys are shown

in figs. 4.4a to 4.4d. In the temperature range of 400 - 800°C, it appears that the coated alloy oxidizes by a linear rate law, indicating an uninterrupted growth of oxides, but the uncoated alloy oxidizes by a parabolic rate law. At 800 and 1000°C the plots indicate relatively heavy weight losses. Surprisingly, the losses at 800°C are much higher than at 1000°C. The shape of the weight loss curve at 800°C shows some typical features of an alloy undergoing scale rupture followed by rapid oxidation due to exposure of the fresh alloy to the oxidising gas. At 1000°C lower weight losses presumably indicate quicker healing of the scales after rupture. The values of linear oxidation rates of the coated alloy are given in Table - 4.1.

4.3.3 Borate coating: Figures 4.5a to 4.5d represent weight gain vs. time plots for the borate coated and uncoated alloys. At 400, 600 and 800°C, the plots are approximately parabolic. The coated alloy shows comparatively higher oxidation rates as compared to uncoated alloy. At 1000°C a weight loss is observed in the first three hours of the oxidation run, followed by a weight increase with increasing time. The weight gain^2/time plots for coated and uncoated alloys are given in figs. 4.6a to 4.6d respectively. The values of activation energy for the borate coated and uncoated alloys are 1.3×10^3 cal/mole and 2.8×10^3 cal/mole, respectively. The values of the parabolic rate constant for the coated alloy are summarised in Table - 4.1.

4.3.4 Oxide coating: The weight gain vs. time plots for the oxide coated and uncoated alloys at 600, 800 and 1000°C are given in figs. 4.7a to 4.7c respectively. In the temperature range of 400 - 800°C the oxide coated alloy follows approximately a parabolic rate law. Upto 600°C the oxidation rates of uncoated alloy are lower than that of coated alloys but at higher temperature (above 600°C) an opposite behaviour is observed. At 1000°C, coated alloy follows nearly linear rate law, thus indicating uninterrupted oxidation due to the formation of non-protective oxide film. The values of parabolic rate constants for the coated and uncoated alloys are given in Table - 4.1 and the weight gain^2/time plots are given in figs. 4.8 a and 4.8b.

4.3.5 Chromate coating: The weight gain vs. time plots for coated and uncoated alloys at 400, 600, 800 and 1000°C are given in figs. 4.9a to 4.9d respectively. In the temperature range of 400 - 800°C, the coated and uncoated alloys follow a proximate parabolic rate law. The oxidation rates of coated alloy are much lower than that of uncoated alloy. The weight gain/time plot of the coated alloy oxidized at 800°C shows parabolic behaviour upto 6h, subsequently there is rapid increase in weight signifying a break away oxidation. Similar behaviour is observed at 1000°C when the weight gain/time plot after 4h indicates very rapid oxidation typically of break away or catastrophic types of oxidation. The weight gain^2/time plots

of the coated and uncoated alloy are shown in figs 4.10a to 4.10f.

4.4 Discussion:

The oxidation behaviour of 18 : 8.5 Cr : Ni (303) steel has been investigated in air in presence of a variety of inorganic coatings, viz., phosphate, borate, silicate, chromate and oxide. Figure 4.11 shows a plot of oxidation rate constant vs temperature for the various coated alloys. The oxidation kinetics of the coated alloy reveal some interesting information regarding the oxidation resistance of the different coatings. Except silicate coated alloy, all the coated alloys as well as uncoated alloy exhibit parabolic behaviour in the temperature range of 400 - 800°C. The silicate coated alloy oxidizes by a linear rate law. Phosphate coated steel oxidizes by a parabolic rate law up to a temperature of 1000°C, whereas other coated alloys (including silicate) and uncoated steel oxidize by a linear rate law at this temperature.

In the temperature range of 400 - 1000°C, the comparative oxidation resistance of the various coatings is as follows: (in order of decreasing corrosion resistance

400°C: chromate $>$ phosphate $>$ oxide $>$ uncoated $>$ borate $>$ silicate

600°C: chromate $>$ phosphate $>$ oxide $>$ uncoated $>$ borate $>$ silicate.

800°C: chromate > uncoated > borate > oxide > phosphate > silicate.

1000°C: phosphate > uncoated > oxide > chromate > silicate ≈ borate.

The oxidation resistance sequence indicates that chromate, phosphate and oxide coatings could prove protective coatings against oxidation in the temperature range of 400-600°C. Chromate coated alloy has better corrosion resistance at 800°C compared to other coatings including uncoated alloy. At 1000°C phosphate coated steel has superior corrosion resistance than the uncoated steel.

The good performance of phosphate coating may be attributed to the presence of compact and adhered coating of phosphate with $FePO_4$ and Fe_2O_3 as the major components. This compact coating is mechanically stable at high temperature, provide healing effect to the protective spinel Cr_2O_3:FeO film at the oxide/alloy interface. The chromate coating is also thermally stable at temperature upto 800°C, the major constituents of the coating: $ZnCr_2O_4$ and $NiCr_2O_4$ provide assistance in the formation of protective layers of $FeO.Cr_2O_3$ and $NiO.Cr_2O_3$. It appears that the outer layers of Fe_2SiO_4 and $MnFe_6O_7$ remain unaffected during oxidation and provide an adhered, mechanically stable coating which is oxidation resistance.

CHAPTER - V

HOT CORROSION BEHAVIOUR OF INORGANIC COATED 303 STEEL.

CHAPTER - V

HOT CORROSION BEHAVIOUR OF INORGANIC COATED 304 STEEL.

5.1 Introduction:

Gas corrosion of metals assumes particularly violent forms in gasturbines used in marine or aircrafts or in land based power generating units. Gas turbine blades, valves and other components are deposited with ash or salt deposits when come into contact with fuel combustion gaseous environment at high temperatures. These deposits liquify and interact with alloy to produce an accelerated type of oxidation which is universally known as hot corrosion. The deposits are predominently composed of Na_2SO_4, but may also contain sulfates of K, Ca & Mg, NaCl, V_2O_5 etc. The corrosion products are usually molten sulfides or molten oxides or the mixture of both. The hot corrosion usually proceeds by a two stage mechanism . initiation stage and the propagation stage. In initiation stage, the alloy forms a protective oxide film and this is followed by a propagation stage in which the unprotective scales are formed and the degradation of the corrosion products is rapid. The duration of initiation stage depends upon several factors such as nature of the deposit, composition of the gases, composition of the alloy, velocity of gases, rate of deposition etc.[83].

Various mechanism have been proposed to explain hot corrosion attack. Direct sulfidation was the earliest which was proposed by Simon et al[84] to explain fire-side corrosion in boilers. It involves reduction of sulfate into sulfur by a reducing agent (such as carbon) followed by sulfidation. At present acid and basic fluxing are the two popular mechanisms which have been used to explain hot corrosion attack. In basic fluxing, the sulfur released from Na_2SO_4 sulfidises the alloy component. On the other hand the O^{2-} released forms metal oxide ions which dissolve in the molten sulfate. The metal oxide ions such as $CrO_4^{=}$, AlO_2^{-}, $NiO_2^{=}$ etc. are reprecipitated as oxide at alloy/salt interface. In this way the fluxing is strongly dependent upon the amount of the deposited salt. The presence of oxides of MoO_3, WO_3 etc. brings about acid fluxing. In acid fluxing the solubility of alloy oxide. For example, Al_2O_3 in Na_2SO_4 is modified by second oxide from alloy such as MO_3 and we have AlO_4 enriched Na_2SO_4. And finally oxide Al_2O_3 is precipitated from solution due to loss of MO_3 from Na_2SO_4 which permits substantial attack with small amount of Na_2SO_4[85-86].

Nickel and cobalt base superalloys (Nimonic, Inconel, Udimet, Hastealloy B 1900 etc.) are the common alloys. Used for the hot corrosion resistance purposes, all the alloys more or less are subjected to corrosion depending upon severity of corrosion environment. It is generally agreed that high concen-

tration (more than 15%) of Cr in alloy are always essential for good corrosion resistance. Cobalt base alloys though are of comparatively inferior high temperature strength than to nickel base alloys, but are superior with respect to their hot corrosion resistance. Whether the superior corrosion resistance of cobalt base alloys is due to cobalt matrix or due to high chromium in the alloy is still disputed but cobalt base alloys indeed have high-chromium contents.

The fact that cobalt or nickel base superalloys to some extent are subjected to corrosion leads turbine manufacturers to think in terms of coated alloys. Nowadays all manufacturers use coated superalloys which under service environment provide protective oxide layer on the alloy components. The earliest coatings used were obtained by inter diffusion of Al with the alloy to form layers consisting mainly of intermetallic compounds such as NiAl or CoAl. These coatings at high temperatures provide protective alumina scales[87].

Diffusion coating[88] with Cr, Al, Si and Al - Si on heat resistant superalloys had been invostigated as early as 1962. Samples coated with Si showed highest stability at 730°C in air, in contact with ash containing 10 and 41.6% V_2O_5. Except Si coating all other coatings disintegrated due to penetration of corrosion medium through the coating to the alloy surface with resulting oxidation at diffusion interface. In silicon

coating there was no penetration, inspite of some decrease in coating thickness. In all cases introduction of $SO_2 + H_2O$ into corrosion environment has no or little effect. On corrosion rate. Diffusion coating with Al + Si has a lower corrosion resistance than coating of each of the elements specially during 40 cycles of cooling from 730 to 20°C (15-20 min).

Besides protecting alloys from salt depositing environments, the diffusion coatings can also be used for protection against other environments. For example, an aluminum coating protects steels from sulfur corrosion. Diffusion coatings obtained by aluminizing is twice more slowly corroded in H_2S atmosphere. The corrosion rate of protective coated alloy steel in the same environment is two order of magnitude lower that of uncoated alloy. Protective coating on 18:8 steel reduces sulfur corrosion rate over 300 times[37].

The chromium steels exhibit good oxidation resistance in temperatures ranging from low temperatures to moderately high temperature (upto 600°C) due to the formation of protective Cr_2O_3 film. However, these steels undergo rapid oxidation in presence of fused salt deposits e.g., Na_2SO_4 due to hot corrosion attack. As mentioned above in presence of diffusion coating of Al on chromium steels, the corrosion rates are lowered by several order of magnitude in sulfur containing environments. A survey of literature indicates that no work has yet been done on the

hot corrosion behaviour of inorganic coated steels.

The work described in this chapter deals with the hot corrosion behaviour of inorganic coated steel in presence of ionic salts viz., Na_2SO_4, NaCl and Na_2CO_3. The 18:8.5 Cr:Ni steel specimens have been coated with thin films of phosphate, silicate, borate, chromate and oxide, and their hot corrosion behaviour has been studied in the temperature range 700-1000^{o}C.

5.2 Experimental:

18 Cr : 8.5 Ni steel (AISI 303) specimens were cut from the sheets and prepared for coatings. Steel specimens were coated with thin films of phosphate, silicate, borate, chromate and oxide. The details of specimens preparation and coating procedures have already been described in chapter II. The steel specimens of 2.5 x 8 x 0.5 cm dimensions were sprayed with saturated solutions of NaCl, Na_2SO_4, Na_2CO_3 and mixtures of NaCl + Na_2SO_4 (1:1) Na_2SO_4 + Na_2CO_3 (1:1) and NaCl + Na_2CO_3 (1:1). During spraying utmost care was taken to have a nearly uniform coating at all the faces of the specimens. The sprayed specimens were then left for complete drying and then weighed. In general, the specimens had salt coatings of about 5 mg/cm^2. The weighed specimens were placed in silica boat and then transferred to a horizontal tubular furnace set at the desired temperature. The corrosion runs were limited to a

period of 6h. After completion of the run, the specimens were taken out, cooled in a desiccator and weighed. The hot corrosion studies were carried out at four different temperatures viz., 700, 800, 850 and 1000°C.

5.2.1 X-ray diffraction analysis: X-ray diffraction patterns of the powdered materials were obtained by using a Debye-Scherrer camera. In some cases a diffractometer was also used. The constituents identified by X-ray diffraction technique are listed in Table - 5.1.

5.2.2 Metallographic studies: A Leitz photographical metallurgical microscope, attached with a plate camera as well as a 35 mm Yashika FX-2 camera, was used for metallographic studies.

5.2.3 S.E.M. studies: A cambridge Electron Scanning Microscope model S_4-10 was used for the S.E.M. studies. The specimens were coated with colloidal silver emulsion before examining through scanning microscope.

5.3 Results:

5.3.1 Hot corrosion behaviour: The hot corrosion behaviour of AISI 303 steel, coated with films of phosphate, silicate, borate, chromate and oxide, was studied in presence of Na_2SO_4, NaCl, and Na_2CO_3 in the temperature range of 700-1000°C. The coated and uncoated specimens were sprayed with nearly saturated

solutions of NaCl, Na_2SO_4 and Na_2CO_3 and mixtures of NaCl and Na_2SO_4 NaCl and Na_2CO_3, and Na_2SO_4 and Na_2CO_3 such that uniform coatings containing about 5 mg/cm^2 of the salt(s) were obtained The samples were placed in silica boats and were heated in a limited supply of air for 6h.

Figures 5.1a to 5.1e show weight gain vs temperature plots for the coated steel specimens in presence of Na_2SO_4, NaCl and Na_2CO_3 and their mixtures, NaCl + Na_2SO_4, NaCl + Na_2CO_3, Na_2SO_4 + Na_2CO_3 and in the temperature range of 700 - 1000°C. Each plot indicates weight gains during 6h corrosion run at 4 different temperatures; 700, 800, 850 and 1000°C. for a particular coating and in presence of an ionic salt(s) film. The plot also indicates weight gains for an uncoated alloy hot corroded in nearly identical conditions.

5.3.1.1 Behaviour in Na_2SO_4: At 700°C, an appreciable increase in weight is observed in all the five coatings. During a 6h corrosion run, the pattern of weight gain in different coatings at this temperature, is as follows (g/cm^2) oxide (0.00013) phosphate (0.00023) chromate (0.0004) silicate uncoated (0.0008) silicate (0.0047) borate (0.0723).

The above sequence indicates that oxide, phosphate and chromate coated alloys have lower corrosion rates than the uncoated alloy, and the borate coated alloy has the highest

corrosion rate at 700°C.

At 800°C, the weight gains in phosphate and oxide coated alloys are nearly the same ($\simeq$ 0.0008 g/cm^2) and similar to those of uncoated alloy. While comparing the weight gains at 700°C with those at 800°C it is noted that the increase in weight gain values at 800°C is much higher in case of phosphate and oxide coated alloy compared to uncoated alloy where there is no or very little change in weight gain. The weight gain values for borate and silicate coated alloys at 800°C are considerably lower than the corresponding values at 700°C. The chromate coated alloy shows a weight loss at 800°C.

The phosphate and chromate coated alloy specimens show weight losses at 850°C whereas silicate and oxide coated alloys show weight gains of 0.0144 g/cm^2 and 0.0068 g/cm^2 respectively at this temperature. The corresponding weight gain for uncoated alloy is 0.0014 g/cm^2.

At 1000°C the oxide and chromate coated alloys show appreciable increase in weight though the chromate coated alloy indicates weight losses at lower temperatures (800 and 850°C). At this temperature (1000°C) the uncoated alloy has a lower weight gain (0.0014 g/cm^2) than the oxide coated alloy (0.0094) but, much higher than the chromate coated alloy (0.0005 g/cm^2). The

results indicate that in presence of Na_2SO_4, the chromate coating is most effective for corrosion protection purposes at 1000°C, compared to other coatings.

5.3.1.2 Behaviour in Na_2CO_3: The temperature/weight gain plots for 303 steel under a thin coating of Na_2CO_3 show largest weight gains at 800°C for borate and phosphate coated alloys, on the other hand, the silicate and chromate coated alloy indicates minimum weight gains at 800°C. In oxide coated alloy after a minimum weight gain (or maximum weight loss) upto 850°C, there is again increase in weight at 1000°C, the weight gains at this temperature are higher then at 800°C. The uncoated alloy behaves like phosphate and borate coated alloy at 1000°C. A comparison of the weight gain values (g/cm^2) for different coatings under Na_2CO_3 film at 800°C shows the following sequence:

oxide (0.00085) < silicate (0.0009) < uncoated (0.0014) < phosphate (0.0048) < borate (0.0066)

The sequence indicates that oxide and silicate coatings have slightly better corrosion resistance in comparison to uncoated alloy in presence of Na_2CO_3.

5.3.1.3 Behaviour in NaCl: In presence of NaCl, phosphate and silicate coated alloys show maximum weight gains at 800°C. The oxide coated alloy and uncoated alloy behave similarly, there is a sharp increase in weight from 700 - 800°C followed by slow increase upto 1000°C. The borate and chromate

coated alloys show exceptional behaviour in the respect that they showed minimum weight gains at 800°C. Only borate (0.001 g/cm^2) and oxide (0.0032 g/cm^2) coated alloys have lower oxidation rates than the uncoated alloy (0.0046 g/cm^2) at 800°C.

5.3.1.4 Na_2SO_4 and NaCl: In presence of a thin film of 1:1 mixture of Na_2SO_4 and NaCl, the phosphate, borate and silicate coated alloy indicates maximum weight gain at 800°C. The table which is given below, summarises the weight gain values of the different coatings at 800°C in presence of Na_2SO_4 NaCl and Na_2SO_4 + NaCl.

Table: Weight gain values (g/cm^2) after 6h corrosion run at 800°C.

Coatings	Na_2SO_4	NaCl	Na_2SO_4 + NaCl
Phosphate	0.0076	0.017	0.006
Silicate	0.0029	0.0223	0.013
Borate	0.0280	0.0010	0.023
Uncoated	0.00076	0.0046	0.0076

In presence of Na_2SO_4 and NaCl mixture, the phosphate coated alloy shows lowest weight gain amongst the three coatings; in this case the weight gain is also lower than the corresponding values, in presence of Na_2SO_4 and NaCl. In presence of Na_2SO_4 and NaCl mixture, silicate and borate coated alloys have weight

gain values lower than the corresponding values obtained in presence of NaCl and Na_2SO_4, respectively. In case of uncoated alloy, the weight gain value, in presence of Na_2SO_4 and NaCl mixture, is higher than the corresponding values in presence of Na_2SO_4 and NaCl. The former is higher than that obtained for phosphate coating but much lower than the corresponding values for silicate and borate coatings.

5.3.1.5 Na_2CO_3 and NaCl: The weight gain/temperature plots for the coated alloys, under a thin film of 1:1 mixture of Na_2CO_3 and NaCl, indicate highest weight gains at 800°C in all but the chromate coated alloy. The weight gain values for the uncoated alloy at 800°C indicates lowest weight increase among all the coatings. Table summarises the weight gain data for different coatings in presence of Na_2CO_3, NaCl and a 1:1 mixture of Na_2CO_3 and NaCl at 800°C

Table: Weight gain data for different coatings after 6h hot corrosion run at 800°C(g/cm^2).

Coatings	Na_2CO_3	NaCl	Na_2CO_3+NaCl
Phosphate	0.0048	0.0170	0.00006
Silicate	0.0009	0.0223	0.0215
Borate	0.0066	0.0010	0.0210
Oxide	0.00085	0.0032	0.0019
uncoated	0.0014	0.0046	0.0013

The data in table indicate lowest weight gains in phosphate coated alloy in presence of Na_2CO_3 and NaCl mixture, whereas borate coated alloy has highest weight gain while comparing with the weight gain data in presence of NaCl and Na_2CO_3 separately. The uncoated alloy has lower weight gain in presence of the mixture of Na_2CO_3 and NaCl than $NaCO_3$ and NaCl alone but this value is only very slightly lower than that from Na_2CO_3. In oxide and silicate coated alloys the addition of Na_2CO_3 in NaCl decreases the corrosion rate considerably.

5.3.1.5 Na_2CO_3 and Na_2SO_4: The behaviour of phosphate and silicate coated alloy in (Na_2CO_3 + Na_2SO_4) is similar to that in Na_2CO_3 + NaCl. In general, the coated alloys show highest corrosion rates at 800°C. The uncoated alloy also shows maximum weight gain of 0.005 g/cm^2 at 800°C corresponding to 0.019 and 0.00076 for phosphate and silicate coated alloy respectively. The borate coated alloy shows weight losses at all the temperatures above 700°C. The oxide coated alloy shows weight losses upto a temperature of 800°C followed by a continuous weight gain upto 1000°C. The chromate coated alloy shows a continuous weight loss upto 850°C, followed by weight increase at higher temperatures. The following table summarises the weight gain data for the coated and uncoated alloy in presence of Na_2CO_3, Na_2SO_4 and 1:1 mixture of Na_2CO_3 and Na_2SO_4 at 800°C.

Table : Weight gain data for the different coatings after 6h corrosion run at 800°C (g/cm^2).

Coatings	Na_2CO_3	Na_2SO_4	$Na_2CO_3 + Na_2SO_4$
Phosphate	0.0048	0.00079	0.019
Silicate	0.0009	0.0029	0.00076
Borate	0.0066	0.028	0.005
Oxide	0.00085	0.0008	0.00085
Chromate	0.0008	0.0008	0.0009
Uncoated	0.0014	0.00076	0.005

At 800°C, the behaviour of phosphate coated and uncoated steel is similar in the respect that both have higher corrosion rates in presence of Na_2CO_3 and Na_2SO_4 but lower than the mixture of Na_2SO_4 and Na_2CO_3.

5.3.2. Morphological studies:

5.3.2.1 Uncoated alloy:

(a) Na_2SO_4 - Figure 5.2a shows a photomicrograph of the 18:8.5 Cr:Ni steel hot corroded in presence of a thin film of Na_2SO_4 at 800°C. The micrograph indicates deep penetration of the salt along the grain boundaries of the alloy resulting in the dissolution of some of the metal. The scale is separated from the alloys presumably due to polishing artifacts.

The porous scale consists of fairly uniform thick white layer of ($FeS.Cr_2S_3$) and outer layer contains FeS in which incorporation of grey FeO could be seen.

(b) NaCl - Figure 5.2b shows photomicrograph of the corroded alloy in presence of NaCl at 800°C. The alloy is again separated from the scale due to polishing artifacts. The inner thin scale presumably contains $FeCl_3$ and outer scale contains Fe_2O_3 with dispersion of Cr_2O_3. NaCl is penetrated through the pores of the oxide scale and forms $FeCl_3$ at the metal/oxide interface. NaCl is also penetrated along the grain boundaries and dissolved outer layer of the metal.

(c) Na_2SO_4 + NaCl - The 18:8.5 Cr:Ni steel corroded in presence of 1:1 mixture at 800°C. (Figure 5.2c)shows thick scales containing two distinct layers. The inner most layers contain mixtures of Cr_2S_3, FeS and some NiS. The outer layer is porous and contains Fe_2O_3 admixed with $NiCr_2O_4$. There is evidence of internal sulfidation: The surface layers of the alloy show presence of iron and chromium sulfides (Fig. 5.2d).

5.3.2.2 Phosphate coating:

(a) Na_2SO_4 - Figure 5.3a shows photomicrograph of phosphate coated 18:3.5 Cr:Ni steel corroded under a thin film of Na_2SO_4 at 800°C. There is some penetration of the salt inside the metal resulting in its dissolution. The scale consists of white ($FeS.Cr_2S_3$) with incorporation of grey FeO.

The scanning electron micrograph Fig. 5.3b of the corroded specimen shows similar features as observed in optical micrograph. There appears to be 3 layered scale; the inner white layer containing ($FeS.Cr_2S_3$); middle grey layer containing FeO with small contamination of Cr_2S_3 and probably NiS. The outer most white layer has Fe_2O_3 admixed with Fe_3O_4 The SEM picture (fig. 5.3a) at higher magnification shows thick white layers of $FeS.Cr_2S_3$ with grey FeO inclusions.

(b) NaCl - Figure 5.4a shows SEM picture of phosphate coated alloy corroded in presence of NaCl at 800°C. The inner portion of the scale consists of a thick uniform layer of grey colour with white inclusion this is presumably Cr_2O_3 with inclusion of $FeCl_3$, the outer scales are in the form of layers containing Fe_2O_3 (white) and Fe_3O_4(light). The high magnification SEM picture (fig. 5.4b) shows the structure of scale consisting $FeCl_3$(white) and Cr_2O_3 (grey) constituents. The photomicrograph (fig. 5.4c) of NaCl - corroded phosphate coated alloy shows mostly the features, which have been observed in the SEM picture. Penetration of the salt at the surface of alloy is clearly visible and this could have resulted in the formation of $FeCl_3$ in the form of white constituent. $FeCl_3$ is also associated with Cr_2O_3 (grey) in the inner most layer. The outer most layer contains Fe_2O_3 as white streak which contains Fe_3O_4 in the form of light inclusion.

(c) Na_2SO_4 + NaCl - The photomicrograph (fig.5.4d) of the phosphate coated steel corroded in the presence of Na_2SO_4 NaCl shows deep penetration of the salt along the grain boundaries. The alloy is seperated from the scale due to polishing artifacts. The detached thick scale contains inner white cluster containing $FeS.Cr_2S_3$ and outer porous scale probably consists of Fe_2O_3 with FeS inclusions.

5.3.2.3 Silicate coating:

(a) Na_2SO_4 - The photomicrograph (fig. 5.5a) of the Na_2SO_4 induced corroded silicate coated alloy shows slightly seperated white inner layers containing ($FeS.Cr_2S_3$) middle layer of Al_2O_3 (from coating) and outer layers of Fe_2SiO_4 (light) and Fe_2O_3(white outer most). The SEM picture (fig. 5.5b) of the corroded alloy shows deep penetration of the salt into the alloy along the grain boundaries.

(b) NaCl - The SEM picture (fig. 5.5c) of the silicate coated steel corroded in presence of NaCl at 800°C, indicates inner stratified layers of Al_2SiO_5 with probable inclusions of $FeCl_3$. The outer most scale which appears in the form of thick uniform and adhered layer presumably contains $Fe_2O_3.SiO_2$. There is some evidence of penetration of the salt through grain boundaries. The photomicrograph (Fig. 5.5d) of the corroded alloy shows the presence of a second phase in the

matrix. This is probably due to the precipitation of graphite as the second phase.

(c) Na_2SO_4 + NaCl - The photomicrograph (fig.5.5c) of alloy corroded in presence of Na_2SO_4 + NaCl shows indication of internal sulfidation involving the formation of FeS and Cr_2S_3. The scales which are detached from the alloy surface due to polishing artifacts, contain $FeS.Cr_2S_3$ (white) incorporated with FeO (grey).

5.3.2.4 Borate coating:

(a) Na_2SO_4 - The SEM picture (fig.5.6a) of the Na_2SO_4 induced corroded borate coated steel shows a very thin uniform inner most layer consisting of Cr_2S_3 followed by a relatively thick middle layer containing FeS and (Fe, Ni) S_2. The outer most layer contains Fe_2O_3 and $CrBO_3$. The alloy matrix shows presence of needle shaped second phase which is presumably containing borides of iron and nickel. The presence of those constituents have been identified by X-ray diffraction analysis.

(b) Na_2SO_4 + NaCl - The photomicrograph (fig.5.6b) of the borate coated alloy hot corroded in presence of 1:1 mixture of Na_2SO_4 and NaCl shows inner most scale in the form of a white thin layer presumably containing $FeS.Cr_2S_3$ with FeO (grey) inclusions. The outer most scale probably constitutes Fe_2O_3 and $CrBO_3$.

5.3.2.5 Chromate coating:

(a) Na_2SO_4 - The chromate coated alloy corroded in presence of a thin Na_2SO_4 film shows thick multilayered scales in its photomicrograph (fig.5.7a). The scales are separated from the

inner one probably due to the polishing artifacts. The multi-layered inner scale contains Cr_2S_3 followed by porous scales of FeS and Cr_2S_3 and the outer most relatively thick scales of mixture containing Fe_2SiO_4, $PbFe_4O_7$ and Fe_2O_3.

The SEM picture (fig.5.7b) of the corroded alloy shows features similar to those observed in the photomicrograph of the same alloy. The inner scale, which is uniform contains Cr_2S_3, is separated from the outer scale by a small gap. The inner portion of the outer porous scale contains FeS and Cr_2S_3 followed by a thick layer containing Fe_2SiO_4, $PbFe_4O_7$ and Fe_2O_3. The latter appears in the form of anouter most thin layer.

(b) NaCl - Figure 5.7c shows SEM picture of chromate coated alloy, corroded in presence of NaCl at 850°C. The alloy is detached from the scales as indicated by a cleavage in the picture. The inner most scale presumably contains Cr_2O_3 followed by a thicker middle layer largely comprising of $FeO.SiO_2$ spinel; $PbFe_4O_7$ forming the outer most layer, appears in the form of distinct strips.

The photomicrograph (fig.5.7d) of the alloy shows detached multilayered scale. The grey inner layer comprises of Cr_2O_3 with white streaks as $FeCl_3$ inclusions, this is followed by a thicker white scale presumably containing Fe_2SiO_4. The outer most layer in the scale most likely contains $PbFe_4O_7$, which appears in the form of a dark band. The alloy matrix also shows evidence of penetration of the salt through grain boundaries.

(c) Na_2SO_4 + NaCl - The photomicrograph (fig. 5.7e) of the chromate coated steel corroded at 850°C in presence of 1:1 mixture of Na_2SO_4 and NaCl is detached from the alloy due to polishing artifacts. The inner grey colour scale is in the form of a band comprising of Cr_2S_3, at the outer ridges of this band there is a white thin discontinuous layer in the form of a hair line, which is $FeCl_3$, the outer most thick porous layer contains Fe_2SiO_4 with FeS and Cr_2S_3 inclusions.

5.3.2.6 Oxide coating:

(a) Na_2SO_4 - Figure 5.8a shows a micrograph of oxide coated alloy corroded in presence of thin film of Na_2SO_4 at 800°C. The scale though looks adhered to the alloy but detached at some places. The inner grey scale presumably contains Cr_2S_3 with some FeS; the outer scale is probably comprised of ZrO_2 in which Fe_2O_3 is incorporated. The SEM picture of the alloy (fig. 5.8b) shows a thin inner most grey scale adhered to the alloy matrix probably containing Cr_2S_3, this is separated from a thick light scale by a gap. The thick scale is that of ZrO_2 in which some Fe_2O_3 is incorporated. Figure 5.8c shows the micrograph of the corroded alloy at 1000°C. There appears to be internal sulfidation deep inside the alloy. The light discontinuous scale comprises of a mixture of white FeS with grey Cr_2S_3 inclusions.

(b) NaCl - The NaCl induced corroded oxide coated alloy (fig. 5.8d) contains scales which comprise of an inner layer of Cr_2O_3 (grey) with $FeCl_3$ as white inclusions (at the outer periphery) this is followed by an outer scale of ZrO_2 with Cr_2O_3, NiO and FeO inclusions.

(c) Na_2SO_4 + NaCl - The metallograph (fig. 5.8e) of the oxide coated alloy corroded in presence of Na_2SO_4 and NaCl mixture shows scales in the form of widely separated bands The inner scale comprises of $FeO.Cr_2S_3$ and the outer scale probably contains ZrO_2 in which there are sulphide inclusions.

5.4 Discussion:

The hot corrosion behaviour of phosphate, silicate, borate, chromate and oxide coated 18:8.5 Cr:Ni austenitic steel has been studied in presence of a thin film of ionic salts e.g., Na_2SO_4, NaCl, Na_2CO_3 and 1:1 mixtures of NaCl and Na_2SO_4, Na_2SO_4 and Na_2CO_3 and a NaCl and Na_2CO_3. The hot corrosion was carried out in the temperature range of 700 - 1000°C, selecting 4 temperatures viz., 700, 800, 850 and 1000°C, for the study. The hot corrosion runs were usually of 6h durations.

The temperature/weight gain plots for 6h corrosion runs indicate sever attack due to hot corrosion in the coated as well uncoated alloys. A number of generalisations emerge from the

analysis of the weight gain data from the hot corrosion studies at different temperatures:

I) In general, the hot corrosion rates are highest at 800°C in the temperature range of 700 - 1000°C although in some cases rates are slightly higher at 1000°C.

II) In a few cases instead of weight gains, weight losses are observed. This is true particularly with chromate coatings at temperatures above 700°C. The weight loss may be attributed to the vaporization of volatile metal halides e.g., $ZnCl_2$ (b.p. 732°C), $FeCl_2$ (m.p. 670°C sublimation) and $CrCl_3$ (m.p. 947°C sublimation) which are formed during interaction with NaCl.

III) In presence of Na_2SO_4 and the mixture of Na_2SO_4 and NaCl, the phosphate coated alloy displays best performance amongst all the coated alloys. The corrosion rates are either lower than those of uncoated alloy or at least of nearly the same values.

IV) Borate and oxide coated alloys have lower corrosion rates in NaCl than the uncoated alloy in similar conditions.

V) In general, the corrosion rate of the coated alloys in presence of NaCl are much higher (at least one order of magnitude) than in presence of Na_2SO_4 or Na_2CO_3.

VI) The addition of NaCl in Na_2SO_4 decreases the corrosion rates of phosphate and borate coated alloys where as in silicate

coated alloy an increase in corrosion rate is observed.

(VII) Except phosphate coated alloy, all the coated and uncoated alloys show increase in corrosion rate by the addition of NaCl in Na_2CO_3. The phosphate coated alloy shows a decrease in corrosion rate and the rate is indeed lower than the rates in NaCl and Na_2CO_3 alone.

(VIII) The phosphate coated and uncoated alloys show increase in corrosion rate on addition of Na_2CO_3 to Na_2SO_4 whereas in silicate coated alloy a decrease in corrosion rate is observed.

(IX) At higher temperatures (above 700°C), in presence of Na_2CO_3 or its mixtures, weight decrease (or weight loss) is noted in fairly large number of cases especially in chromate coated alloy. This is attributed to the loss of CO_2, formed during the decomposition of Na_2CO_3.

In general the hot corrosion study indicates that like uncoated steel none of the five coatings is capable of withstanding severe attack of corrosion in presence of Na_2SO_4, NaCl and Na_2CO_3, and their mixtures.

Uncoated alloy

(I) Na_2SO_4: The 18:8.5 Cr:Ni austenitic steel was corroded in presence of a thin film of Na_2SO_4, in the temperature

range of 700 - 1000°C. The alloy is severely corroded at all the four temperatures chosen for the hot corrosion study. The weight gain/temperature and scale thickness measurements indicate highest corrosion attack at 800°C.

The scales are relatively thick and porous due to polishing artifacts. The scales predominantly contain sulfide scales ($FeO.Cr_2O_3$) with inclusions of $(Fe,Ni)_3S_2$ especially in the outer scales. The following mechanism is presumably operated during hot corrosion attack.

In the initiation stage, oxidation of the alloy occurs with the predominant formation of FeO and Cr_2O_3 and with little NiO

$$Fe \longrightarrow FeO$$

$$Cr \longrightarrow Cr_2O_3$$

$$Ni \longrightarrow NiO$$

$$FeO + Cr_2O_3 \longrightarrow (FeO.Cr_2O_3) \quad \ldots\ldots \text{ I}$$

thus in the initiation stage protective inner layer of $(FeO.Cr_2O_3)$ is formed.

This is followed by minor reactions of the types

$$Na_2SO_4 + 2FeO \longrightarrow Na_2S + Fe_2O_3 + 3O \qquad \text{II}$$

$$Cr_2O_3 + 3Na_2S \longrightarrow Cr_2S_3 + 3Na_2O \qquad \text{III}$$

Finally, the propagation stage which can be represented by the following S-induced degradation reactions

$$Na_2SO_4 \longrightarrow S + 3/2\ O_2 + Na_2O \qquad IV$$

$$2\ Cr_2O_3 + 9S \longrightarrow 2\ Cr_2S_3 + 3SO_2 \qquad V$$

$$2FeO + 3S \longrightarrow 2\ FeS + SO_2 \qquad VI$$

$$Cr_2S_3 + FeS \longrightarrow FeS.Cr_2S_3 \qquad VII$$

$$2\ NiO + 3S \longrightarrow 2\ NiS + SO_2 \qquad VIII$$

$$FeS + NiS \longrightarrow (FeS.NiS) \qquad IX$$

The possibility of regeneration of Na_2SO_4 can not be excluded as evident by the following reaction:

$$Na_2O(III \text{ and } IV) + SO\ (V,\ VI \text{ and } VIII) + O(II \text{ and } IV) + O\ (II \text{ and } IV) \longrightarrow Na_2SO_4 \qquad X$$

In such a situation, the hot corrosion attack will not depend upon the amount of Na_2SO_4 and will be self sustaining. However, the reaction X can only proceed to forward direction if sufficient partial pressure of SO_2 is developed from reactions V, VI and VIII. The micrograph of the corroded alloy indicates deep penetration along the grain boundaries with in the alloy matrix due to sulfidation via reactions V and VI and to some extent by reaction VIII. Figure 5.9 represents a schematic diagram showing hot corrosion of 303 steel in presence of Na_2SO_4.

NaCl - The photomicrographs of the steel corroded in presence of NaCl indicates the presence of inner thin scale of Fe_2O_3 with dispersions of Cr_2O_3. The outer layers are porous and disrupted at some places. At high temperature NaCl penetrates through the pores of the oxide scales and form $FeCl_3$ at the metal/oxide interface. NaCl is also penetrated into the alloy matrix along the grain boundaries and dissolves outer layer of the alloy. The following reactions are expected

$$6\,NaCl + Fe_2O_3 \longrightarrow 2FeCl_3 + 3\,Na_2O \qquad XI$$

$$2\,NaCl + FeO \longrightarrow FeCl_2 + Na_2O \qquad XII$$

$$Cr_2O_3 + Na_2O \longrightarrow Na_2Cr_2O_4 \qquad XIII$$

$$2\,FeCl_2 + O_2 \longrightarrow FeO + 2Cl_2 \qquad XIV$$

$$2\,FeCl_3 + O_2 \longrightarrow 2\,FeO + 3Cl_2 \qquad XV$$

Reactions XI and XII proceed at oxide/alloy interface and Na_2O thus formed, fluxes the alloy according to the reaction XIII. The $Cl_2(g)$ evolved according to reactions (XIV) and (XV) disrupts the scales and is also available for further chlorination of the alloy. At all temperatures the weight gain data indicate much higher corrosion in presence of NaCl, when compared to Na_2SO_4. For example, the weight gains in presence of NaCl and Na_2SO_4 are 0.0046 and 0.0076 g/cm^2 respectively at 800°C. during a 6h corrosion run. The corrosion mechanism is repre-

sented schematically by a model given in Fig.5.10 as according to reactions:

$$FeS + Cl_2 \longrightarrow FeCl_2 + S \qquad \text{XVI}$$

$$2FeO + 2Cl_2 \longrightarrow 2FeCl_2 + O_2 \qquad \text{XVII}$$

$$Cr_2O_3 + 3Cl_2 \longrightarrow 2CrCl_3 + 3/2\ O_2 \qquad \text{XVIII}$$

The reactions (XVI) to (XVIII) are only possible when the S or O activates at the salt/oxide interface are [illegible] minimum.

Na_2SO_4 + NaCl - In general, the corrosion rate of the alloy in presence of 1:1 mixture of Na_2SO_4 + NaCl is higher than in presence of Na_2SO_4 but lower than NaCl alone. In presence of mixtures the scales are thicker and show two distinct layers. The inner thin layer containing Cr_2S_3.FeS with inclusions of $FeCl_3$, and the outer layer which is thicker and contains Fe_2O_3 with $NiCr_2O_4$ inclusions. The presence of NaCl in Na_2SO_4 has promoted the corrosion rate as is evident by the internal sulfidation which is not found in Na_2SO_4. Besides, reactions I to X taking place in presence of Na_2SO_4, the following reaction is also expected to take place at oxide/salt interface.

$$NiO + Cr_2O_3 \longrightarrow NiCr_2O_4 \qquad \text{XIX}$$

Figure 5.11 represents schematic diagram for sulfidation of AISI 303 steel in presence of Na_2SO_4 + NaCl.

Phosphate coating

Na_2SO_4 - Figure 5.12 represents a schematic diagram for sulfidation of phosphate coated steel in presence of Na_2SO_4. The phosphate coated 18:8.5 steel when corroded in presence of a thin film of Na_2SO_4 shows a 3-layered scale in which the inner white layer contains $FeS.Cr_2S_3$, middle layer containing FeS, with small contaminations of Cr_2S_3 and probably NiS. The outermost layer has $FePO_4$ with inclusions of phosphides. Molten sodium sulfate penetrates through the pores of phosphate coating and induces a sulfidation degration reactions as represented by reactions IV to VIII. Reactions II and III initially occur at the alloy surface due to interaction of Na_2SO_4 with coating materials. Na_2S form in reaction II also fluxes $FePO_4$ and Fe_2O_3 present in the coating material according to the following reactions:

$$FePO_4 + Na_2S + Fe_2O_3 \longrightarrow Fe_3P + Na_2SO_4 + 3O \qquad XX$$

$$FePO_4 + Na_2S + 3NiO \longrightarrow (Fe,Ni)_3P + 2O_2 \qquad XXI$$

However, all the $FePO_4$ is not consumed and some of it is left unreacted. Thus the outer scale should contain particulates of Fe_3P and $(Fe,Ni)_3P$ in $FePO_4$. The formation of this layer to some extent provides protection against hot corrosion. This is evident by the lower corrosion rate of phosphate coated alloy in comparison to steel in presence of Na_2SO_4.

NaCl: The SEM picture of phosphate coated alloy, corroded in presence of NaCl shows a uniform grey inner layer of Cr_2O_3 with white inclusions of $FeCl_3$, the outer scales are in the form of multilayers containing Fe_2O_3 (white) and FeO_4 (light). We expect the formations of $FeCl_2$ and $FeCl_3$ and fluxing of the alloy by the reactions depicted in equations XI to XIII. The fact that the presence of NaCl increases the corrosion rate is evident from its higher corrosion rate than that in presence of Na_2SO_4. The FeO_4 layer of the coating remains unaffected by NaCl though it provides passage for transport of NaCl to the alloy/coating interface.

NaCl + Na_2SO_4: The photomicrograph of the phosphate coated alloy in presence of NaCl + Na_2SO_4 shows severe corrosion in the alloy, the alloy is separated from the scale due to polishing artifacts. The presence of NaCl again accelerates the corrosion as is evident from consumption of the alloy during fluxing. The corrosion rates of the alloy are about one order of magnitude higher than the corresponding rate in Na_2SO_4. The detached scale contains inner white cluster of Fes.Cr_2S_3 and the outer scale contains Fe_2O_3 with Fes inclusions. There is a strong possibility of the presence of $FeCl_3$ at the alloy/scale interface although it has not been identified either by X-ray diffraction or metallographically.

Silicate coating:

Na_2SO_4: The photomicrographs and the SEM pictures of the silicate coated alloy in presence of Na_2SO_4 shows white inner layers of $FeS.Cr_2S_3$, middle layer of Al_2O_3 (from coating) and outer layers of Fe_2SiO_4 (light) and Fe_2O_3 (white, outer most). Apart from the reactions I to VII and X, we may expect the following reactions:

$$Al_2SiO_3 \text{ (from coating)} \longrightarrow Al_2O_3 + SiO_2 \qquad \text{XXII}$$

$$Al_2O_3 + Na_2O \text{ (from reaction III)} \longrightarrow 2\,NaAlO_2 \qquad \text{XXIII}$$

$$2NaAlO_2 + SO_2 \text{ (from reaction V \& VI)} \longrightarrow Na_2S + Al_2O_3 + 3O \text{ (regeneration)} \qquad \text{XXIV}$$

$$Na_2SO_4 + 2SiO_2 \longrightarrow Na_2SiO_3 + Fe_2SiO_4 + SO_2 \qquad \text{XXV}$$

$$3Na_2SiO_3 + 6FeS \text{ (from reaction VI)} + Cr_2O_3 + 6O_2 \text{ (from reaction XXIV)} \longrightarrow 3Fe_2SiO_4 + 3Na_2SO_4 + Cr_2S_3 \text{ (regenerated)} \qquad \text{XXVI}$$

(Al_2O_3 regenerated from XXIV and Fe_2SiO_4 form middle and outer layers of the scale, respectively,)

NaCl: The SEM pictures of the silicate coated alloy corroded in presence of NaCl shows inner stratified layers of Al_2SiO_5 with inclusions of $FeCl_3$. The outer most scale which

appears in the form of relatively thick uniform layer of Fe_2SiO_4. The presence of a second phase in the matrix is attributed to the precipitation of FeSi. When NaCl penetrates through silicate coating itattacks the alloy forming $FeCl_3$ (equation XI to XIII). However, some of the SiO_2 is penetrated into the scale along the grain boundaries and form silicides of iron, FeSi, NaCl seems to play the following role in the silicide formation.

$$Al_2SiO_5 \text{(from coating)} \longrightarrow Al_2O_3 + SiO_2 \qquad \text{XXVII}$$

$$3SiO_2 + 12\,NaCl + 7Fe \longrightarrow 3FeSi + 4FeCl_3 + 3Na_2O \qquad \text{XXVIII}$$

$$Na_2O + Cr_2O_3 \longrightarrow Na_2Cr_2O_4 \qquad \text{XXIX}$$

$NaCl + Na_2SO_4$: Due to the presence of NaCl in Na_2SO_4 the silicate coated alloy corroded at a much higher rate then in presence of Na_2SO_4 at temperatures higher than 700°C. The presence of NaCl indeces internal sulfide formation as observed in case of uncoated steel, otherwise the main features are similar to those observed in presence of Na_2SO_4.

Borate coating:

Na_2SO_4: The diagram for the sulfidation of borate coated steel in presence of Na_2SO_4 is schematically represented in Fig. 5.13. The corroded borate coated alloy shows a uniform thin layer at the alloy interface (SEM picture). The thin layer

contains white $FeS.Cr_2S_3$ with grey inclusions of Cr_2S_3. this is followed by a relatively thick but discontinuous middle layer of FeS and $(Fe, Ni)S_2$. The outer most layer contains Fe_2O_3 and $CrBO_3$. Na_2SO_4 penetrates through the borate coating and undergoes reactions represented by equation IV to X. The constituents in the coating also react with Na_2SO_4, giving the following reaction products.

$$2Fe_3BO_6 \text{ (from coating)} + 3Na_2SO_4 \longrightarrow 3FeS + 2Na_3BO_3 + Fe_2O_3 + FeO + 7O_2 \quad XXX$$

$$2Na_3BO_3 + Cr_2O_3 \longrightarrow 2CrBO_3 + 3Na_2O \quad XXXI$$

Na_2O and O_2 from reactions XXX and XXXI are consumed in X. The alloy matrix shows the presence of needle shaped second phase which presumably represents borides of iron and nickel. There is no plausible explanation for the formation of these borides, but their presence has been confirmed by X-ray diffraction analysis.

The presence of NaCl in Na_2SO_4 does not have any significant effect on the corrosion rate of the borate coated alloy upto a temperature of 800°C; however, at higher temperature, a considerable increase in rate is observed. It appears that the dispersion of metal borides in the alloy matrix considerably retards the corrosive action of NaCl which is otherwise observed in uncoated alloy and phosphate and silicate coated alloys.

Chromate coating:

Na_2SO_4 - The chromate coated alloy corroded in presence of a thin Na_2SO_4 film shows multilayered thick scales. The inner scales contain mixture of Cr_2S_3, FeS and Cr_2S_3 where as the outer scale, contains Fe_2SiO_4, $PbFe_4O_7$ and Fe_2O_3 as the main constituents. Molten Na_2SO_4 diffuses through the pores of chromate coating and interacts with the alloy at the oxide/ alloy interface and undergoes reactions IV to IX. The chromate coating itself reacts with Na_2SO_4 according to the following reactions.

$$4Na_2SO_4 + NiCr_2O_4 \text{(from coating)} \longrightarrow 4Na_2O + Cr_2S_3 + NiS + 8O_2 \quad \text{XXXII}$$

$$4Na_2SO_4 + ZnCr_2O_4 \text{(from coating)} \longrightarrow ZnSO_4 + 4Na_2O + Cr_2S_3 + 6O_2 \quad \text{XXXIII}$$

Na_2O formed in above reactions is used up in reaction X.

X-ray diffraction analysis indicates the presence of $PbFe_4O_7$ and Fe_2SiO_4 in the coating as well as in the corrosion product, this shows that these constituents remain unaffected during the corrosion process.

NaCl - The photomicrograph and SEM picture of the chromate coated alloy corroded in presence of NaCl at 850°C shows a grey inner layer of Cr_2O_3 with $FeCl_3$ inclusions, in the form of thin white stripe. The outer scale which is thicker

contains mostly Fe_2SiO_4 with $PbFe_4O_7$ as the outer most distinct layer. The structure of the alloy matrix shows severe attack in the form of salt penetration inside the alloy.

$NaCl + Na_2SO_4$ - The chromate coated alloy corroded in presence of 1:1 mixture of Na_2SO_4 and NaCl shows multilayered scales which are separated. The inner grey layer contains Cr_2S_3 followed by a detached thick layer which contains Fe_2SiO_4 with inclusions of FeS and Cr_2S_3. $PbFe_4O_7$, which appeared in the form of outer most layers in Na_2SO_4 and NaCl corroded alloys, is not visible in the metallograph of the Na_2SO_4 - NaCl corroded alloy. A white inclusion in between the outer and inner layers of the scale indicates the presence of $PbCl_2$. The presence of NaCl brings detrimental effects on the coated alloy is evident by the greater degree of internal sulfidation in the alloy matrix.

Oxide coating:

Na_2SO_4 - Figure 5.8c shows the micrograph of the oxide coated alloy corroded in presence of Na_2SO_4 at 1000°C. The inner scale is grey coloured presumably containing Cr_2S_3 with FeS inclusions. the outer scale is that of ZrO_2 in which Fe_2O_3 is incorporated. Internal sulfidation in alloy matrix is also noted. The SEM picture also gives more or less the same features.

Na_2SO_4 is penetrated through the oxide coating and has carried out sulfidation as represented by the reaction IV to X. Some of the constituents in the coating e.g. $(FeCr)_2O_3$ and $NiCr_2O_4$ undergo sulfidation reactions whereas ZrO_2 by and large remain unaffected.

NaCl - The oxide coated alloy undergoes severe corrosion in presence of NaCl. There is deep penetration of the salt along the grain boundaries. Reactions represented by XI to XXI take place. Whereas ZrO_2 present in the coating material remain unaffected. Inner layer of Cr_2O_3 (grey) with inclusions of $FeCl_2$(white hair line) and outer layer of the scales containing ZrO_2 with Cr_2O_3, NiO and FeO inclusions are observed in the micrograph.

Na_2SO_4 + NaCl - The oxide coated alloy exposed in presence of 1:1 mixture of NaCl + Na_2SO_4 at 1000°C shows scales in the form of two widely separated thick bands, the inner band consists of Cr_2S_3. Fes admixed with Cr_2S_3 and outer band contains ZrO_2 with sulfide inclusions. As in the other cases the presence of NaCl in Na_2SO_4 seems to increase the severity of corrosion.

CHAPTER - VI

HIGH TEMPERATURE OXIDATION AND HOT CORROSION BEHAVIOUR OF INORGANIC COATED MILD STEEL.

CHAPTER - VI

HIGH TEMPERATURE OXIDATION AND HOT CORROSION BEHAVIOUR OF INORGANIC COATED MILD STEEL

6.1 Introduction:

A wide range of iron, cobalt and nickel base alloys have been developed, with chromium as one of the major elements, to meet industrial requirements of specific mechanical properties and good corrosion resistance at high temperatures. The oxidation resistances of these alloys is determined by the transport properties and mechanical integrity of the protective oxide layer which is formed on the surface of the metal.

Iron base alloys with chromium as a major component are the principal materials used in elevated temperature regions of power generating units, and coal gasification and petro-chemical plants. Molten deposits of salt(s) or ash and gaseous mixtures of S-bearing gases (H_2S and SO_2) and oxidants (CO_2/CO and H_2/H_2O) are the common environments. The corrosion behaviour in such complex environment is strongly influenced by gas composition, alloy composition, nature of the deposit and temperature.

Cr_2S_3 and FeS (in low Cr steel) and $FeS.Cr_2S_3$ and FeS are the predominant species of the scale composition. Sulfide layers on the metal are in general not protective and their

growth rates are orders of magnitude higher than the oxide layers. Considering the serious effects of sulfidation on alloy steel, a study was carried out to investigate the hot corrosion behaviour of 321 steel in presence of different inorganic coatings (Chapter V).

Plain carbon steels exhibit relatively poor high temperature oxidation resistance mainly due to decarburization which disrupts the otherwise protective oxide scales. The disrupted scale provide easy passage for vanadia growth resulting in abnormally high oxidation rates. In a salt deposit environment such as that of Na_2SO_4, cementite or free carbon encourages sulphidation to an extent that long exposures may result in complete annihilation of the metal.

The objective of the present work is to investigate the high temperature oxidation and hot corrosion behaviour of mild steel in air and Na_2SO_4, respectively. The corrosion study has been further extended to the borate, carbide and chromate coated mild steel.

6.2 Experimental:

6.2.1. Specimen preparation: Mild steel (C:0.1; Si 0.15; S:0.03; Fe: balance) strips of 2.0 x 0.8 x 0.1 cm. size were cut from the sheet. The strips were abraded with different grades of SiC papers, and annealed at 700°C in an evacuated

pyrex glass-tube (Pressure 1 x 10^{-4} torr.) for 5h. The annealed specimens were polished and cooled with inorganic materials (Borate Carbide and Chromate). The details of the preparations of coatings and their methods of application are described in Chapter - II.

6.2.2 High temperature oxidation studies: The oxidation behaviour of coated and uncoated specimens was studied at 3 different temperatures viz., 400, 600 and 800°C, in a limited supply of air. The oxidation runs were usually of 5h durations. The kinetics measurements were carried out by using a laboratory fabricated thermal balance with a sensitivity of ±0.5 mg (fig.4.1).

6.2.3 Hot corrosion studies: The borate, chromate and carbide coated and uncoated mild steel specimens were uniformly coated with thin films of Na_2SO_4 of varying concentrations using spraying technique. During the spraying utmost care was taken to have a nearly uniform coating of the salt on all the faces of the specimens. The Na_2SO_4 coated specimens were dried in air, transferred to a silica boat and then further dried in a hot air oven at 110°C. The dried specimens were finally weighed along with silica boats and transferred to a tubular furnace maintained at the required temperature. The hot corrosion runs were limited to a period of 5 h. After the completion of the run, samples were taken out and cooled in a desiccator, and

weighed. The hot corrosion studies were performed at 5 different temperatures viz., 650, 700, 750, 800 and 850°C.

6.2.3 X-ray diffraction analysis: The identification of the various constituents in the corroded specimens was carried out by X-ray diffraction analysis, using a diffractometer with Mo as target and Zr as the filter. The constituents identified in the scales of corroded alloy specimens are listed in Table - 6.1.

6.2.4 Metallographic studies: A Leitz metallurgical microscope attached with a 35 mm Yashica FX-2 camera, was used for metallographic studies. The corroded specimens were mounted in paper moulds using Araldite as a cold setting mounting resin. The mounted specimens were abraded on 180, 320, 400 and 600 grade SiC papers respectively. The abraded specimens were then polished with 30 and 6 μ diamond pastes using kerosene as a lapping compound. A 5% Nital solution was used as an etchant.

6.2.5 Scanning Electron microscopic studies: A cambridge electron scanning microscope model S_{4-10} was used for the SEM studies. The specimens were coated with colloidal silver emulsion, before examining through scanning microscope.

6.3 Results:

6.3.1 Behaviour of coatings in various salts: The general behaviour of borate, chromate and oxide coatings was studied

in air, water, acids, alkalies and organic solvents at ambient temperature. This was carried out by immersing the coated specimens in 0.5M solutions of the acid and alkali e.g., HNO_3 HCl, H_2SO_4, KOH and NaOH as well as immersing in solvents like benzene, acetone, alcohol and H_2O for 24h. The immersed specimens were subsequently dried and weighed. The weight changes occurred after immersion are given in Table - 6.2. The coated mild steel specimens were also dipped in 15 ml of 0.5M solutions of the above mentioned liquids and boiled for 10 min. In general, the coatings did not show any change in weight.

6.3.2 Oxidation studies: Oxidation kinetics of the chromate, borate and carbide coated mild steel was studied, in the temperature range of 400 - 800°C, in a limited supply of air. The oxidation kinetics of mild steel was also studied under the identical conditions.

In the following section, the results of oxidation kinetics are described considering each coating separately.

6.3.2.1 Chromate coatings: Figures 6.1a to 6.1e present weight gain/time plots for the oxidation of chromate coated mild steel, at 5 different temperatures viz., 400, 600 and 800°C. The figures also show plots for uncoated mild steel under similar conditions. In the temperature range: 400 - 600°C, both the coated and uncoated mild steel follow a parabolic rate law. At 800°C,

the weight gain/time plot is approximately parabolic for chromate coated alloy though the corresponding plot for the mild steel is linear.

The weight gain^2/time linear plots for the chromate coated and uncoated mild steel at 400, 600 and 800°C are shown in figs. 6.3a to 6.3c. The values of parabolic rate constant are summarized in Table - 6.3. In general, the chromate coated mild steel shows lower oxidation rate than the mild steel in the temperature range of 400 - 800°C.

6.3.2.2 Carbide coating: In the temperature range 400 - 800°C, the weight gain/time plots (figs. 6.3a to 6.3c) for the carbide coated alloy are parabolic in nature. At 400 and 800°C, oxidation rates of the coated alloy are lower than those of mild steel but at 600°C, the case is reverse. The weight gain^2/time plots (figs. 6.4a to 6.4c) are linear and the values of the rate constants, computed from these plots, are listed in Table 6.4.

6.3.2.3 Borate coating: The borate coated mild steel shows a parabolic oxidation behaviour in the temperature range of 400 - 800°C as indicated by the parabolic and linear shape of the weight gain/time and weight gain^2/time plots, respectively (figs. 6.5a to 6.5c). Furthermore, the oxidation curves indicate that the borate coated alloy oxidizes at a

much slower rate than the mild steel in this temperature range.

6.3.3 Hot corrosion studies. In the following section, the results of hot corrosion studies, carried out on chromate, borate and carbide coated mild steel under a thin film of Na_2SO_4 of varying concentrations (0.4 to 8 mg/cm^2), are given. These studies have been carried out in the temperature range of 650 - 850°, in a limited supply of air. A hot corrosion run was usually of 5h duration.

6.3.3.1 Chromate coating: Figure 6.7a shows weight gain/Na_2SO_4 concentration plots at 5 different temperatures (650, 700, 750, 800 and 850°C). Some interesting information is emerged from the study of these plots. At lower temperatures (650 and 700°C), the weight gains are similar at all the concentrations of Na_2SO_4, in other words, the corrosion rate is independent of salt concentration.

At higher temperatures (750 - 850°C), the concentration of Na_2SO_4 giving maximum weight gain (or quantitatively highest corrosion rate) decreases with increasing temperature. This behaviour is similar to that of chromated steel. The concentrations of Na_2SO_4 which give maximum weight gains in chromate coated alloy, in the temperature range 750 - 850°C, are given below; the corresponding figures for mild steel are also given.

Temperature	Chromate coated concentration of Mg / cm^2	Uncoated Na_2SO_4
750°	7.4	6.5
800°	4.5	4.0
850°	0.4	4.0

6.3.3.2 Borate coating: In borate coated mild steel, at 850°C the corrosion rate does not show any change with varying concentrations of Na_2SO_4. In the temperature range 700 - 850°C the weight gain/concentration of Na_2SO_4 plots (Fig. 6.7b) indicates that the amount of Na_2SO_4 corresponding to maximum weight gain decreases with increasing temperature. This is illustrated by the data given in the following table.

Temperature	Amount of Na_2SO_4 required for max. wt. gain (mg/cm^2)	
	Borate	Uncoated
700°	4.4	-
750°	4.3	6.5
800°	3.8	4.0
850°	0.5	0.4

6.3.3.3 Carbide coating: At 650°C, the carbide coated alloy shows nearly the same weight gain values with increasing Na_2SO_4 concentrations (fig. 6.7d). At 700°C, maximum weight gain is observed at a salt concentration of 1.6 mg/cm^2. Above 700°C, the pattern is somewhat regular resembling with chromate, borate and uncoated alloys. With increasing temperature the amount of Na_2SO_4 required to produce maximum corrosion decreases. The amounts of Na_2SO_4 required to produce maximum weight gains at different temperatures for carbide coated alloy are given in the following table.

Temperature	Amount of Na_2SO_4 (mg/cm^2)	
	Carbide coating	Uncoated
750°	7.8	6.5
800°	4.6	4.0
850°	2.0	0.4

6.3.3.4 Uncoated: Figure 6.7d shows weight gain/Na_2SO_4 plots for mild steel at 5 different temperatures in the temperature range of 650 - 850°C. At 650°C, the Na_2SO_4 concentration does not affect the corrosion rate, i.e., the weight gains are independent of salt concentrations (range 0.2 - 8 mg/cm^2). Above 700°C, the value of maximum weight gain is shifted to the direction of the lower Na_2SO_4 concentration

as the temperature increases. At 650°C, the corrosion rates are highest at 0.5 mg/cm^2 of Na_2SO_4 corresponding to 4.0 and 6.5 mg/cm^2 at 800° and 750°C, respectively.

6.3.4 Morphological studies: Table lists the different constituents, as identified in the scales of Na_2SO_4 corroded uncoated and coated mild steels by X-ray diffraction analysis.

Figures 6.8 shows a photomicrograph of annealed mild steel (0.3% C). The steel contains polygonal grains of ferrite and pearlite.

Figure 6.8b shows a photomicrograph of the uncoated alloy corroded in presence of Na_2SO_4 at 750°C. The inner most layer consists of FeS which is followed by a discontinuous layer containing FeO and FeS, and the outer most layer which is thicker presumably contains Fe_2O_3 with Na_2SO_4 inclusions. From the metallographic examination there appears to be a strong evidence of fluxing of cementite (from pearlite) leaving a predominantly ferritic structure in the steel matrix.

Figures 6.9a and 6.9b show photomicrographs of chromate coated mild steel at 800°C and 650°C respectively in presence of a thin film of Na_2SO_4. The chromate coated alloy corroded at 800°C shows scales in which a thin uniform layer is present at the alloy interface and contains FeS, this followed by a thick layer containing $FeO.Cr_2O_3$ and Fe_2O_3. The structure of

the alloy matrix shows transformation of pearlite into ferrite due to the fluxing of cementite with Na_2SO_4. At 850°C the alloy matrix is fragmented due to severity of corrosion attack. The structure of the steel matrix shows complete dissolution of pearlitic phase in molten Na_2SO_4. The thick porous scale predominantly contains FeS with contamination of Cr_2S_3. The S.E.M. picture (fig. 6.9c) of the corroded alloy at 800°C shows a thin layer at the alloy/scale interface containing FeS, this is followed by a thick scale containing 2 phases, FeO and Cr_2O_3 and the outer thin layer contains Fe_2O_3.

Figures 6.10a to 6.10c represent photomicrographs of the corroded borate coated mild steel in presence of Na_2SO_4 at 650, 700 and 800°C, respectively. The morphology of the scales at these temperatures is similar though scales thickness increases with increasing temperature. The FeS is distributed through out the scale though it is more concentrated in the inner layers. The outer layers show the presence of 2 other constituents besides FeS which are presumably Fe_2SO_6 and Fe_2O_3. Unlike chromate and the uncoated alloy, the alloy matrix in borate coated is not much affected by sulfidation and the distribution of ferrite and pearlite is similar to that observed in the uncoated mild steel. The S.E.M. picture (fig. 6.10d) of the corroded borate coated alloy indicates the presence of microcrystals of FeS in the inner layers of

scale, the outer layer contains constituents which are presumably Fe_3SO_6 and Fe_2O_3.

The carbide coated alloy seems to be severely corroded in presence of Na_2SO_4. The photomicrograph (fig. 6.11a) and SEM picture (fig. 6.11b) of the coated alloy at 800°C show multilayered discontinuous scales. The inner layers predominantly contain FeS and the outer layers contain Fe_3O_4 admixed with ZrO_2 and SiC. The alloy matrix shows evidence of internal sulfidation., sulfidation attack is more pronounced at the regions containing pearlite phase.

6.4 Discussion

The high temperature oxidation behaviour of chromate, borate and carbide coated mild steel has been studied in the temperature range of 400 - 800°C. The weight gain/time plots are usually parabolic or approximately parabolic in nature at three temperatures viz., 400, 600 and 800°C chosen for oxidation studies. On the other hand, the uncoated mild steel shows parabolic behaviour only at 400 and 600°C. at 800°C a linear behaviour is observed. The values of parabolic rate constant evaluated from weight gain^2/time plots (and the linear plots in case of mild steel at 800°C) indicate slightly better oxidation resistance of coated alloys at temperatures upto 600°C. At 800°C the coated alloy

has much superior corrosion resistance when compared to mild steel. In the temperature range of 650 - 800°C, the oxidation resistance of different coatings follows the sequence

Borate > Carbide > Chromate > mild steel

surprisingly, the results of oxidation studies indicate that the presence of chromium does not induce better corrosion resistance in chromate coating in comparison to borate and carbide coatings though the chromate coating has much better corrosion resistance than the mild steel (Table - 6.3). The better oxidation resistance of borate and carbide coatings in comparison to chromate coating is probably due to the presence of relatively low chromium content in the coating (3.2% Cr_2O_3).

The hot corrosion studies of borate, carbide and chromate coated alloys have been carried out in the temperature range of 650 - 850°C, under thin films of Na_2SO_4 of varying thicknesses.

The weight gain/concentration of Na_2SO_4 plots for the different coatings and those for the mild steel indicate that at a critical concentration of Na_2SO_4 the rate is maximum. This critical concentration is strongly dependent upon temperature (range: 700 - 800°C). The critical amount of Na_2SO_4 at which the weight gain is maximum decreases rapidly with

increasing temperature. Table - 6.4 gives the critical amounts of Na_2SO_4 for the borate, carbide and chromate coatings as well as for the mild steel.

Figure 6.12a shows temperature/maximum weight gain plots for different coatings and the mild steel. From the plots some important generalisations emerge:

I) At 650°C, the corrosion rates for the different coatings and the uncoated alloy are similar.

II) In the temperature range of 650 - 800°C, the carbide coated alloy has the maximum corrosion rate followed by the uncoated alloy.

III) Mild steel has the highest corrosion rate in the temperature range of 800 - 850°C.

IV) Chromate coated mild steel, in general, has the lowest corrosion rate.

The temperature vs Na_2SO_4 concentration plots (fig.6.12b) show that except carbide coated alloy, the chromate and borate coated mild steel and the uncoated mild steel require nearly the same amount of Na_2SO_4 i.e., 3.8-4.4 and 0.4-0.8 mg/cm^2 at 800 and 850°C, respectively, for achieving maximum corrosion rate.

The mild steel when corroded in presence of a thin film of Na_2SO_4 shows extensive sulfidation, the inner layers

entirely contain FeS followed by middle layers of FeS and FeO which is porous and the outer most thicker layer of Fe_2O_3 with Na_2SO_4 inclusions. There is a strong evidence of decarburization in the alloy matrix during hot corrosion process cementite from the pearlite phase in the alloy and carbon from the solid solution phase are presumably responsible for initiation of the sulfidation reactions. In all probability, the hot corrosion reaction in mild steel proceeds by a sulfidation mechanism. The various reaction steps can be hypothesized in the form of the following equations:

$$Na_2SO_4 + 3C(\text{from ferrite}) = Na_2O + 3CO \qquad \text{I}$$

$$2Na_2SO_4 + Fe_3C\ (\text{from pearlite}) = 2Na_2O + 3FeS + CO \qquad \text{II}$$

Sulfidation:

$$Na_2SO_4 + 3FeS \longrightarrow 4S + 3FeO + Na_2O \qquad \text{III}$$

$$Fe + S \longrightarrow FeS \qquad \text{IV}$$

$$Fe_3O_4 + S \longrightarrow Fe_2O_3 + FeS + O \qquad \text{V}$$

$$S + O_2 \longrightarrow SO_2 \qquad \text{VI}$$

$$Fe_3O_4 + CO \longrightarrow 3FeO + CO_2 \qquad \text{VII}$$

$$Fe_2O_3 + CO \longrightarrow 2FeO + CO_2 \qquad \text{VIII}$$

Regeneration

$$Na_2O + SO_2 + O \longrightarrow Na_2SO_4 \qquad IX$$

The possibility of the reaction IX cannot be ruled out because of the two important observations: firstly the sulfidation rate is not a function of salt. Concentration, only at the definite concentration of Na_2SO_4 maximum corrosion rate is obtained; infact this critical amount is capable to accomplish all the reaction steps (I to VI) involved during hot corrosion. Secondly in all cases a white deposits of Na_2SO_4 is invariably found on the surface of the corroded alloy. Figure 6.13 illustrates a schematic diagram of sulfidation for the mild steel.

The chromate coated alloy when corroded in presence of Na_2SO_4 shows similar features as those observed in case of uncoated mild steel. However, due to the presence of chromates e.g. $FeCr_2O_4$ and Cr_2O_3 in the coating there is a formation of Cr_2S_3 layer at the alloy/scale interface. Figure 6.14 shows a schematic diagram representing a plausible model for sulfidation of chromate coated alloy. In the initial stages, the fused Na_2SO_4 penetrates through the chromate coating and most likely initiate sulfidation reactions (I and II). Subsequently reactions III to IX also take place along with the following reactions at the alloy/scale interface during the initial stages of sulfidation

$$2FeO(\text{from coating}) + 2S \longrightarrow 2Fe + \phi_2 \qquad X$$

$$2Cr_2O_3(\text{from coating}) + 6S \longrightarrow 2Cr_2S_3 + 3O_2 \qquad XI$$

Thus the chromate coated alloy in a typical Na_2SO_4 induced hot corrosion condition at 900°C undergoes sulfidation, and produces a morphology in which a thin layer of Cr_2S_3 is present at the alloy/scale interface followed by a duplex scale of Cr_2O_3 and FeO. At 850°C the hot corrosion attack is very severe and thick porous scales of Cr_2S_3 and FeS are obtained, the latter is a predominant species. At lower temperatures (650 - 800°C), the alloy matrix shows decementitization of the pearlite giving a ferrite structure in the corroded alloy - a situation resembling to mild steel. However, at 850°C the severity of hot corrosion attack is indicated by the complete annihilation of pearlite during sulfidation.

Among the coated mild steels under investigation carbide coated alloy seems to corrode to a maximum extent. By and large, SiC, ZrO_2 present in coating are not affected during the hot corrosion but these constituents do not supposedly produce any beneficial effect as far as hot corrosion resistance is concerned. Molten Na_2SO_4 penetrates through the pores of coating and directly attack the mild steel by a sulfidation mechanism via a triggering stage. During triggering stage presumably small amount of cementite are consumed, however, when the sulfidation reactions start,

gradually the whole pearlite is consumed during sulfidation. Due to the presence of some amount of Cr_2O_3 in the coating, the inner most layers which predominantly contain Fes also have Cr_2S_3 inclusions. At all the temperatures, the corroded alloy leaves some Na_2SO_4 deposit, which has also been observed in uncoated and chromate coated mild steel. The regeneration of Na_2SO_4 by reaction IX is also possible in this case on the basis of the same reasonings. The diagram for the sulfidation of the carbide coated alloy is shown schematically in fig. 6.5.

Borate coated mild steel is subjected to a lesser degree of corrosion attack compared to chromate and carbide coatings . The matrix of the corroded alloy indicates little attack on pearlite phase which is otherwise severely attacked in chromate and carbide coating. This suggests that in borate coating triggering is initiated by the trace amount of carbon from ferrite. The weight gain/temperature and weight gain/Na_2SO_4 concentration plots (discussed in the previous section) indicate lowest corrosion rates for borate coating in the temperature range 650-850°C. The critical concentration of Na_2SO_4 required to provide a maxima in corrosion rate at a particular temperature, is also lowest in borate among all the coatings. This indicates that Na_2SO_4 is continuously regenerating according to reaction IX and initially a small amount of Na_2SO_4 required to trigger the sulfidation reaction.

The main constituents of the borate coating, Fe_3BO_6, by and large remain unaffected and is probably responsible for restricting the corrosion attack. ZnB_2O_4 which is also present in the coating material could not be detected in the corroded alloy and presumably converted into ZnO and Fe_3BO_6 according to the following reactions.

$$ZnB_2O_4 \longrightarrow ZnO + B_2O_3 \qquad \text{XII}$$

$$3Fe_2O_3 + B_2O_3 \longrightarrow 2Fe_3BO_6 \qquad \text{XIII}$$

$$ZnO + Na_2BO_4 \longrightarrow ZnO_4 + Na_2O \qquad \text{XIV}$$

The diagram for the sulfidation of borate coated alloy is represented schematically in fig. 6.16.

CHAPTER - VII

SUMMARY

CHAPTER - VII

S U M M A R Y

The use of coatings for protection against corrosion has been an area of active investigations ever since the materials were first used for engineering and technological purposes. Painting, galvanising, metal plating, aluminising, chromising etc., were employed for corrosion protection as well as decoration purposes for quite some time. The polymer coatings e.g., poly vinyl, epoxy, silicones, are some of the recent additions to a long list of coatings which are currently used in industry. These coatings act as suitable barrier against corrosion at ambient to moderately high temperatures. In recent years interest has been developed to produce coatings for metals and alloys, providing satisfactory protection against high temperature oxidation and corrosion under severe environments. This is largely due to the development of new high temperature corrosion resistant materials for applications in aerospace and marine industries and high efficiency power generating units working on low grade fossil fuels, and coal gasification plants. Aluminide, boride, silicide, carbide, nitride and refractory oxide are some of the base materials which proved promising as corrosion resistant coatings on heat resistant or high temperature alloys.

The main objective of the investigations which are described in this thesis is to study the high temperature performance of some inorganic coatings and to explore the possibility of application of some of the coatings on high temperature materials to improve corrosion resistance AISI 303 steel, which is 18Cr : 8.5 Ni austenitic steel and mild steel (0.2%C) have been chosen as materials for these investigations.

The work described in this thesis deals with the corrosion behaviour of AISI 303 steel and mild steel in presence of inorganic coatings. The alloys have been coated with phosphate, silicate, borate, oxide, chromate and carbide coatings. The corrosion behaviour has been studied at ambient temperature in aqueous medium using electrochemical techniques. The high temperature oxidation behaviour has been studied in air and in presence of ionic salts (e.g., Na_2SO_4, NaCl, Na_2CO_3 and their mixtures) in the temperature range 400 - 1000°C. Oxidation kinetics, metallography, scanning electron microscopy and X-ray diffraction are the main tools on which high temperature corrosion studies are based.

Chapter - I presents a critical survey of the coating materials with especial emphasis on the coating materials and coating techniques introduced during the last 20 years or so. Some of the recent techniques include pack cementation, ion

implantation, gas phase chemical vapour deposition, Electroplating plus pack cementation and Electrophoretic.

Chapter - II deals with the preparation, properties and mechanism of formation of coatings which have actually been used in the work and described in the preceding chapters. The coatings include: phosphate, chromate, carbide, oxide, borate and silicate. The first 4 coatings have been applied on polished alloy specimens, surfaces using a coating slurry, whereas the other two viz., borate and silicate are formed on alloy surfaces by diffusion technique. The composition of the coating materials or the constituents present in the coatings have been determined on the basis of X-ray diffraction analysis and analysis of the scanning electron micrographs of the coated surfaces. The following are the main constituents identified in the coating materials.

Phosphate[a]	Silicate[a]	Chromate[a]	Borate[a]	Oxide[a]
$FePO_4$	Y_2SiO_4	$NiCr_2O_4$	Fe_3BO_6	ZrO_2
	Al_2SiO_5	$MnCr_2O_4$	Fe_2B, NiB	

Borate[b]	Chromate[b]	Carbide[b]
Fe_3BO_6	$FeCr_2O_4$	SiC
MnB_2O_4		

a- coating on Aisi 304 steel; b-coatings on mild steel.

Chapter - III describes electrochemical studies on the corrosion behaviour of coated 303 steel in presence of mineral acids (e.g., HCl, H_2SO_4 and HNO_3). The corrosion potential/time plots indicate that in H_2SO_4 medium oxide, phosphate and chromate coatings are stable where as other coatings show the tendency of dissolution, in HNO_3. Corrosion potential for coated alloy specimens initially shifted in the cathodic direction which is followed by no or little variation in potential, for the rest of the period. In HCl, phosphate and borate coated alloy specimens show better corrosion performance than the uncoated alloy steel. The scanning electron micrographs of the coating surfaces (after treatment with acids) show features typical of passivated coating metal, roasted metal/detached coating/undetached coating. For example, phosphate (H_2SO_4 and HCl) and oxide (H_2SO_4 and HNO_3) show nearly uniform coatings with close resemblance to uncoated coatings, where as in HCl the SEM pictures indicate some features typical of acidic corrosion.

Chapter - IV contains oxidation studies of phosphate, ali silicate, borate oxide and chromate coated 303 steel alloy in air at temperatures ranging from 400 to 1000°C. In the temperature range 400 to 800°C the kinetic curves (wt. gain/time) show parabolic behaviour. Above 800°C, however, most of the coatings show deviation from the parabolic rate law. Chromate, phosphate and oxide coatings show better corrosion resistance than uncoated alloy in the temperature range 400 - 600°C. At 800°C, only chromate coating has better corrosion resistance than the uncoated steel. At 1000°C phosphate coated alloy has superior corrosion resistance than the

uncoated alloy. It has been concluded that phosphate and chromate coatings are the promising materials for high temperature corrosion resistance purpose in environments containing air or oxygen.

In Chapter - V, the high temperature oxidation behaviour of phosphate, borate, silicate, oxide and chromate coated 303 steel, has been discussed in presence of ionic salts. The hot corrosion studies have been carried out at four different temperatures viz., 700, 800, 850 and 1000°C, in air.

In general, the corrosion rates of the coated alloys in presence of NaCl are much higher (at least one order of magnitude) than in presence of Na_2SO_4 or Na_2CO_3. Moreover, the addition of NaCl to Na_2SO_4 or Na_2CO_3 increases the corrosion rates appreciably in nearly all the cases. This indicates the pivotal role of NaCl in enhancing the corrosion attack in all the coated alloys as well as in the uncoated alloy. The phosphate coated alloy has lower corrosion rates than the uncoated alloy in presence of Na_2SO_4 and 1:1 mixture of Na_2SO_4 and NaCl. Like uncoated steel none of the five coatings is capable of withstanding severe attack of corrosion in presence of ionic salts.

The morphological studies of the corroded alloys indicate similarities in the scale structures. Multilayered scales are usually formed. In presence of Na_2SO_4, a sulfide spinal ($FeS.Cr_2S_3$) is invariably present as the inner most layer followed by a sulfide rich layer predominantly containing FeS., the penultimate layer contains oxide(s) and the coating materials form the outer

most layer, $FePO_4$, Al_2SiO_3, $CrBO_3$, Fe_2SiO_4 and ZrO_2 present initially in phosphate, silicate, borate, chromate and oxide coatings, respectively, remain unattacked during hot corrosion and appear in the form of outer layer in the scale. During hot corrosion, Na_2SO_4 penetrated through coating pores and attack the alloy at coating/metal interface, a sulfur induced degradation mode is operative ; this is perhaps produced by a fluxing mode involving reprecipitation of oxide near the coating interface. The coated alloys corroded in presence of NaCl show penetration of the salt through grain boundaries and in some cases are accompanied by fragmentation of the alloy surface. The oxide scales are discontinuous and porous and chloride phase is presumably accumulated at the alloy interface. The Na_2SO_4 - NaCl corroded alloys show extensive sulfidation, though the nature of the sulfide scale is similar to that observed in case of Na_2SO_4 alone but they are thicker and more porous. The alloy matrix of the corroded alloy shows evidence of internal sulfidation in some cases (uncoated, silicate and chromate) whereas in other cases the alloy is fragmented extensively.

Chapter - VI presents the results of high temperature oxidation and hot corrosion studies carried out on chromate, borate and carbide coated mild steel.

The high temperature oxidation studies have been carried out in air in the temperature range 400 - 800°C. The coated mild steel alloys usually follow a parabolic rate law in the temperature range 400 - 800°C, however, the mild steel shows a linear rate law at 800°C. In general, all the three coatings

offer better oxidation resistance than the mild steel. The oxidation resistance of different coatings follows the sequence: Borate > Carbide > Chromate > Mild steel.

The hot corrosion studies carried out on borate, carbide and chromate coated mild steel under thin films of Na_2SO_4 of varying concentrations (0.4 to 8.0 mg/cm^2) at 5 different temperatures. Concentration of Na_2SO_4/wt gain and concentration of Na_2SO_4 / temperature plots indicate that at a particular temperature there is a critical concentration of Na_2SO_4 at which corrosion rate is maximum. This critical amount of Na_2SO_4 decreases with increasing temperature. For example, the chromate, borate and mild steel require 3.8 - 4.4 and 0.4 to 0.5 mg/cm^2 of Na_2SO_4 at 800 and 850°C respectively for achieving maximum corrosion rate.

The scale morphology of the coated alloys is similar to that of mild steel. Invariably all the coatings show a thick sulfide layer of FeS adjacent to the alloy followed by a oxide or a duplex oxide scale which is porous, and the outer scale usually comprising of coating material. The Na_2SO_4 penetrates through the coating pores and attacks the alloy at the coating alloy interface. The corrosion proceeds by sulfidation in which carbon (from the solid solution phase in the alloy) and cementite (Fe_3C) react with sodium sulfate to give S and Na_2S respectively. The removal of cementite from the alloy is

indicated by the absence or depletion of the pearlite phase in the matrix of the corroded alloy.

Future Plan of Work.

It is proposed to extend the present work on inorganic coatings on steels and iron base alloys by using some new coatings.

Preparation of coatings:

The chemical vapour deposition (CVD) seems to be a promising technique for the preparation of some new coatings especially from high temperature oxidation point of view.

The following types of coatings, prepared by CVD method are under consideration for high temperature oxidation and aqueous corrosion studies.

i) Coatings of B, Al, Si, Ti, Zr, Nb and Ta by thermal decomposition of the corresponding tri-isobutyl compound.

ii) Coatings of nitride, boride, silicide and carbide using refractory metal halide as the starting material.

iii) Coatings of rare earth oxide (e.g., Y, Ce, La, Pr, Nd, Gd etc.) by choosing an appropriate organo-rare earth compound.

Alloys to be chosen:

Among steels, low and medium carbon steel will be the substrate alloy materials. Iron base alloys will include commercial alloy steels (including stainless steels) and 0.1-0.8 wt% C steels containing carbide and non carbide formers as alloy additions e.g., Cr, W, Ti, Nb, Ta, Ni, Al and Mn.

Studies to be conducted:

i) Mechanical testing: Mechanical testing is an essential tool for determining the competence of a coating. It provides information regarding the adherence of coating to the substrate, the bond strength between coating and the metal, strength of the coating and plasticity of the coating. It is proposed to carry out tensile, tensile impact, hardness and creep test on uncorroded as well as corroded coated alloys.

ii) Wet corrosion: The corrosion behaviour of the coatings in aqueous solutions of acid, base and salts, will be studied by using polarisation technique employing potentio static and potentio dynamic methods of analysis.

iii) High temperature oxidation: The high temperature oxidation studies will include kinetics and morphological aspects under environments relevent to industry. The main emphasis will be to study the relative performance of the

different coatings in mild (air) to severe (ionic salt, V_2O_5, SO_2, SO_3 etc.) corrosive environments.

iv) Electrochemical behaviour at higher temperature: It is also proposed to study the high temperature corrosion behaviour of different coating by using electrochemical technique. The anodic polarisation technique is most suitable for this purpose especially under ionic salt environments. It provides more quantitative information and is a quick way to assess the relative compatibility of different coatings in a given corrosive environment.

REFERENCES

1. J. E. Restall.
   J. Metallurgia. Vol. 46, No. 11, November 1979.

2. A. Ya. Drinberg, E. S. Gurevich and A. V. Tikhomirov - Technology of non-metallic coating (translated from the Russian and Edited by E. Bishop), Pergamon Press Oxford, London, New York, Paris 1960.

3. Pichoir, R. Aluminide coatings on nickel or cobalt - base super-alloys: main factors determining their morphology and composition. Proc. COST - 50 Conference (Liege) 1978 High temp. alloys for gas turbines Applied science publisher.

4. Llewelyn, G. Ubank, R. G. Improvements in metal surface treatments (Packaluminising) U.K. Patent 1093322 (1968).

5. Goward, G. W. Current research on the surface protection of superalloys for gas turbine engines. Jof Metals, 22, Oct. 1970, pp 31-39.

6. N. J. Archer.
   J. Phys. Technol. July 1979, 10(4), 153-161 English - 0305-4624.

7. Sermaloy (R) J solutions for hot corrosion, Sermetal Incorporated Brochure, 301 (C) 1977.

8. Saifullin, R. S., Zaitseva, L. V. The electrophoretic

deposition of Inorganic Components from organic media. Paint Technology, 2eff January 1966.

9. Coward, G. M. Coatings and coating processing for gas turbine aerofoils operating in a marine environment. Proc. 1974 NAVSEC Conference, pp 277-296.

10. Boone, D. H. et al. The electron beam coating of turbine components and ion plating. Conference on Ionplating and Allied Techniques. 1 PAT 1967 (Edinburgh) pp 141-148.

11. Mattox, D. M. Fundamentals of ionplating. J. Vac. Sci., Technol. 10, No. 1 (1973) 47 ff.

12. M. J. Bennett, et al., The influence of the surface ion implantation of Al and Y upon the oxidation behaviour of A Fe-15% Cr-6% Al FERRALLOY Stainless Steel in air at 1100°C. J. Corr. Sci., Vol. 20, No.1, pp. 69-72.

13. M. J. Bennett, et al., The influence of surface ion implantation upon the oxidation behaviour of a 20% Cr-25% Ni, Niobium stabilised austenitic stainless steel in carbon dioxide at 625°C. J. Corr. Sci., Vol. 20, No. 1, pp 73-89.

14. M. J. Bennett, The role of ion-implantation in High temperature oxidation studies AERE-R10091 (Paper

presented to NACE International Conference on High Temperature Corrosion, San Diego, March 2-6, 1981.

15. Coating Technology Bulletin, C83 E762M. Union Carbide UK Ltd., Coatings Service Division, Swindon Wilts.

16. K. Brennfleck, E. Fitzer and D. Kahr, CVD 1977 (Proc. Conf.) Los Angeles, Calif. 14-19 Oct. 1977, The Electrochemical Society, Box 2071 Princeton, N.J. 08540, 1977 (Met. A. 8008-730381) (2) 518-529.

17. M. Ozan and Vanmar, Vacuum, Dec. 1978, 28(12), 567-570 (English) 0042-207.

18. Lavendel, Henry W. J. Met. 27(7), 4-10, 1975 (Chem. Abst. 84:80892r).

19. I. V. Kuotan Izvest. Sektora, Fiz-Khim. Anal. Inst. Obshchei. Inorg. Khim. Akad. Nauk, SSSR, 26, 304 - 12(1955) (Chem. Abst. 50-1956, 2393 i).

20. Tadahiko, Haruya and Katsuhiro, Matsuo, Kogai Kenkyu No. 9, 1-8 (1956).

21. Roger Lagarde, Corrosion et anticorrosion 4, 289-89 (1956); Chem. centr. 129. 1973 (1958) (Chem. Abst. 53-1959, 21561h).

22. John. A. Henrike & To Geraldine D Henrike, U.S. 3, 178, 319 (Cl 148-615), Apr. 13-1956 (Chem. Abst. 63, 1965, 2960h).

23. Final treatment of phosphate coatings. Cupr, Vestav. (Brno, Czech), Povrchone upravy 1970 (5-6), 38-41 (Czech) (Chem. Abst. 75 - 1971, R 78194j).

24. Rhim, William A. (Pennwalt Comp. Philadelphia, Pa.) Prod. Finish. (Cincinnati) 1972, 37(1), 66-79 (Eng) (Chem. Abst. 78 - 1973, 5448x).

25. Kayser, Friedrich (Frankfurt/Ger.) Galvano - Technik 1974-65(2) 119-23 (Ger.) (Chem. Abst. 80 - 1974, 136358a).

26. Jones, Kamlet (to American Potash and Chemical Corp.) U.S. 2, 646, 344, July 21, 1953 (Chem. Abst. 47 - 1953, 10815i).

27. Nachard, Nelson J., Jr. (Am. Chem. prod. Ins. Ambler, Pa.) Metal Finish 1972, 70(7). 49-53 (8) 66-9 (English) (Chem. Abst. 77- 1972, 117259x).

28. Nakajima, Jun, Iwai, Hiroshi, Nomiyama, Iwao (Matsushita Electric Works Ltd., Kansai Paint Co., Ltd.). Japan, Kokai 72-30, 731 (Cl. 24, NO. 24 F_3) 09 Nov 1972 (Chem. Abst. 78 - 1973,86111g).

29. Ved. V. E. Grigorev, L. S. Simbirskii. D. F. Pyzhenko, S. I. (Kharkov, Aviation Inst.) U.S.S.R. 614, 134 (Cl C_{23} D 5100) 05 Jul 1978 Appl. 2, 426, 498, 06 Dec. 1976.

30. Anticorrosive Composition for Metal Surfaces, International Standard Electric Corp. Neth. Appl. 7805,

896 (Cl. C23F7/08) 05 Dec 1978, Brit. Appl. 77/23. 790, 03 Jun 1977.

31. J. Mogl, R. Mac. Millan (Phosphate Conversion Coatings on Steel) Journal of Materials Science 12 (1977) 2235 - 2240.

32. F. Winlow and Earl W. Balis (to General Electric Co.) U.S. 2, 529, 206, Nov.7, 1950 (Chem. Abst. 45-1951, 1496).

33. P. A. J. Gate Product Finishing (London) 9, No. 8. 46-51 (1956) (Chem. Abst. 51-1957, 7381).

34. Jesse R, Connor, Jr (to Allegheny Ludlum Steel Corp.), U.S. 3, 208, 874 (Cl 117-135 1) Sept. 28, 1965 (Chem. Abst. 63-1965, 15950c).

35. J. I. Richardson, Trav, Centre, Rech. Etud, Oceanogr. (Paris) 6 (1-2-3-4), 221-3 Discussion 223 (1965 (Eng) (Chem. Abst. 66- 1967, 97693 y).

36. Sullivan, James, D. (Havey Industries, Inc.) Ger. Offen. 2,003, 332 (Cl C_{23} 4. Co 3C) 30 July 1970, 46 (Chem. Abst. 73 - 1970, 101404).

37. R. Rolls the structure and properties of protective oxides scales on Iron-base alloys, Review on High Temperature Materials (Editor. J. BARDCH) Dept. of

Materials Engineering. Technion, Israel Institute of Technology, Vol. 1, No. 4, 1973.

38. N. N. Rozov, and A. A. Appen. Zh. Prikl. Khim. 42, 2716 (1969).

39. Faber, Guy, Moggi Carlo, M. Trindler, Walter (BBC A-G. Brown, Boveri und cie) Swiss 599, 382 (Cl. C_{23} 15/00) 31 May 1978. (Chem. Abst. 1978(89), 167870h).

40. Mahan Richard Lloyed, Moreloek, Charles, Robert. (General Electric Co.) Ger offen, 2, 754, 660 (Cl C04B 41/06) 15 June 1978 U.S. (Appl. 748, 930, 09 Dec 1976). (Chem. Abst. 1978, (89) 94079 v).

41. Higuchi, Hisashi, Ohsumi, Hirotada, Uchino, Kazuo, Makijima, Hiroshi, Toyota, Tsuneshiko (Nippon Kokan K. K. Dai Nippon Toryo Co., Ltd.) Japan. 7638, 962, (Cl C 21d C_{23}f). 22 Oct. 1974. Appl. 7050, 734, 13 June 1970 (Chem. Abst. 1975(82), 30035 w).

42. Abe, Kazumori, Nakamura, Takumori, Motoki, Hideo (Shikoku Koken Kogyo K. K.) Jpn. Kokai, Tokkyo Koho 78, 132, 024 (Cl C 04B 21/02) 17 Nov. 1978 Appl. 77/47, 673, 23 Apr 1977. (Chem. Abst. 1980 (90) 186519c).

43. F. V. Arnold and R. Rolls. Published in Nask, U. Kerren (1972).

44. J. A. Antill, European Corrosion Federation, Duesseldorf Conference, Dec. 1970.

45. Bareas, H. Krikorian, John D. Farr, and Willard, G. Whitman (to U.S. Atomic Energy Commission) U.S. 3, 020, 632, Feb. 13, 1962 (Chem. Abst. 56-1962, 11341g).

46. Chihiro, Kawashima, Yoshihiro Murata and Soichiro Motoi, Japan, 145 (63) Jan, 16, (Chem. Abst: 59-1963, 4088h).

47. G. A. Semenova, A. N. Minkevich, E. V. Panchenko, and S. B. Maslenkov (Steel & alloy inst. Moscow) Metallot/od i term-obrabotka Meta. 1965(11) 37-8 (Russ.)(Chem. Abst. 64-1966, 4689b).

48. Glanki, Fredrunk A, (Fan, Steel Inc.) U.S. 3, 640, 699 (Cl 29/195 B 326), 08 Feb., 1972, (Chem. Abst. 76-1972, 116999b).

49. Ruppert, W. (Ed. Deerrenberg, Soehne,-Remdscheth, Ger.) C.V.D. Inst. Conf., 2nd 1970, 443-59 (Ger)(Chem. Abst. 74-1971, 1454-24d).

50. Kasai, Masami (Suwa Seikosha Co Ltd.)Japan 72, 42, 013 (Cl 2827, C04b, C23a) 26Oct 1972 (Chem. Abst. 78-1973, 129668d).

51. Sasaki, Shinobu, Asano, Yukihide, (Toyota, Motor Co. Ltd) Japan, Kokai, 77, 107, 248, (Cl C23 F15/00), 08 Sept.1977. (Chem. Abst. 88 (1978), 29868x).

52. Shibata, Isao, Ohno, Saigo, Hwang, Yun Chung (Oki Electric Industry Co. Ltd.) Japan, Kokai, 77, 108, 378 (Cl 23, $C_1$3/04), 10 Sept. 1977 (Chem. Abst. 89 (1978) 28666y).

53. John, M. Blocher, Jr, Carl, J. Ish. Don P. Leiter Layne F. Block and Ivore E. Campbell, Cambell, US At. energy commission, R. Ml 130068 pp (1958) (Chem. Abst.54-1960, 182604).

54. J. H. Oxley, R. B. Landrigan, A. C. Seareut, C. F. Powell, and J. M. Blocher, Jr. (Battel Mem. Inst. Columbus, Ohio) U.S. At. energy comm. BMI-X-160, 47 pp (1960) (Chem. Abst. 58-1963, 8455a).

55. E. A. Antonova and N. N. Popov. Zashchita Meta 1 (6), 687-91(1965) (Russ) (Chem. Abst. 64-1966, 9321a).

56. Minkenich, A. N., Semenova, G. A. (U.S.S.R.) Metallord, Term, obreb, 1968 No. 5 109-15 (Russ) (Chem. Abst.70-1969, 60165n).

57. Dyakova, A. V. Loshutov, V. F., Gordan, G. N. (Kiev, Politekh, Inst. Kiev USSR) IzV, Vyssh. Uchebn. Zaved, Chem Metal 1978, (6) 114-17 (Russ) (Chem. Abst. 89-(1978) 93218c).

58. E. C. Rhem, and C. A. Culpepper; NaCl, Technol. Aug. 1977, 35(1), 173-177.

59. Metal gesellschaft A - G (by Arnold Muenster Guenther Schlemp and Imtraut Friedrich) Ger, 1, 116, 499 (Cl 48b) Nov 2, 1961 (Chem. Abst, 57-1962, 9536e).

60. Ogino, Tenso, Seo, Takeo (Sumiki, Moto, Co., Ltd.) Japan, Kokai, 74, 82, 544, (Cl, 12A 34) 08 Aug 1974, (Chem. Abst. 82-1975, 62738y).

61. L. B. Moskowitz, and E. Kler, Sc M. Corp. off. Gas. 11. Mar. 1980, Patent no US 4192672 (USA) 18 Jan - 1978.

62. A. P. Epik, C. A. Borkum, I. V. Golubchik, and L. P. Sinitsina, Diffusion, Pokrytiyama Metal., Akad, Nauk Ukr, SSR, Inst. Prchl. Material- cmed 1965, 127-42 (Russ) (Chem. Abst. 64-1966, 7814c).

63. Ivor E. Campbell, Bruce W. Gonser, and Carroll F. Powell (to Fan Steel Metallurgical Corp.) U.S. 2, 771, 666, Nov. 27, 1956 (Che. Abst. 51-1957, 2520a).

64. Richard, L, Wachtell and Richard P. Seeling (to chromally Corp.) U.S.3, 037, 883, June 5, 1962 (Chem. Abst.57-1962, 6998d).

65. M. S. Patel, Eutectic Corp. off, Gas., 4 Mar. 1980. Patent No. U.S. 4191565 (USA), 15 June 1978.

66. Bernard, J., Aylett and Howard, M. Colquhoun, J.C.S. Dalton. 1977 (20) p. 2058.

67. Wilhelm Ruppert and Gottfried Schneider (to Metallgea. Unchaft Akt - Ges) U.S.3965, 791, Dec. 23, 1968 (53-1969). 111611).

68. Riemann, Udo K. P. Lynch, Brian, Vandewijgert, Willi Heraeus, W. (W. C. Philips - Glocilampen fabrieken) Ger. offen. 2, 516, 296 (Cl C23C) 23 Oct. 1975.

69. Karpinos, D. M. Listovnichaya, S. P. Alvanyk, V. Ya. Bogomaz, N.A. (Inst. Probl. Materialoved., Kiev, USSR) Borpolosh. Strukt. Svoistva. Mater. Mashinostr. sinp. Boru, 4th 1972 (Pub: 1974) 1, 251-6.

70. Kuniyasi, Tsuyio, Miyai, Akira, (Denki Kagaku Kogyo K.K.) Japan Kokai, 75 156, 519 (Cl. CO 4B) 17 Dec. 1975.

71. R. Rhumbam and Grey. Thin Solid films 15 sept. 1973, 53 (3) 313-321.

72. S. Motojima, Y. ohtsuka, S. Kawajiri, Y. Tokuhashi, and K. Sugiyama, J. Mater. Sci. Feb. 1974, 14 (2) 496-498 (Eng) 0022-2461.

73. Zhuravlev, G. I. Avgustinik, A. I. Borisenko, A. A. (USSR) Kharoteshkie, Teplostoikie pokrytiya. Tr. Vses. soveshch, 4th 1968 (Pub.1969) 38-36 (Russ) Edited by Kharitonov, N. P. Izd. "Nauka" Leningrad. Otd. Leningrad USSR (Theory of high temperature gas-corrosion).

74. Furnace and high velocity oxidation of aluminide - coated cobalt superalloy. Wg-25 Grisaffe, Salvator, J., Deadmore, Daniel, L. Sandruss, William, A. (Lewis Res. Center, NASA, Cleveland Ohio). NASA tech. Note 1970 NAS A TN. D-5834-24 pp (Eng) (Chem. Abst. 73-1970, 69268m).

75. Fenet, C., "Sbior prac. Pt. Zharoprochnye splavy Vysokoyakh pletev so sverkhzvyni skorostiami" (Collection of works on scaling-Resistant alloys in conditions of supersonic Rate flight) Metallurgizdat, Moskva 1962, Translation from English.

76. Buckle, H., Rev. Metallurgie, 54, 16 (1957).

77. Gorbunov, N. "Diffusionnye pokrytiyena zhelezeistali" (Diffusion coating on iron and steel) A.N. SSSR, Moskava, 1958.

78. Drankiewicz T., Gabelski S., "Zarovzpurne, pewloki, aluminiowe na. stali i. zelazie" (Scaling resistant Aluminium coatings on Steel and iron) PWT. Warszawa 1975.

79. J. H. Payer,
Electrochemical methods for coatings study and evaluation (Paper presented at the symposium on Electrochemical Techniques for Corrosion at the NACE) Corrosion/76 meeting held in Houston, Texas, March 22-26, 1976.

80. S. R. Maloof, J. Electrochem. Soc., Vol. 116, p. 1293 (1969).

81. Wilhelm Schwerk, Mannesmann Forschungsber 1977(728), 1-5 (German) (Met.Abst. Jan. 1978).

82. G. N. Walter, Metals 77the 30th Annual Conference of the Australasian institute of Metals 1977, 7A?-78 (Met. Abst. 7803-72002?) (Eng).

83. Gas Corrosion of Metals (Korozja gazowa metali) by Stanislaw Mrowec, Teodor Werber, Translated from Polish (1978) pp. 511-530.

84. Simons, E. L. Browning, G. V. and Liebhafsky, H. A. Corrosion 11 (1955) 305t.

85. Goebel, J. A. and Pettits, F. S. Met Trans 1(1970) 1943-3421.

86. Goebel, J. A. Pettits, F. S. and Goward G. W. Met. trans. 4 (1975) 261.

87. G. William Goward,
Protective coatings for high temperature alloys state of technology "Proceedings of the Symposium on properties of high temperature alloys". Edited by Z. A. Foroulis and F. S. Pettits. Published by the Electrochemical Socity Vol. 77-1(1976) pp 806-819.

88. N. S. Borbunov et al.
Diffusion coatings for the protection of heat resistant gas turbine alloy from corrosion in presence of vanadium

Pentecostals. Nauchn. Ateizm. obshchestv. Rus pan korrespondentskiy, Direktsiyalari, vnutar, Sqsraniya, 1982, 245-58.

Table - 2.1

List of constituents present in phosphate, silicate, chromate, borate and oxide coated AISI 303 steel identified by the X-ray analysis.

Coatings	Constituents
Phosphate	FeO, FeO, Cr_2O_3, $FePO_4$ and $Ca_3(PO_4)_2$
Silicate	Fe_2O_3, Cr_2O_3, Al_2O_3, Fe_2SiO_4 and Al_2SiO_5
Chromate	Fe_2O_3, $PbFe_6O_7$, $NiCr_2O_4$, Fe_2SiO_4 and $ZnCr_2O_4$
Borate	Fe_2O_3, Cr_2O_3, Fe_2B, $NaTiO_2$ and Fe_3BO_6
Oxide	Fe_2O_3, $(Cr,Fe)_2O_3$, $NiCr_2O_4$ and ZnO_2

Table - 2.2

List of constituents present in borate, carbide and chromate coated mild steel identified by X-ray analysis.

Coatings	Constituents
Borate	Fe_3BO_6, Fe_3O_4, Fe_2O_3 and MnB_2O_6
Carbide	SiC, ZnO_2, Fe_2O_3, Fe_3O_4 and Cr_2O_3
Chromate	$FeCr_2O_4$, Fe_2SiO_4, Fe_3O_4, Fe_2O_3 and $PbFe_6O_7$

Table - 3.1

Results of 24 hours immersion tests coated and uncoated AISI 303 steel ($\times 10^{-3}$ g/cm^2).

Coatings	H_2O	HNO_3	HCl	H_2SO_4	Benzene	Acetone	Ethyl alcohol
Phosphate	N.C.	0.3	0.8	2.4	N.C.	N.C.	N.C.
Chromate	N.C.	0.2	1.4	1.5	N.C.	N.C.	N.C.
Borate	N.C.	0.3	1.8	0.25	N.C.	N.C.	N.C.
Oxide	N.C.	0.24	1.4	1.4	N.C.	N.C.	N.C.
Uncoated	N.C.	0	0.5	2.4	N.C.	N.C.	N.C.

N.C. = No change.

Table - 3.2

Visual Observations of the Corroded Samples in Acids and the Constituent (soluble Specimens) Present: ($X\ 10^{-3}$ g/cm^2)

Coatings	Weight loss	Time of Immersion	Colour of the Solution	Soluble specimens present		Remarks
HCl						
Phosphate	1.3	150 hours	colourless	$FeCl_3$	$CrCl_3$	a
Chromate	13.2	"	Blue	"	"	b
Borate	12.6	"	Light blue	"	"	b & c
Oxide	5.6	"	Colourless	"	"	(d)
Uncoated	8.1	"	Blue	"	"	White & grey
HNO_3						
Phosphate	0.5	72 hours	Colourless	$Fe(NO_3)_2$	-	a
Chromate	11.4	"	Brown	"	$Cr(NO_3)_3$	b
Borate	13.0	"	Colourless	"	"	b & c
Oxide	5.4	"	Colourless	"	-	b
Uncoated	0	"	Colourless	-	-	a

..... contd .....

Table - 3.2 : ..... contd .....

Coatings	Weight loss	H_2SO_4 Time of immersion	Colour of the solution	Soluble specimens present		Remarks
Phosphate	3.0	120 hours	Colourless	$Fe_2(SO_4)_3$	-	a
Chromate	4.0	"	Brown	"	$Cr_2(SO_4)_3$	b & c
Borate	0.3	"	Colourless	"	"	b & e
Oxide	2.9	"	Colourless	"	"	b
Uncoated	2.4	"	Blue	"	"	(d) White to black

a = appearence of coating remains unchanged

b = coating is detached at some place

c = coating is detached completely

d = coating remains adhered but colour changes

e = some coatings particle (insoluble) present in the solution.

Table - 4.1

Parabolic rate constant K_p ($\times 10^{-13}$ g^2 cm^{-4} sec^{-1}) and linear rate constant K_l ($\times 10^{-9}$ g cm^{-2} sec^{-1}) of the coated and uncoated alloy in the temperature range 400 - 1000°C.

Coatings	400°C	600°C	800°C	1000°C
Phosphate	7.4	6.0	182.0	158.0
Borate	138	950	31.0	-
Chromate	0.069	0.59	15.0	270.0*
Oxide	-	33.0	13.0	97.0*
Silicate	19.4*	13.8*	-	-
Uncoated	85.0	24.7	19.8	-

* Linear rate constat Kl.

Table – 5.1

Constituents present in the coatings, scales (corroded under varying ionic salt environment) of coated and uncoated steel, identified by X-ray analysis.

Coatings	Constituents of coating analysed by X-ray.	salt	Corrosion products	Constituents identified metallographically
Uncoated	–	Na_2SO_4	$FeCr_2S_4$ $(FeNi)S_2$, Cr_2S_3, Fe_2O_3 and Na_2S.	X $FeS.Cr_2S_3$ XX FeS
"	–	NaCl	$Fe_2O_3.FeCl_3$ & Cr_2O_3	X $FeCl_3$ XX $Fe_2O_3.Cr_2O_3$
"		Na_2SO_4 + NaCl	FeS, Cr_2S_3, NiS, $NiCr_2O_4$	X Cr_2S_3, FeS, NiS, XX Fe_2O_3, NiO, Cr_2O_3
Phosphate	$FePO_4$, FeO, Fe_2O_3, Cr_2O_3, $Ca_3(PO_4)_2$, $Fe_3(PO_4)_2$ (OH)	Na_2SO_4	$FeCr_2S_4$, FeS, $FePO_4$, CrO_3, Ni_3P, NiS, Fe_2O_3	X $FeS.Cr_2S_3$. XX FeS, Small inclusion of Cr_2S_3, NiS XXX Fe_2O_3, $FePO_4$.
"	" " "	NaCl	$FeCl_3$, Fe_2O_3, $FePO_4$, Cr_2O_3, Cr_3O_4, NiO	X Cr_2O_3 and $FeCl_3$ XX Fe_2O_3, $FePO_4$
"	" " "	Na_2SO_4 + NaCl	$FeS.Cr_2S_3$, Fe_2O_3, FeS	X $FeS.Cr_2S_3$ XX Fe_2O_3, FeS.

..... contd .....

Table - 5.1 : ..... contd .....

Coatings	Constituents of coating analysed by X-ray.	Salt	Corrosion products	Constituents identified metallographically.
Silicate	Fe_2O_3, Fe_2SiO_4, Cr_2O_3, Al_2O_3 Al_2SiO_5	Na_2SO_4	$(Fe,Ni)S_2$, Cr_5S_6, Fe_2SiO_4, Cr_2O_3, Al_2O_3	X FeS, Cr_2S_3 XX Al_2O_3 XXX Fe_2SiO_4, Fe_2O_3
"	" "	NaCl	$FeCl_3$, Fe_2SiO_4, Fe_2O_3, $CrCl_3$, $NiCl_2$ & Al_2SiO_5	X Al_2SiO_5, $FeCl_3$ XX Fe_2O_3, SiO_2
"	" "	Na_2SO_4 + NaCl	FeS, Cr_2S_3, FeS	X FeS, Cr_2S_3 XX Fe.
Borate	Fe_2B, Fe_3BO_6, Fe_2O_3, Cr_2O_3, NiB, NaBO	Na_2SO_4	$(FeNi)S_2$, Fe_2O_3, FeS, Cr_5S_6, $CrBO_3$, Cr_2O_3, Ni_2B_2	X Cr_2S_3 XX FeS, $(FeNi)S_2$ XXX Fe_2O_3 & $CrBO_3$
"	" "	NaCl	Fe_3B, $FeCl_3$, FeO, Fe $(BO_2)_2$, Cr_2O_3 & NiO.	-
"	" "	Na_2SO_4 + NaCl	FeS, Cr_2S_3, Fe_2O_3, $CrBO_3$	X FeS, Cr_2S_3 XX Fe_2O_3 and $CrBO_3$
Chromate	Fe_2SiO_4, $ZnCr_2O_4$, $NiCr_2O_4$, $PbFe_6O_7$	Na_2SO_4	Cr_3S_4, Fe_2SiO_4, FeS, Fe_3O_4, $PbFe_6O_7$	X Cr_2S_3 XX FeS, Cr_2S_3 XXX Fe_2SiO_4, $PbFe_6O_7$, Fe_2O_3
"	" "	NaCl	Fe_2O_3, $FeCl_3$, Fe_2SiO_4, $PbFe_6O_7$	X Fe_2SiO_4, $FeCl_3$ XX $PbFe_6O_7$
"	" "	Na_2SO_4+NaCl	$PbFe_6O_7$, Fe_2O_3, Fe_3O_4 FeS, Cr_2S_3	X Cr_2S_3, $FeCl_3$ XX Fe_2SiO_4, FeS, Cr_2S_3

..... contd .....

Table - 5.1 : ..... contd .....

Coatings	Constituents of coating analysed by X-ray	Salt	Corrosion products	Constituents identified metallographically.
Oxide	$(CrFe)_2O_3$, $NiCr_2O_4$, ZnO_2, Fe_2O_3	Na_2SO_4	ZnO_2, Fe_2O_3, FeO, Cr_3S_4, FeS	X Cr_2S_3, FeS, XX ZnO_2, Fe_2O_3
"	"	"	NaCl	Fe_3O_4, Cr_2O_3, $FeCl_3$, NiO, ZnO_2	X Cr_2O_3, $FeCl_3$ XX ZnO_2, Cr_2O_3, NiO and FeO
"	"	"	Na_2SO_4 + NaCl	ZnO_2, Fe_2O_3, FeS, Cr_5S_6, Cr_2O_3	X FeS, Cr_2S_3 XX ZnO_2

X inner layer

XX middle layer

XXX Outer layer.

Table - 6.1

Constituents present in the scales of coated and uncoated steel, identified by X-ray analysis.

Coatings	Salt	Constituents present in the corroded scales at 650°C.	Constituents present in corroded scales at 850°C.
Borate	Na_2SO_4	Fe_3BO_6, Fe_2O_3, FeS	Fe_3BO_6, Fe_2O_3, FeS and Fe_3O_4
Carbide	Na_2SO_4	Fe_2O_3, ZrO_2, FeS, SiC, Cr_2O_3	ZrO_2, FeS, Fe_2O_3, Fe_3O_4 and SiC.
Chromate	Na_2SO_4	Fe_2O_3, $PbFe_6O_7$, $FeCr_2O_4$, Cr_2O_3 FeS and Cr_2S_3	$PbFe_6O_7$, $FeCr_2O_4$, Fe_2O_3 Cr_2O_3, FeS, Cr_2S_3
Uncoated	Na_2SO_4	Fe_2O_3 and FeS	Fe_2O_3, FeS and FeO.

Table - 6.2

Immersion tests on coatings at ambient temperature for 24 hours (% wt. loss) in 0.5N concentration of the following solvents.

Coatings	H_2SO_4	HNO_3	HCl	NaOH	Acetone	Benzene	Alcohol	H_2O
Borate	3.5	2.5	5	N.C.	N.C.	N.C.	N.C.	N.C.
Carbide	4.5	3.5	6	N.C.	N.C.	N.C.	N.C.	N.C.
Chromate	1.2	3.0	4.5	N.C.	N.C.	N.C.	N.C.	N.C.
Uncoated	7.5	5.0	10	N.C.	N.C.	N.C.	N.C.	N. C.

Table - 6.3

Parabolic rate constant K_p ($g^2\ cm^{-4}\ sec^{-1}$) of coated and uncoated alloy in the temperature range 400 - 800°C ($\times 10^{-10}\ g^2\ cm^{-21}\ sec^{-1}$).

Coatings	400°C	600°C	800°C
Borate	0.001	17.3	1100
Carbide	0.009	97.0	1300
Chromate	0.28	24.0	1600
Uncoated	2.9	110.0	2700

Table - 6.4

Critical amount of Na_2SO_4 required for maximum corrosion of coated and uncoated mild steel in the temperature range 700 - 850°C ($\times 10^{-3}\ g/cm^2$).

Coatings	700°C	750°C	800°C	850°C
Borate	4.4	4.3	3.8	0.5
Carbide	1.3	7.8	4.6	3.0
Chromate	6.0	7.4	4.2	0.4
Uncoated	3.1	6.5	4.0	0.4

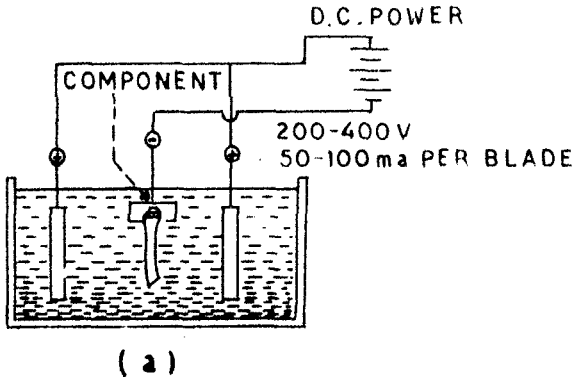

ELECTROPHORESIS

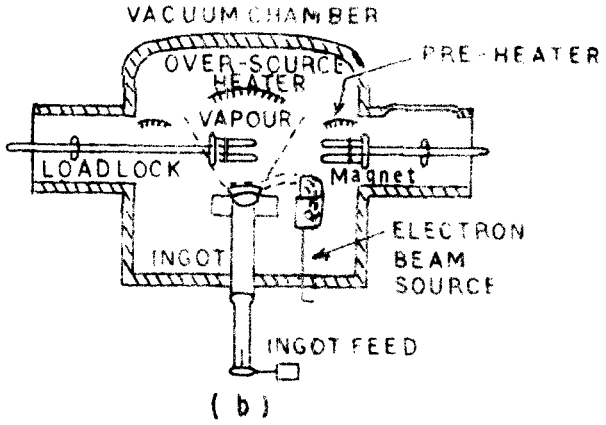

ELECTRON BEAM EVAPORATION

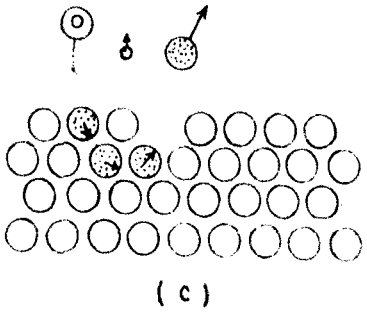

BASIC SPUTTER MECHANISM

FIG. 1

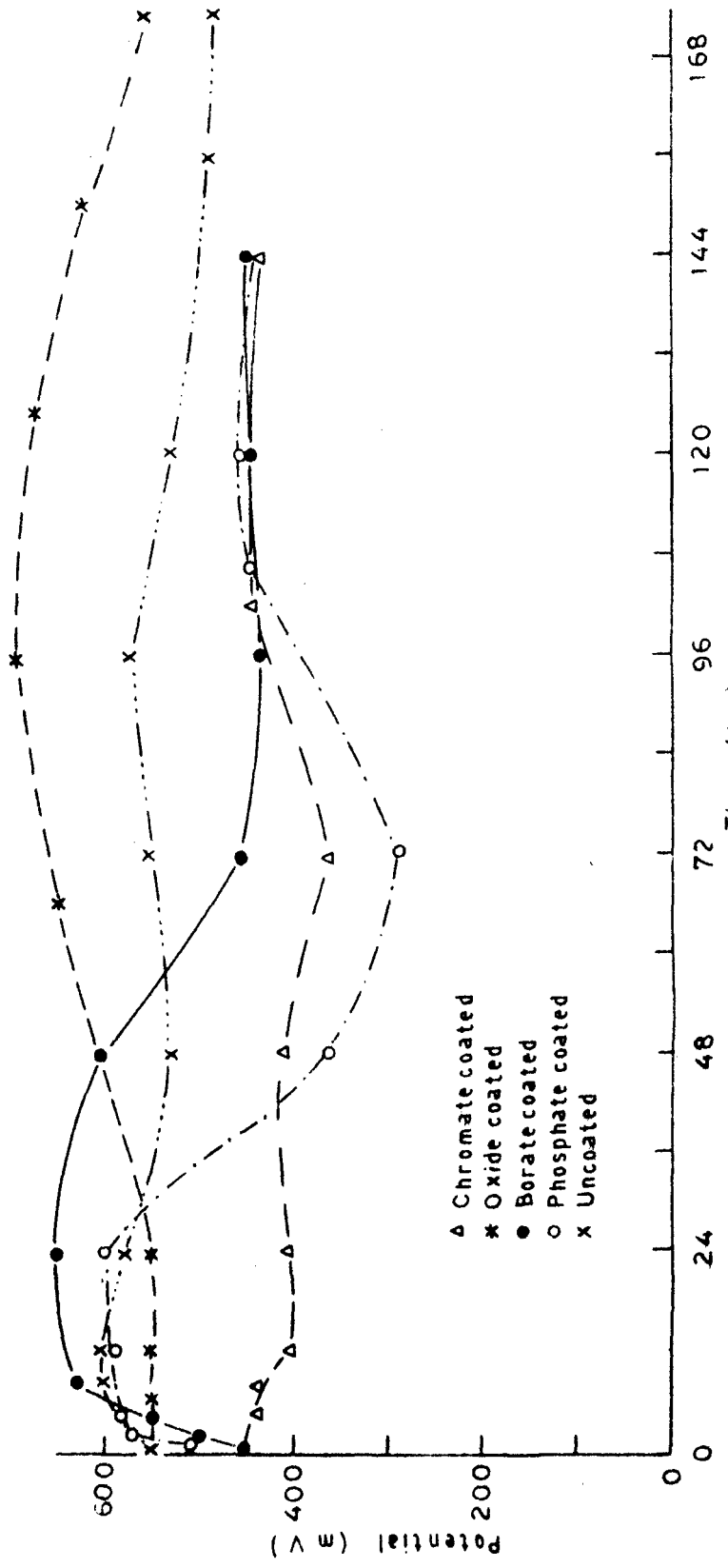

FIG.3.1 POTENTIAL VS. TIME PLOTS OF COATED AND UNCOATED STEEL IN HCl

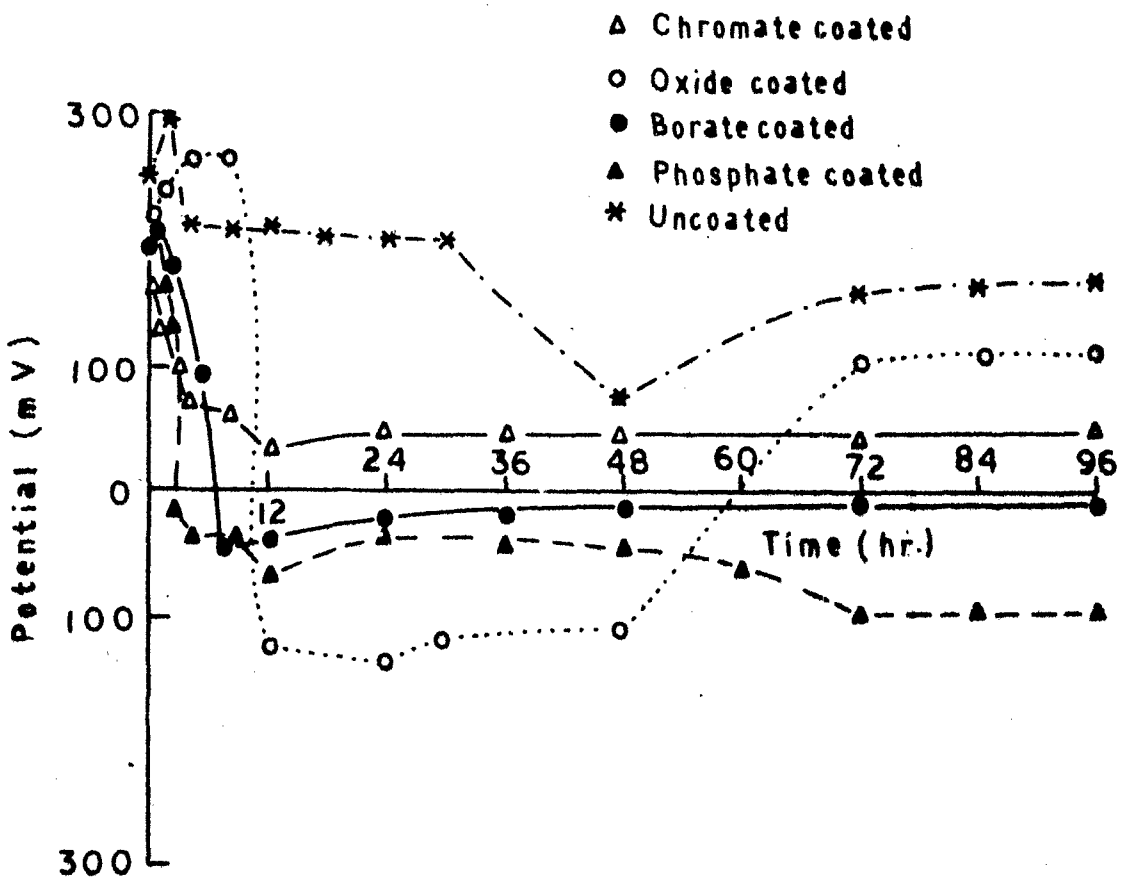

FIG. 3.2 POTENTIAL VS. TIME PLOTS OF COATED AND UNCOATED STEEL IN HNO_3

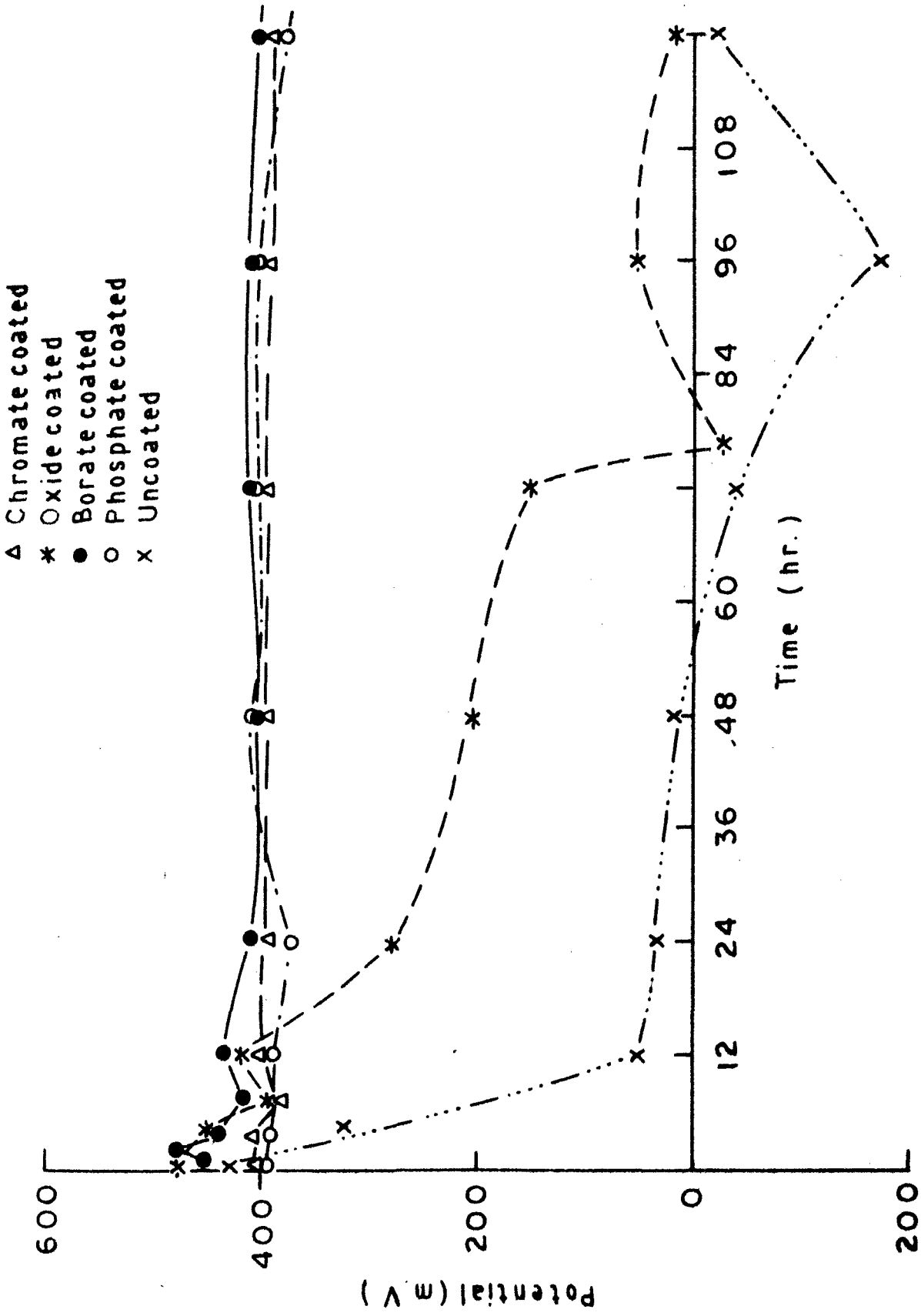

FIG. 3.3 POTENTIAL VS. TIME PLOTS OF COATED AND UNCOATED STEEL IN H_2SO_4

Figure 4.1 Thermogravimetric apparatus for investigation of the oxidation kinetics of metals in air.

1. Semimicroanalytical balance,
2. Platinum wire,
3. Heat - insulation plate,
4. Ceramic plug,
5. Thermoelement,
6. Aluminium tube,
7. Sample,
8. Heat insulating mass,
9. Heater.

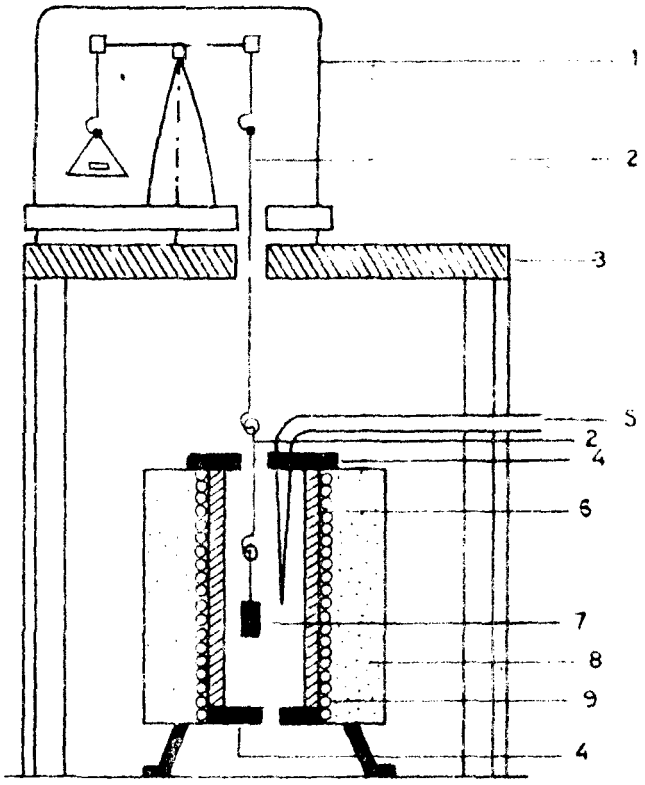

FIG. 4.1 THERMOGRAVIMETRIC APPARATUS

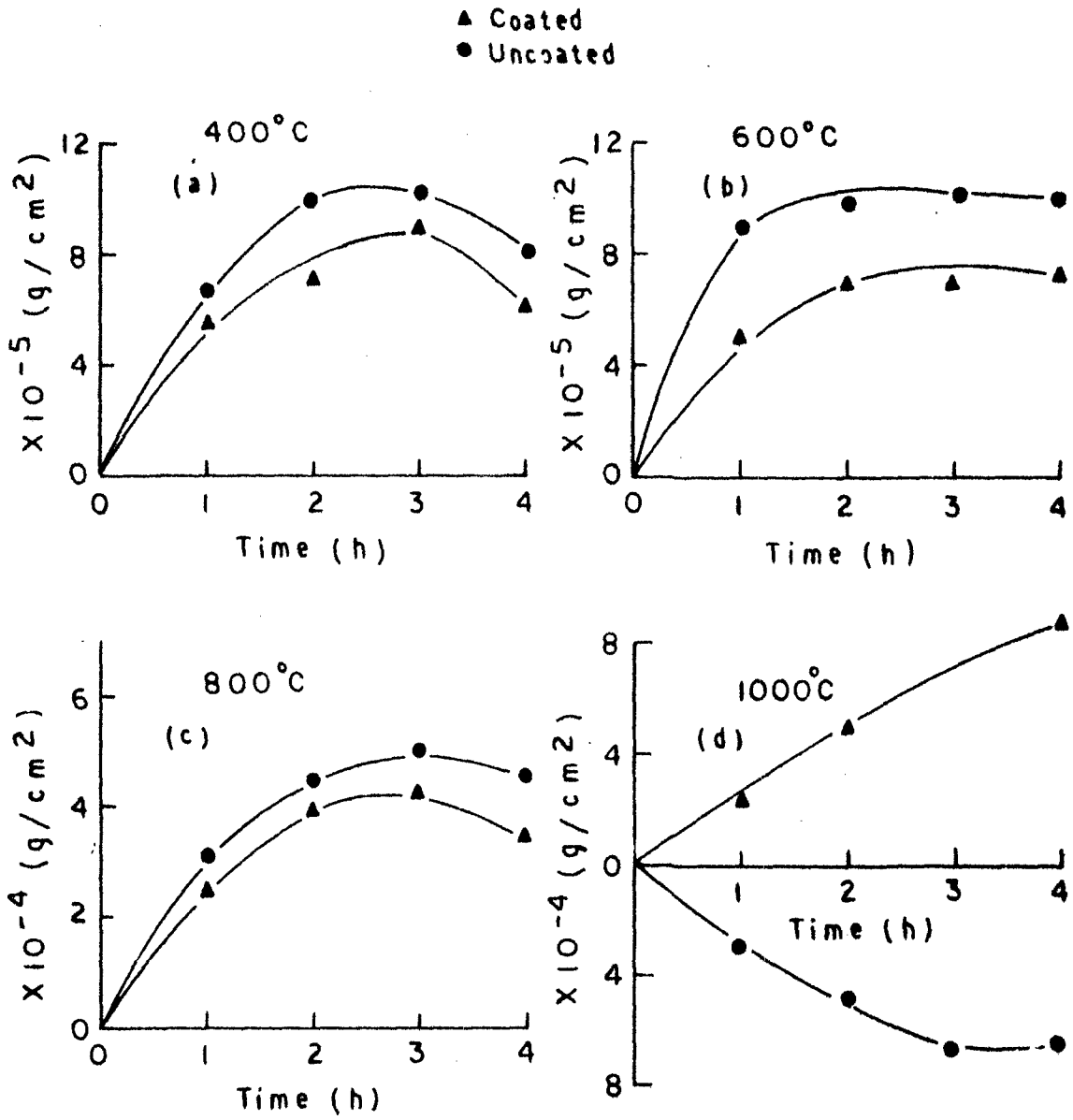

FIG.4.2 WEIGHT GAIN VS. TIME PLOTS OF PHOSPHATE COATED AND UNCOATED STEEL

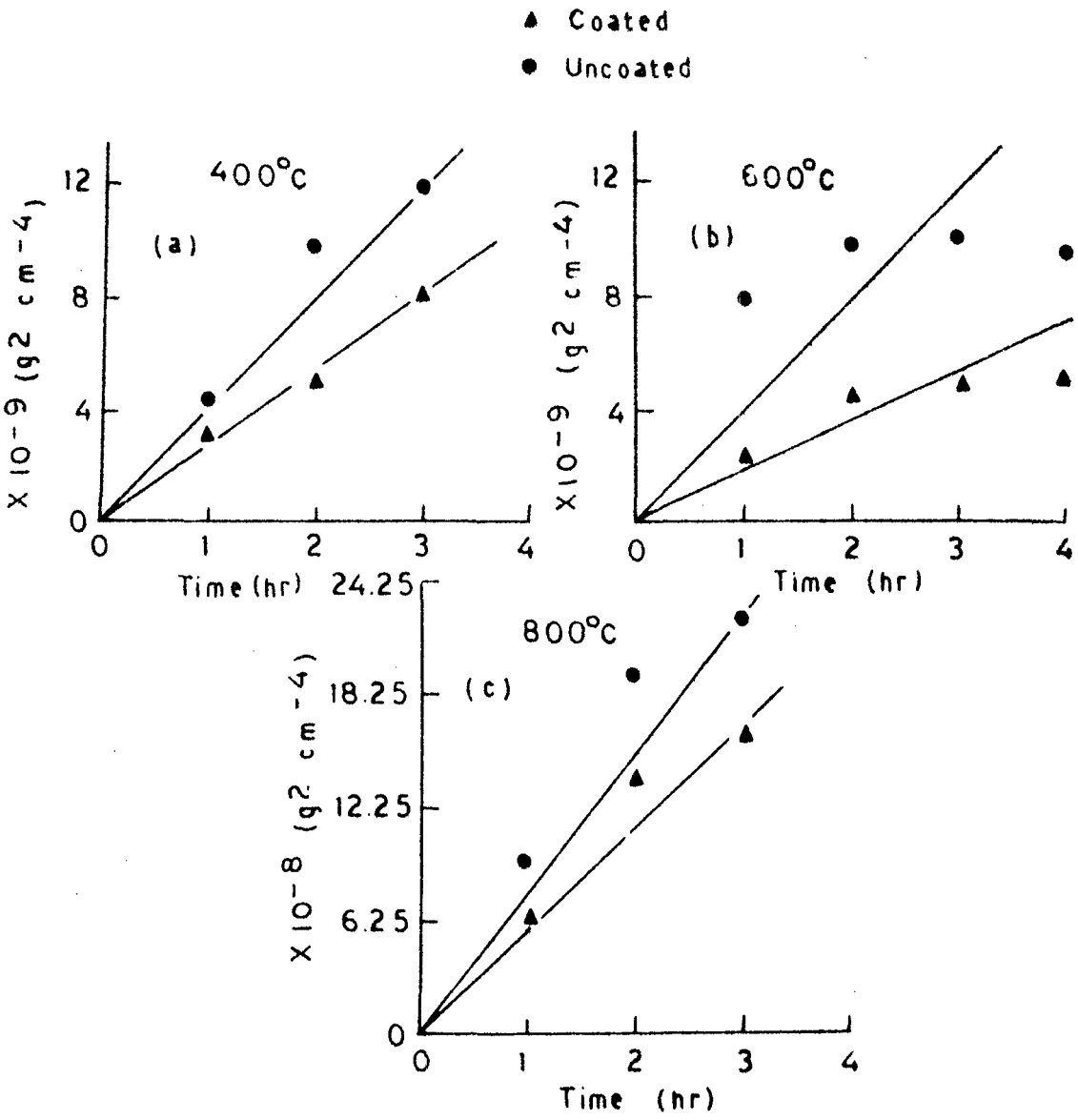

FIG. 4.3 WEIGHT GAIN^2 VS. TIME PLOTS OF PHOSPHATE COATED AND UNCOATED STEEL

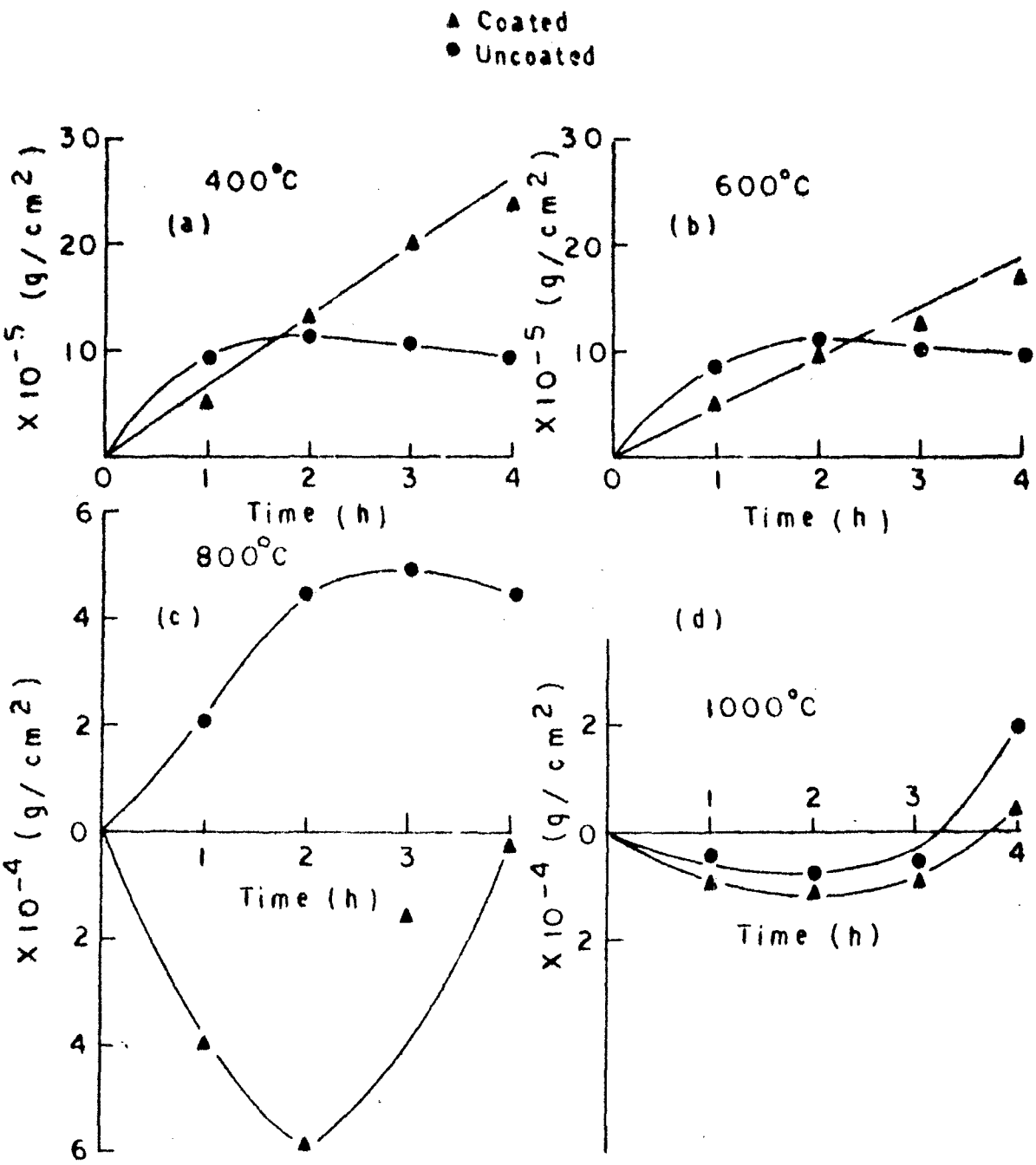

FIG.4.4 WEIGHT GAIN VS. TIME PLOT OF SILICATE COATED AND UNCOATED STEEL

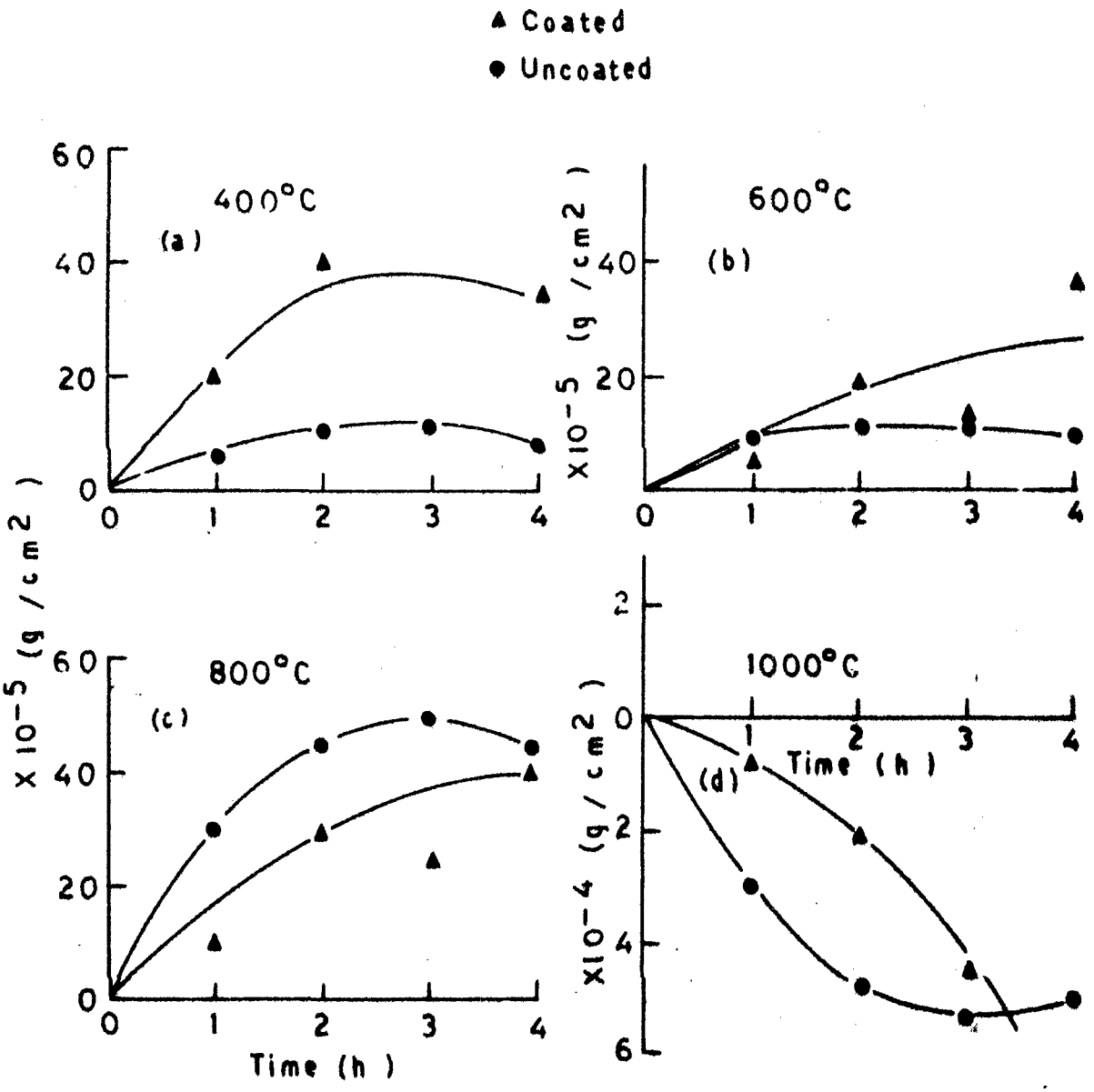

FIG. 4.5 WEIGHT GAIN VS. TIME PLOTS OF BORATE COATED AND UNCOATED STEEL.

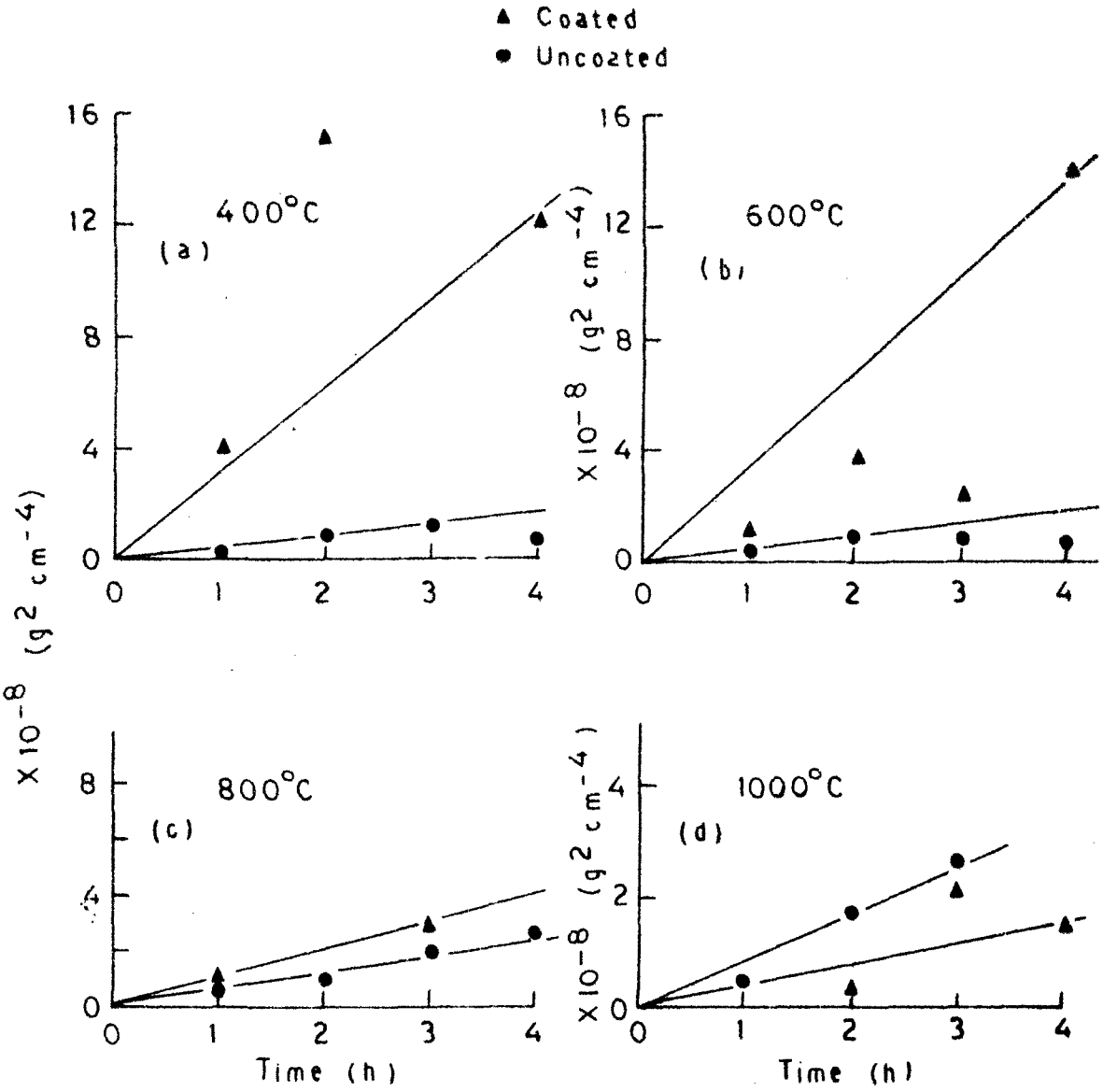

FIG. 4.6 WEIGHT GAIN^2 VS TIME PLOTS OF BORATE COATED AND UNCOATED STEEL

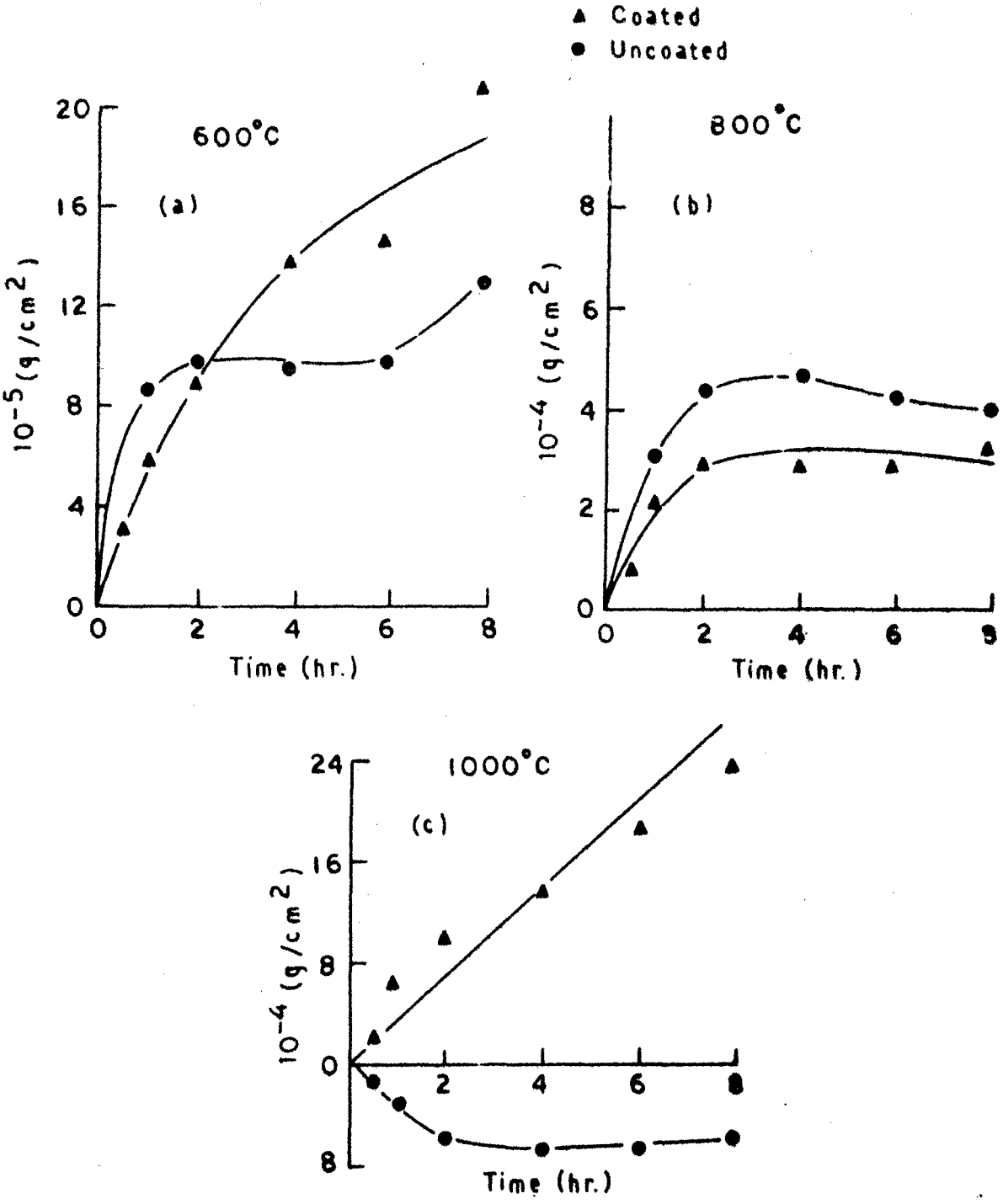

FIG. 4.7 WEIGHT GAIN VS. TIME PLOTS OF OXIDE COATED AND UNCOATED STEEL

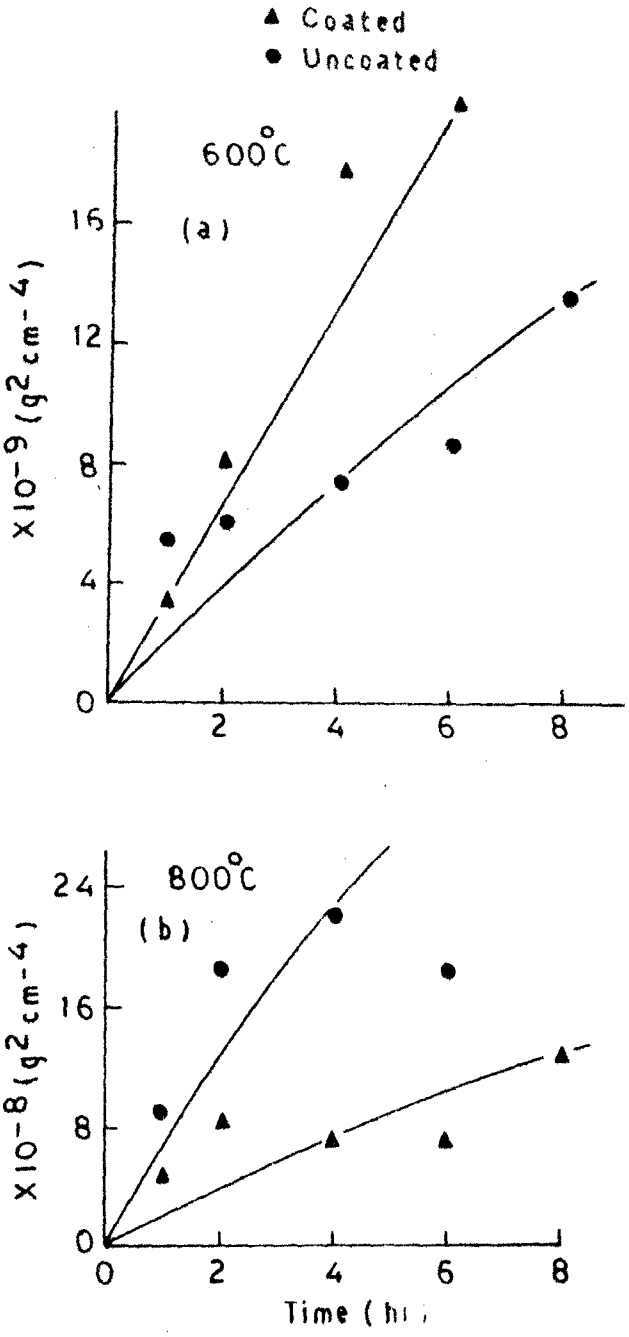

FIG. 4.8 WEIGHT GAIN^2 VS. TIME PLOTS OF OXIDE COATED AND UNCOATED STEEL

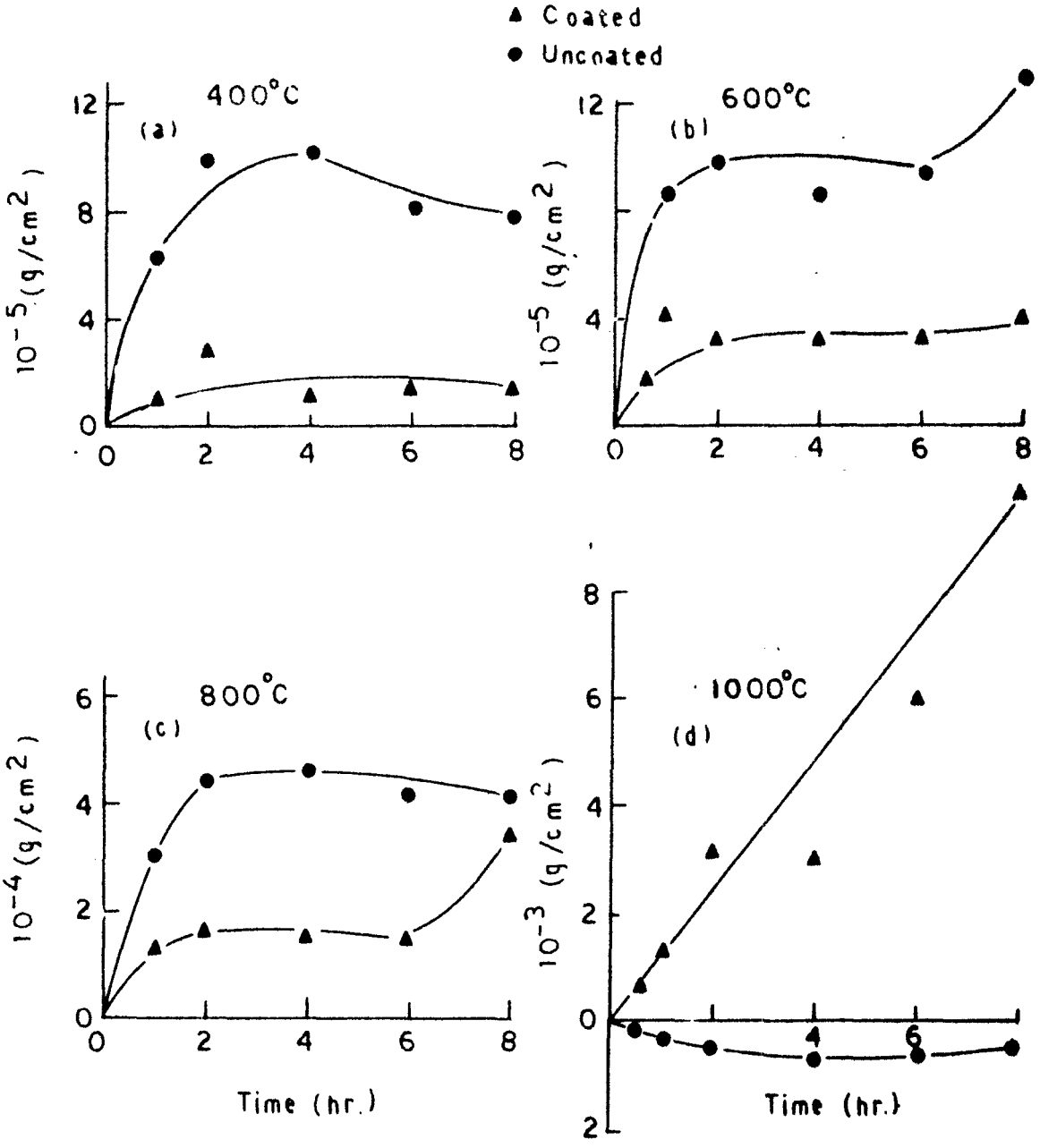

FIG. 4.9 WEIGHT GAIN VS. TIME PLOTS OF CHROMATE COATED AND UNCOATED STEEL.

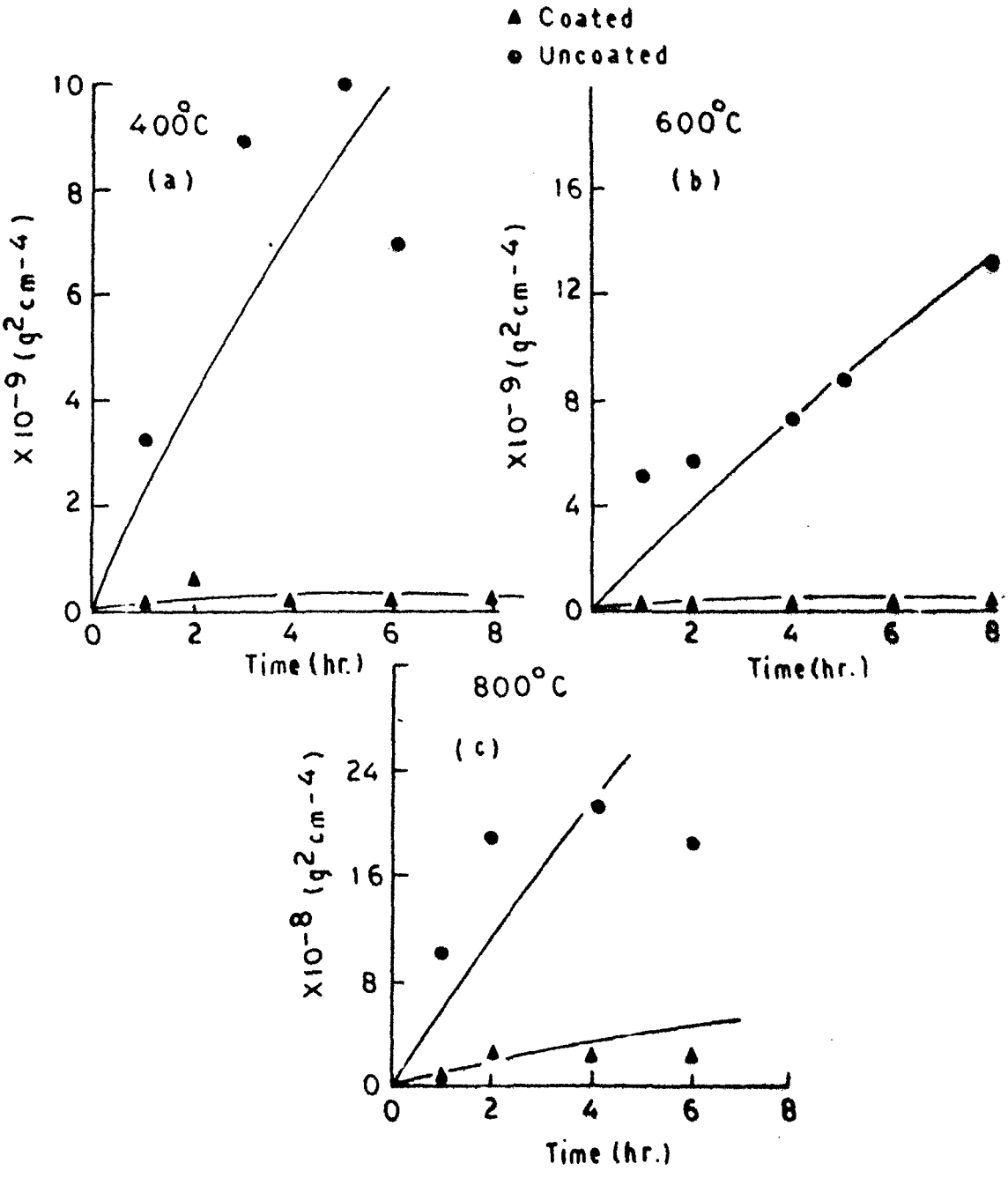

FIG. 4.10 WEIGHT GAIN^2 VS. TIME PLOTS OF CHROMATE COATED AND UNCOATED STEEL

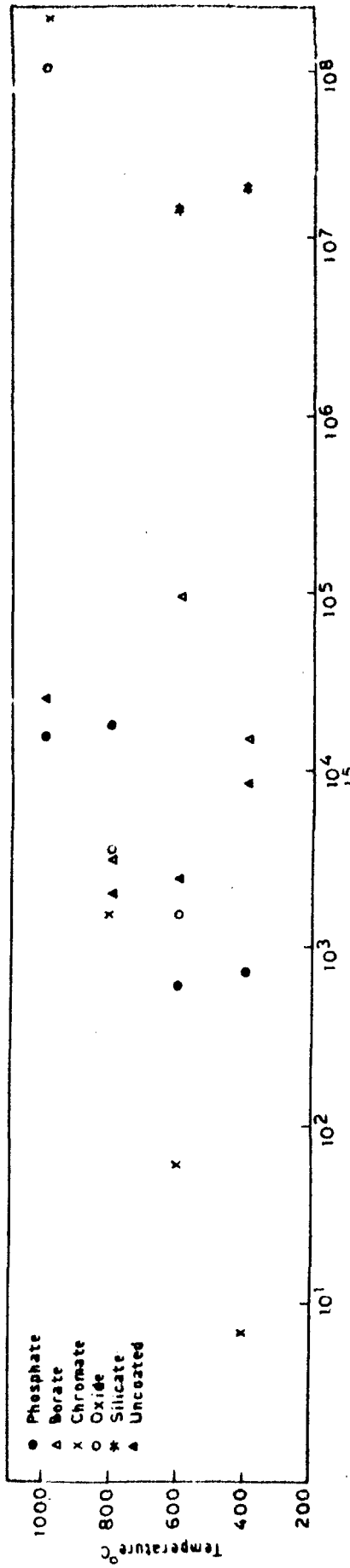

FIG. 4. 11 PLOTS OF OXIDATION RATE CONSTANT VS. TEMPERATURE FOR COATED AND UNCOATED STEEL

Figure 5.1(a) Weight gain vs temperature plots of phosphate coated and uncoated steel.

1. Na_2SO_4 sprayed on phosphate coated steel.
2. Na_2CO_3 sprayed on phosphate coated steel.
3. NaCl sprayed on phosphate coated steel.
4. Na_2SO_4 + NaCl sprayed on phosphate coated steel.
5. Na_2SO_4 + Na_2CO_3 sprayed on phosphate coated steel.
6. Na_2CO_3 + NaCl sprayed on phosphate coated steel.
7. Na_2SO_4 sprayed on uncoated steel.
8. Na_2CO_3 sprayed on uncoated steel.
9. NaCl sprayed on uncoated steel.
10. Na_2SO_4 + NaCl sprayed on uncoated steel.
11. Na_2SO_4 + Na_2CO_3 sprayed on uncoated steel.
12. Na_2CO_3 + NaCl sprayed on uncoated steel.

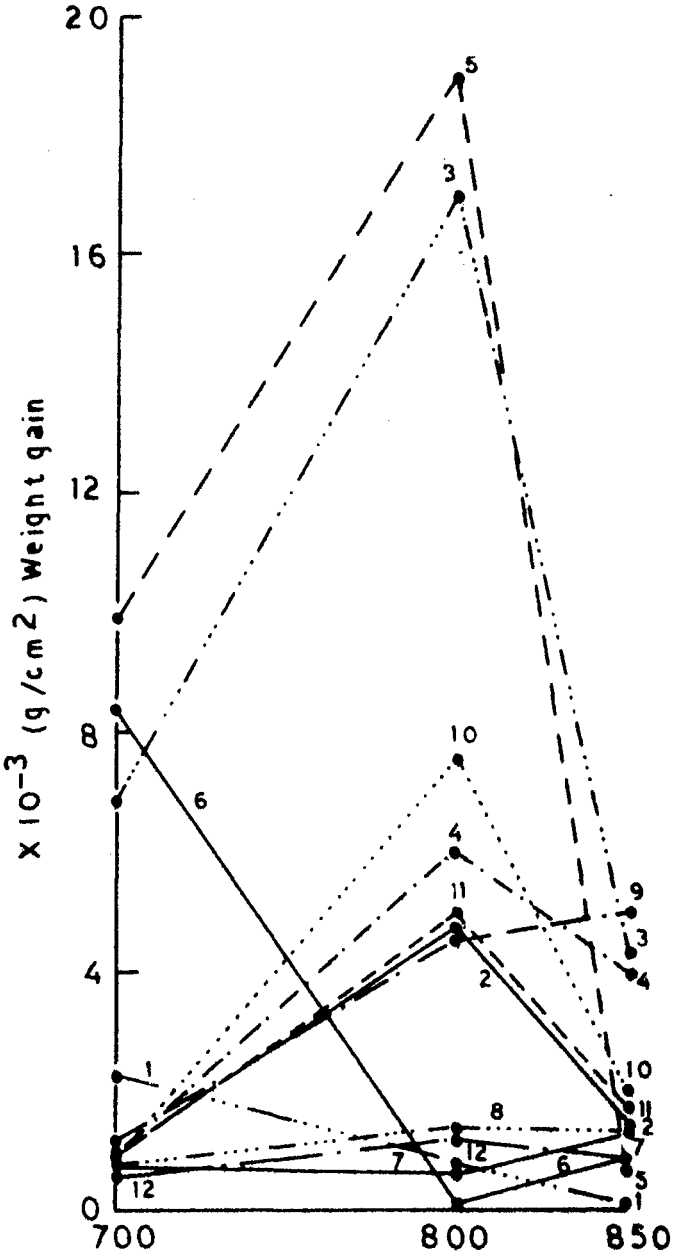

FIG. 5.1 (a) WEIGHT GAIN VS. TEMPERATURE PLOTS

Figure 5.1(b) Weight gain vs temperature plots of silicate coated and uncoated steel.

1. Na_2SO_4 sprayed on silicate coated steel.
2. Na_2CO_3 sprayed on silicate coated steel.
3. NaCl sprayed on silicate coated steel.
4. Na_2SO_4 + NaCl sprayed on silicate coated steel.
5. Na_2SO_4 + Na_2CO_3 sprayed on silicate coated steel.
6. Na_2SO_4 + NaCl sprayed on silicate coated steel.
7. Na_2SO_4 sprayed on uncoated steel.
8. Na_2CO_3 sprayed on uncoated steel.
9. NaCl sprayed on uncoated steel.
10. Na_2SO_4 + NaCl sprayed on uncoated steel.
11. Na_2SO_4 + Na_2CO_3 sprayed on uncoated steel.
12. Na_2CO_3 + NaCl sprayed on uncoated steel.

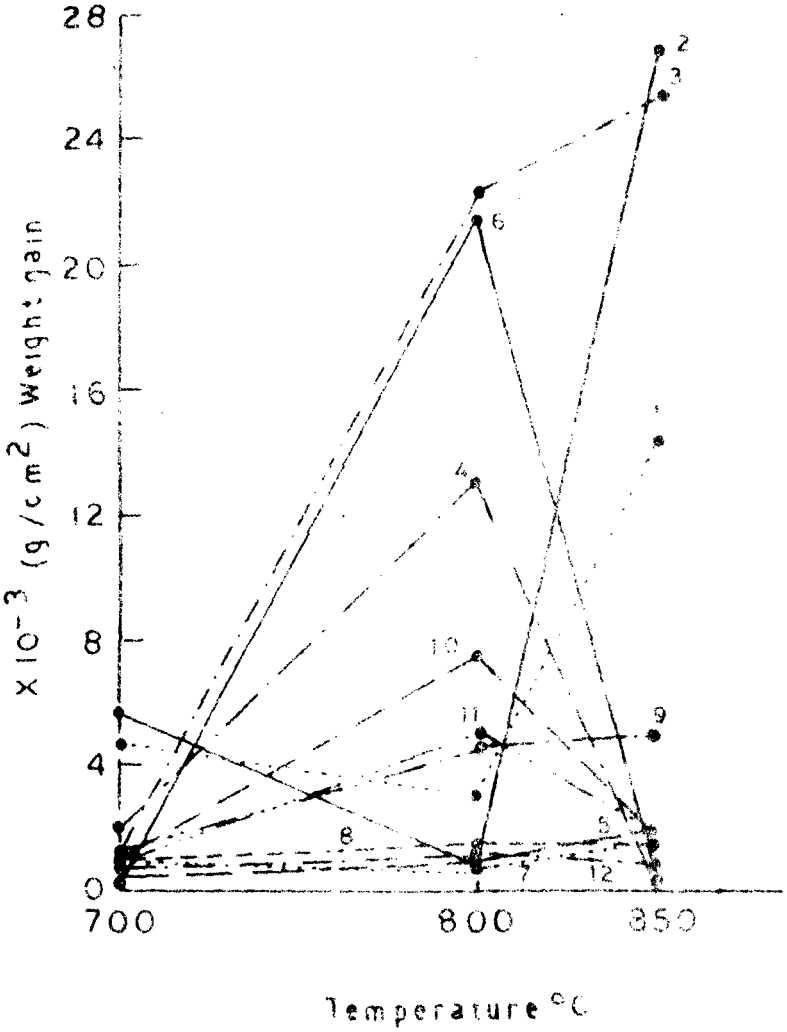

FIG 5.1(b) WEIGHT GAIN VS TEMPERATURE PLOTS

Figure 5.1(c) Weight gain vs temperature plots of borate and uncoated steel.

1. Na_2SO_4 sprayed on borate coated steel.
2. Na_2CO_3 sprayed on borate coated steel.
3. NaCl sprayed on borate coated steel.
4. Na_2SO_4 + NaCl sprayed on borate coated steel.
5. Na_2SO_4 + Na_2CO_3 sprayed on borate coated steel.
6. Na_2CO_3 + NaCl sprayed on borate coated steel.
7. Na_2SO_4 sprayed on uncoated steel.
8. Na_2CO_3 sprayed on uncoated steel.
9. NaCl sprayed on uncoated steel.
10. Na_2SO_4 + NaCl sprayed on uncoated steel.
11. Na_2SO_4 + Na_2CO_3 sprayed on uncoated steel.
12. Na_2CO_3 + NaCl sprayed on uncoated steel.

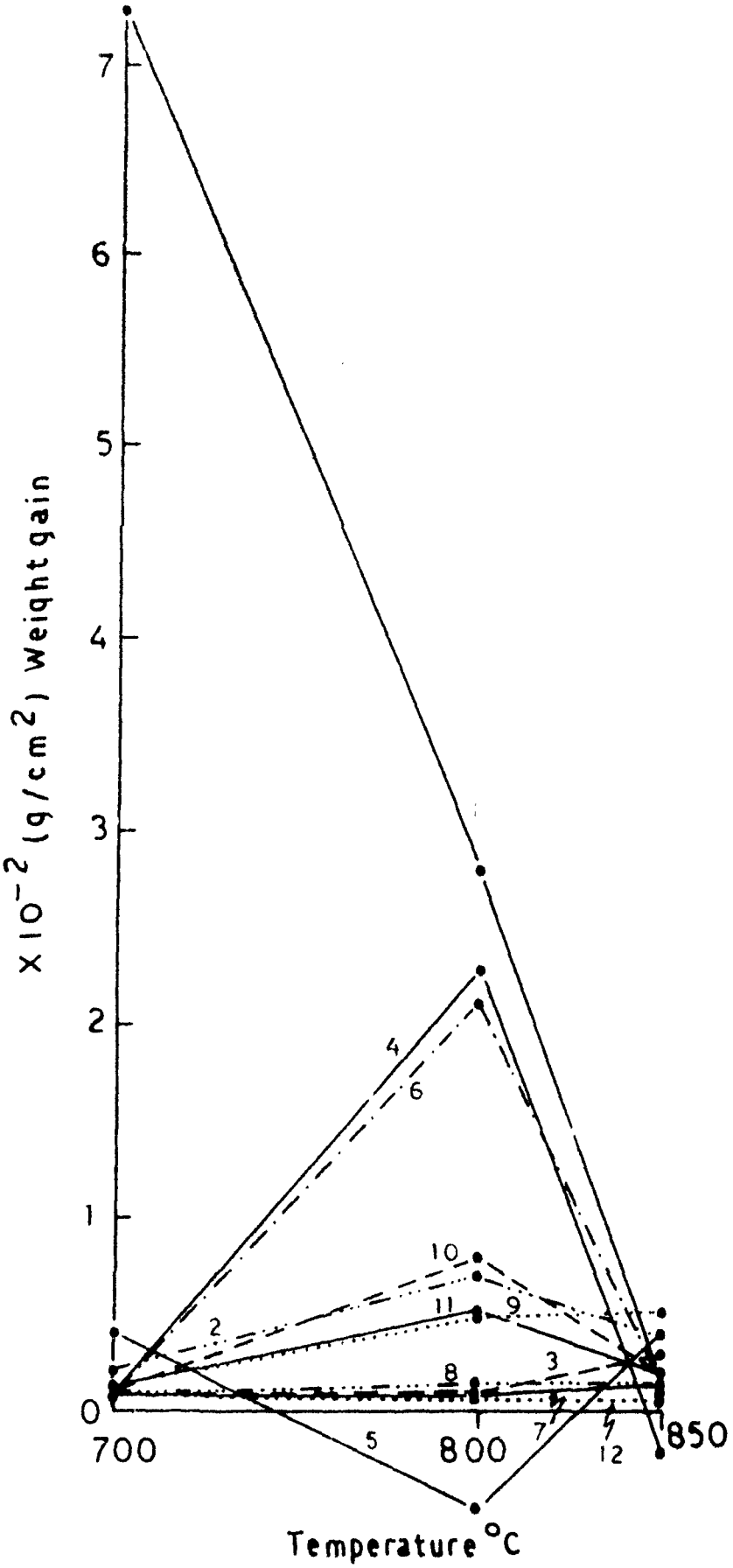

FIG. 5.1 (c) WEIGHT GAIN VS. TEMPERATURE PLOTS

Figure 5.1(d) Weight gain vs temperature plots of chromate coated and uncoated steel.

1. Na_2SO_4 sprayed on chromate coated steel.
2. Na_2CO_3 sprayed on chromate coated steel.
3. NaCl sprayed on chromate coated steel.
4. [illegible] + Na_2SO_4 + Na_2CO_3 sprayed on chromate coated steel.
5. Na_2CO_3 + NaCl sprayed on chromate coated steel.
6. Na_2SO_4 sprayed on uncoated steel.
7. Na_2CO_3 sprayed on uncoated steel.
8. NaCl sprayed on uncoated steel.
9. Na_2SO_4 + Na_2CO_3 sprayed on uncoated steel.
10. Na_2CO_3 + NaCl sprayed on uncoated steel.

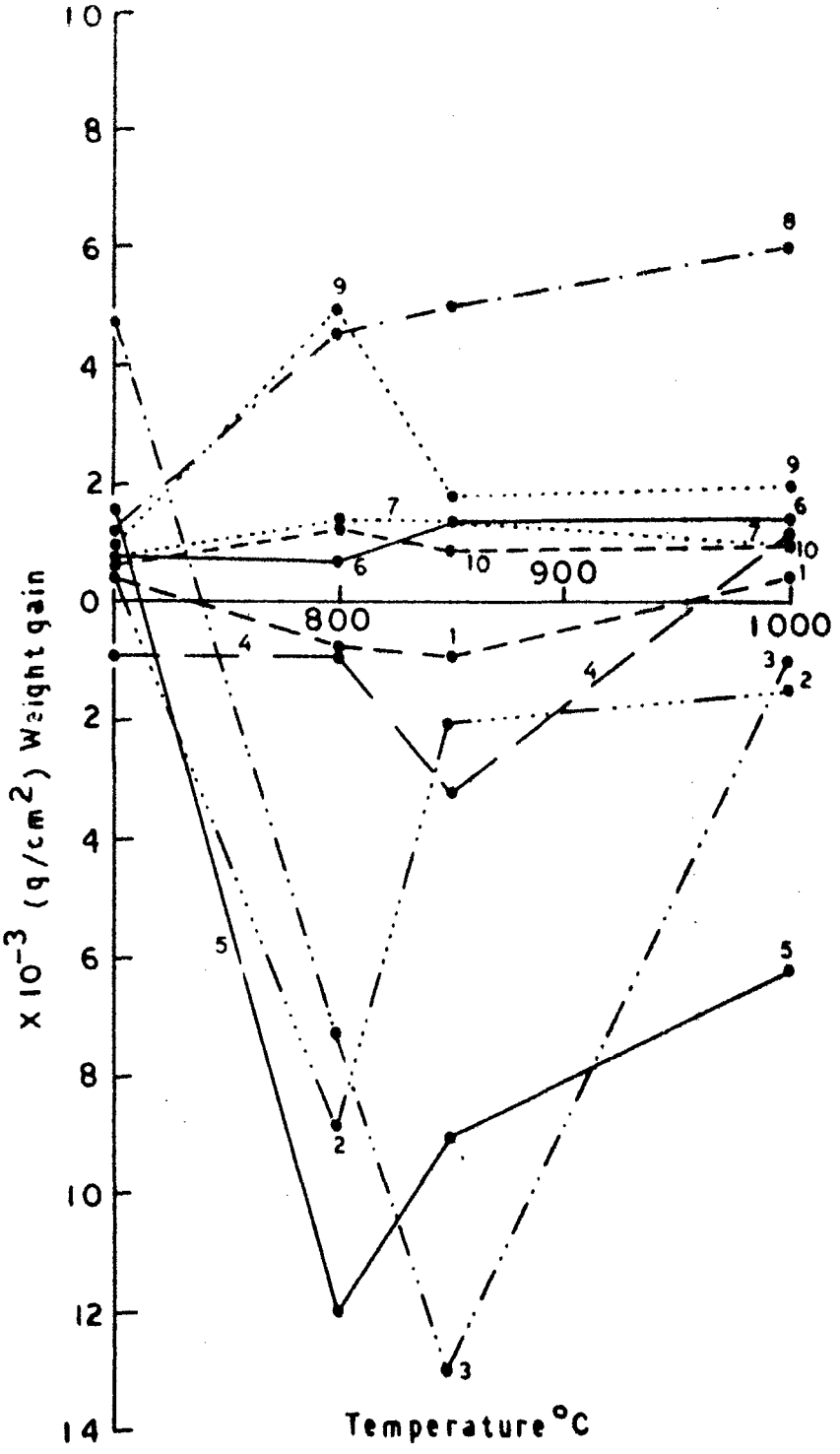

FIG. 5.1 (d) WEIGHT GAIN VS. TEMPERATURE PLOTS

Figure 5.1(a) Weight gain vs temperature plots of oxide coated and uncoated steel.

1. Na_2SO_4 sprayed on oxide coated steel.
2. Na_2CO_3 sprayed on oxide coated steel.
3. NaCl sprayed on oxide coated steel.
4. $Na_2SO_4 + Na_2CO_3$ sprayed on oxide coated steel.
5. $Na_2CO_3 + NaCl$ sprayed on oxide coated steel.
6. Na_2SO_4 sprayed on uncoated steel.
7. Na_2CO_3 sprayed on uncoated steel.
8. NaCl sprayed on uncoated steel.
9. $Na_2SO_4 + Na_2CO_3$ sprayed on uncoated steel.
10. $Na_2CO_3 + NaCl$ sprayed on uncoated steel.

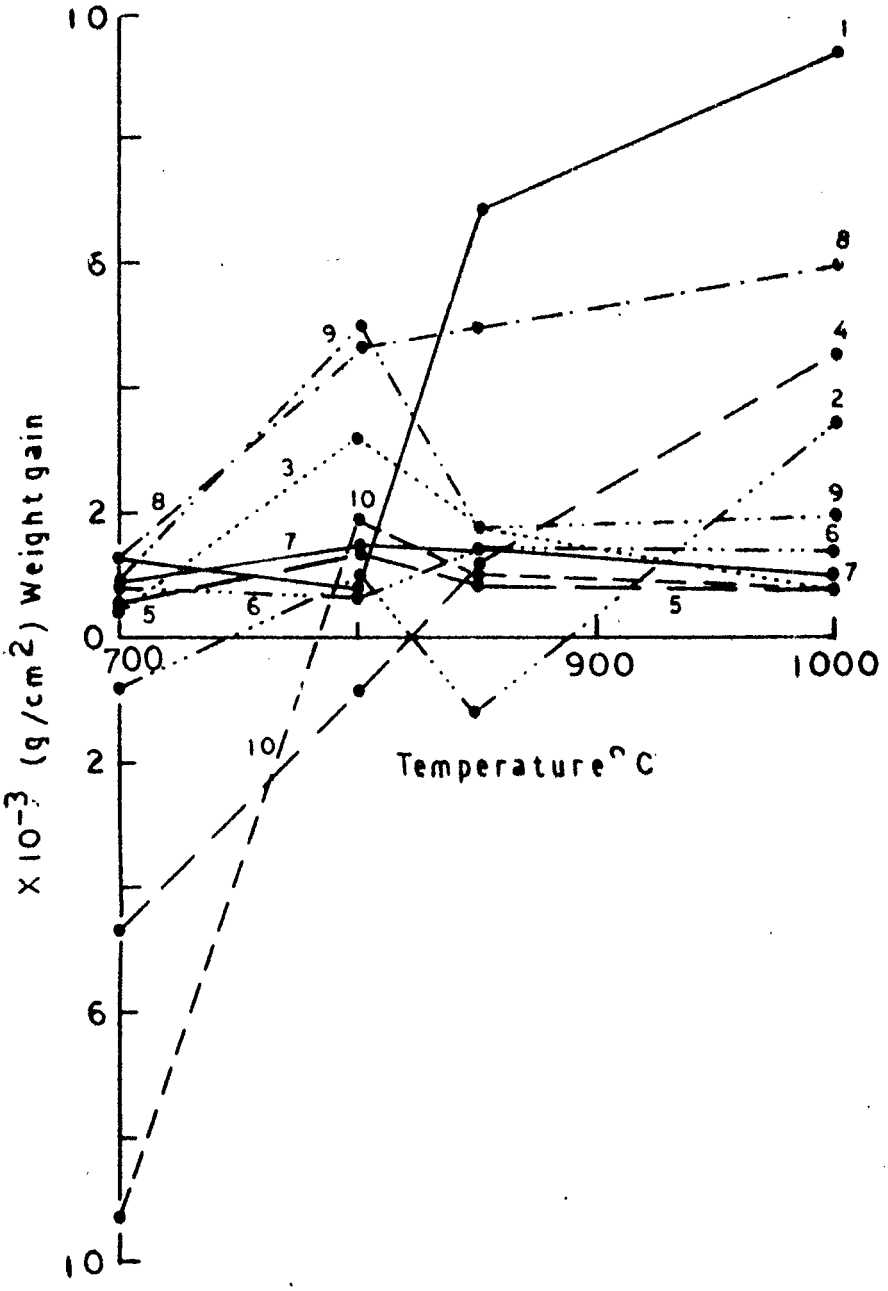

FIG. 5.1 (e) WEIGHT GAIN VS. TEMPERATURE PLOTS

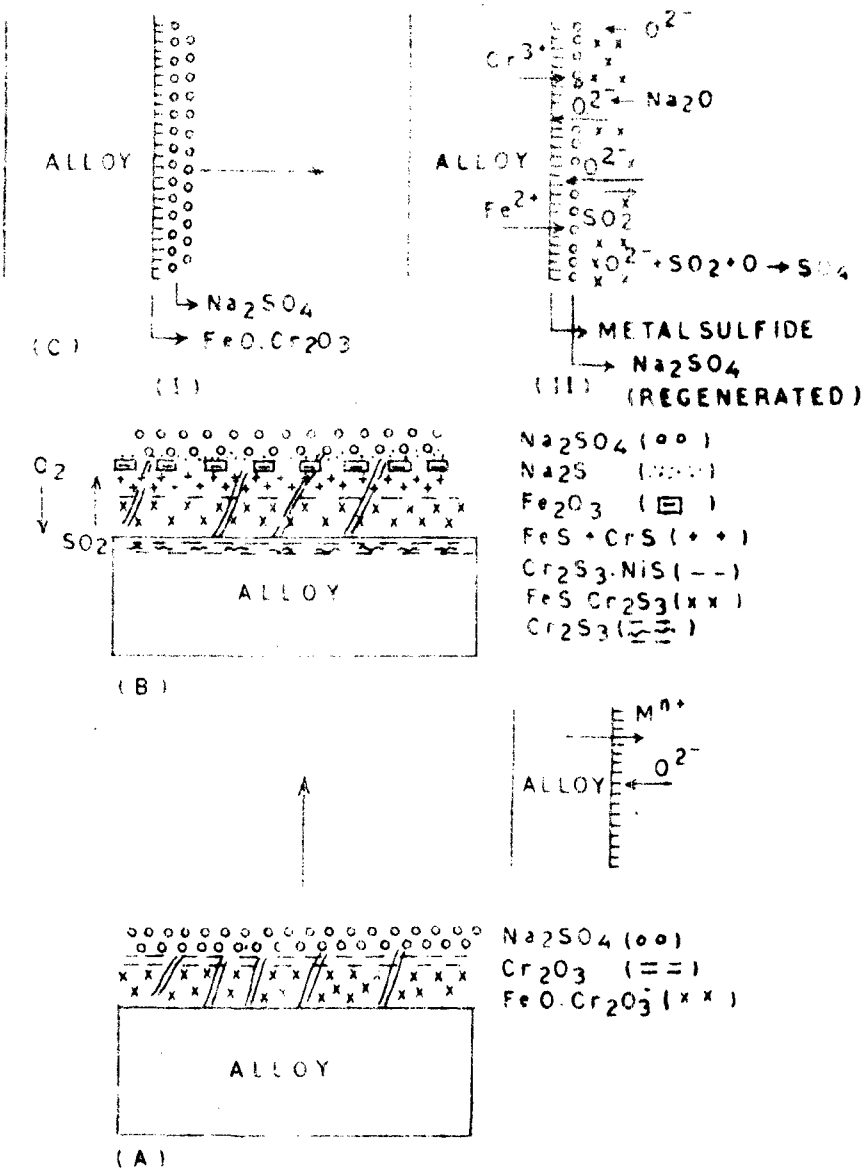

FIG. 5.9 SCHEMATIC DIAGRAMS FOR SULFIDATION OF 303 STEEL IN PRESENCE OF Na_2SO_4

A - Initiation stage B - Propagation stage
C - Sulfidation mechanism.
(I & II Initiation and propagation stages)

Figure 5.10 Schematic diagram for chlorination of AISI 303 steel in presence of molten NaCl.

(a) Initiation stage: Formation of protective oxide layer of spinel $FeO.Cr_2O_3$.

(b) Intermediate stage: NaCl( ) penetrates through the protective oxide and accumulates at the oxide/alloy and penetrates inside the metal.

(c) Propagation stage: NaCl reacts with FeO and Fe_2O_3 (if present) to form $FeCl_2$ and $FeCl_3$. $FeCl_3$ reacts with O_2 to form Fe_2O_3 and $Cl_2(g)$.

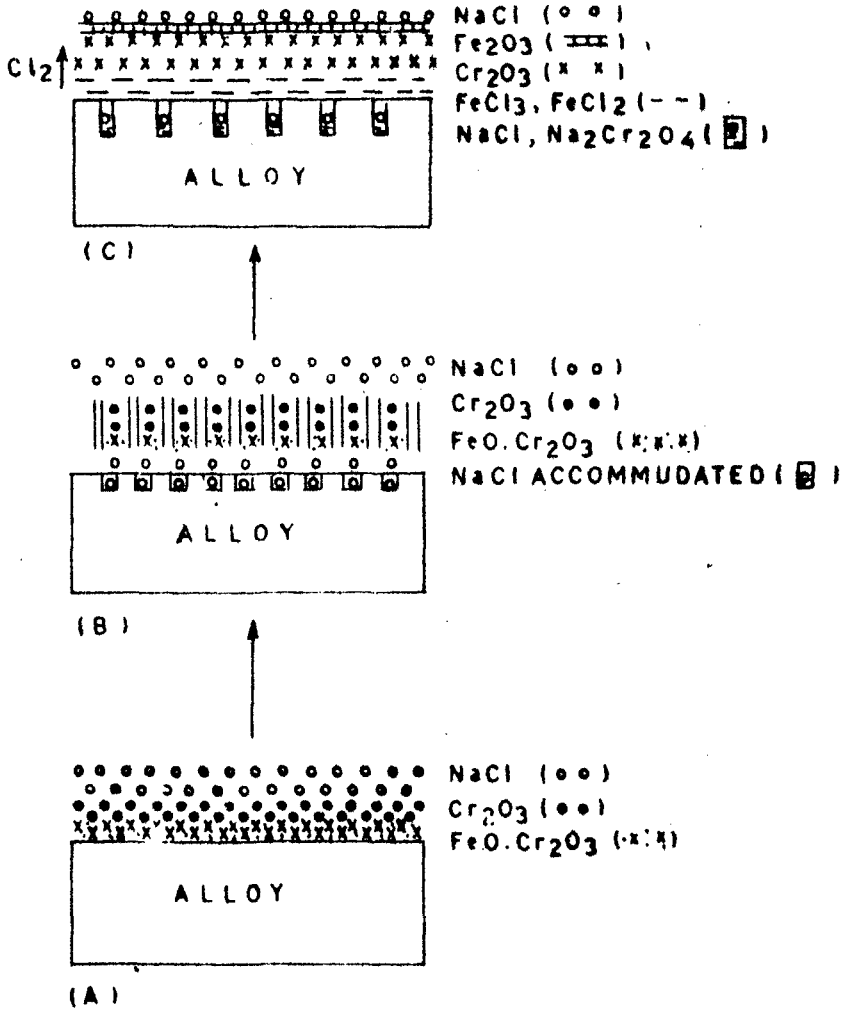

FIG. 5.10 SCHEMATIC DIAGRAMS FOR THE CHLORINATION OF 303 STEEL IN PRESENCE OF NaCl
A - INITIATION STAGE B - INTERMEDIATE STAGE
C - PROPAGATION STAGE

Figure 5.11 Schematic diagram for the sulfidation of AISI 303 steel in presence of Na_2SO_4 and NaCl.

(a) Initiation stage: Alloy forms protective coating of spinel $FeO.Cr_2O_3$ in air.

(b) Intermediate stage: The molten salt mixture penetrates through the protective layer.

(c) Propagation stage:

i) Sulfidation of the alloy occurs by S released from Na_2SO_4 resulting in the formation of Cr_2S_3, FeS and NiS scales.

ii) Formation of $FeCl_2$ by interaction of oxides of iron and NaCl.

iii) Release of Cl_2 by dechlorination of $FeCl_2$ resulting on the formation of pores.

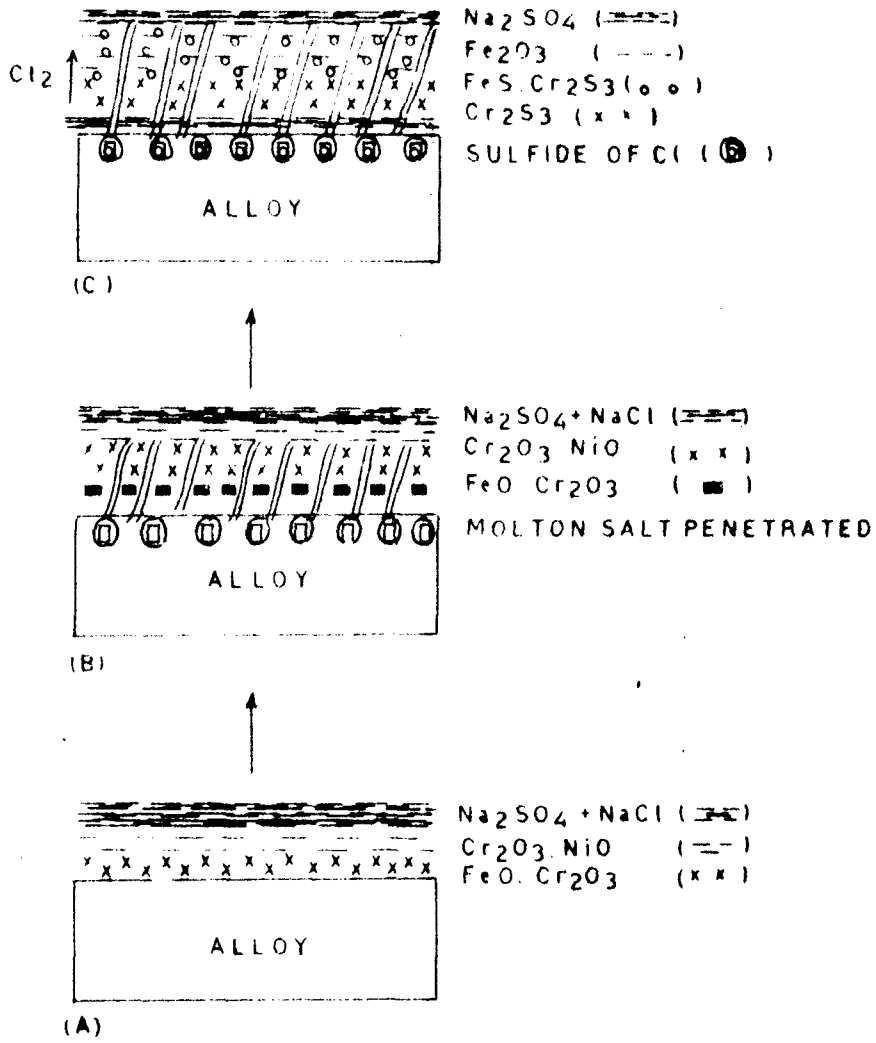

FIG. 5.11 SCHEMATIC DIAGRAMS FOR THE SULFIDATION OF 303 STEEL IN THE PRESENCE OF Na_2SO_4 AND NaCl
A - INITIATION STAGE B - INTERMEDIATE STAGE
C - PROPAGATION STAGE

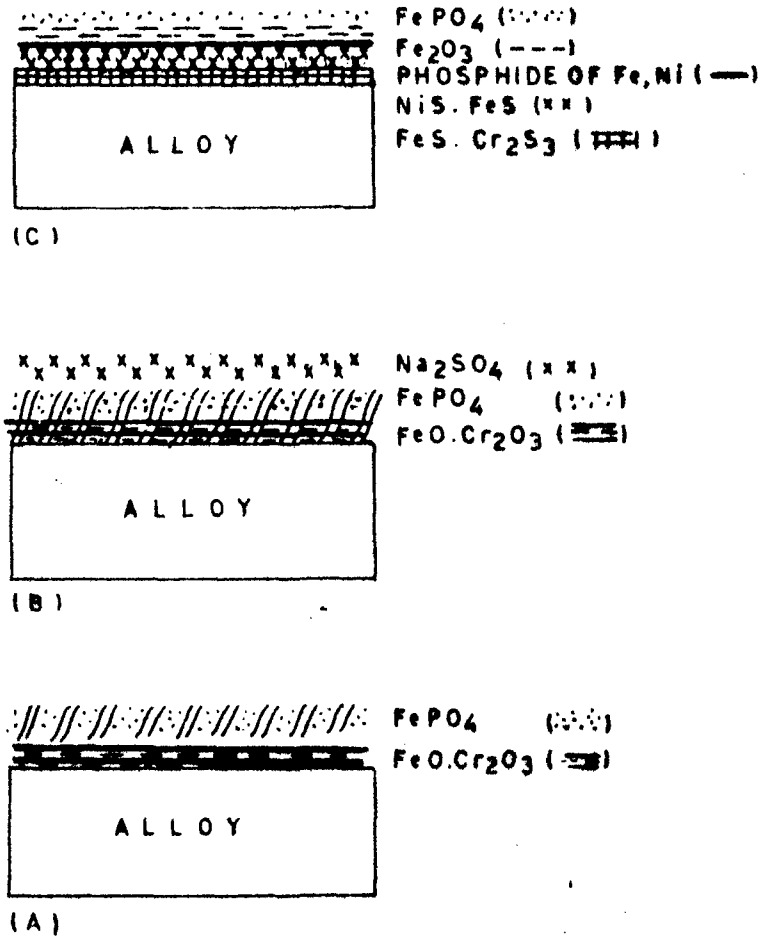

FIG. 5.12 SCHEMATIC DIAGRAMS FOR THE SULFIDATION OF PHOSPHATE COATED 303 STEEL IN PRESENCE OF Na_2SO_4
A - INITIATION STAGE B - PHOSPHATE COATING IN PRESENCE OF Na_2SO_4
C - PROPAGATION STAGE

Figure 5.13 Schematic diagram for the sulfidation of borate coating in presence of Na_2SO_4.

(a) Borate coated 303 steel.

(b) Borate coated 303 steel under a thin film of Na_2SO_4.

(c) Initiation stage

(d) Propagation stage, formation of sulfides Cr_2S_3, $(Fe\ Ni)S_2$ while coating materials remain intact.

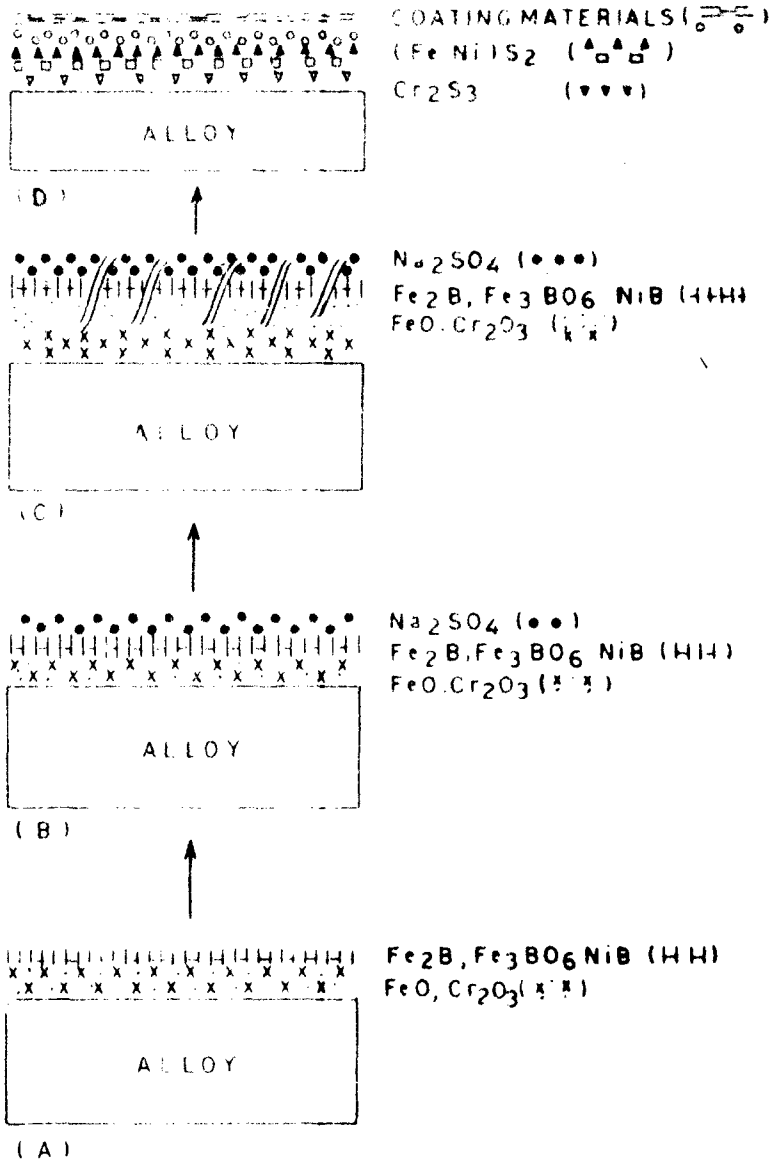

FIG. 5.13 SCHEMATIC DIAGRAMS FOR THE SULFIDATION OF BORATE COATED 303 STEEL IN PRESENCE OF Na_2SO_4

A - Borate coated steel B - Borate coated steel under a thin film of Na_2SO_4

C - Initiation stage D - Propagation stage

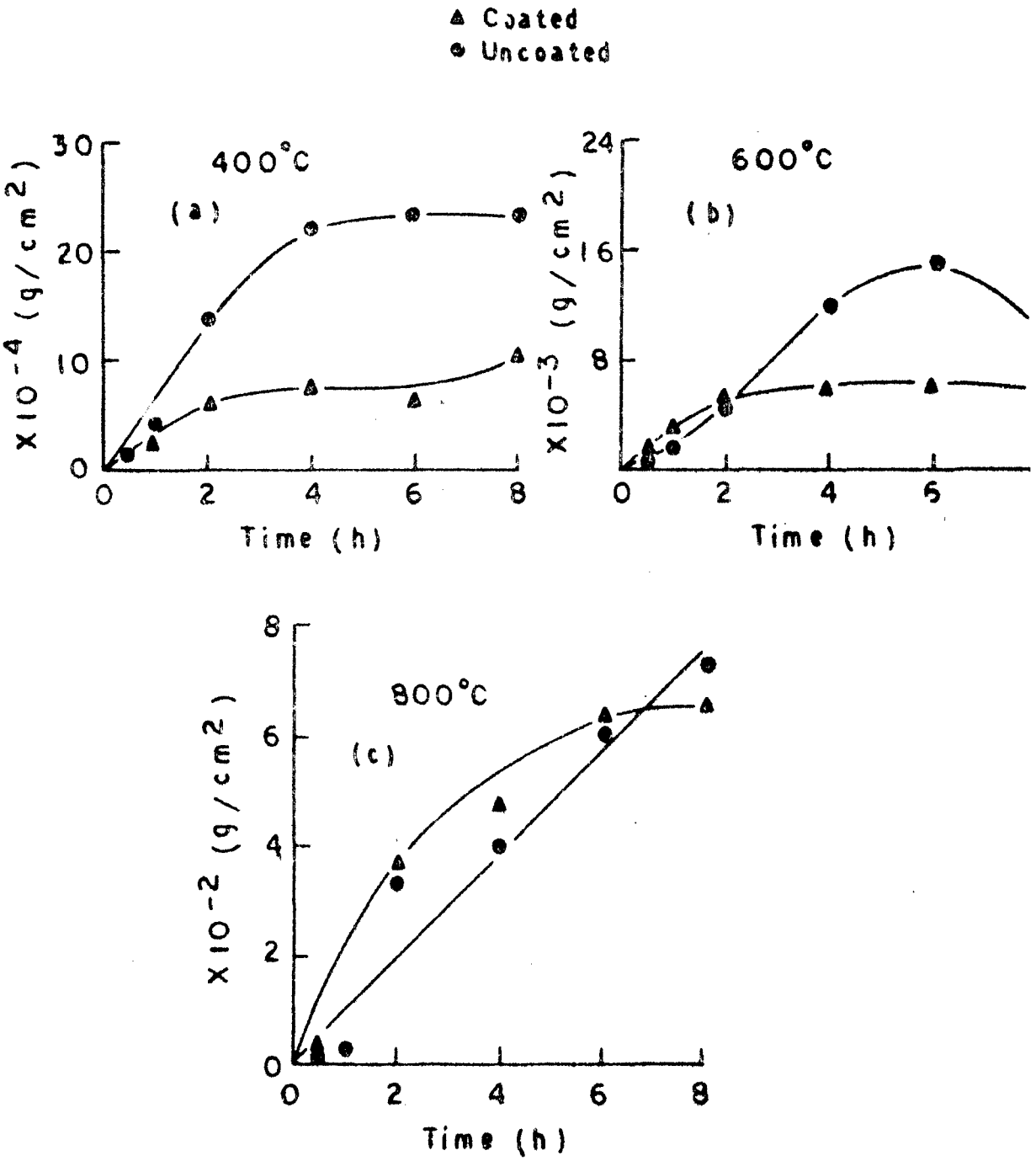

FIG 6.1 WEIGHT GAIN VS. TIME PLOTS OF CHROMATE COATED AND UNCOATED MILD STEEL

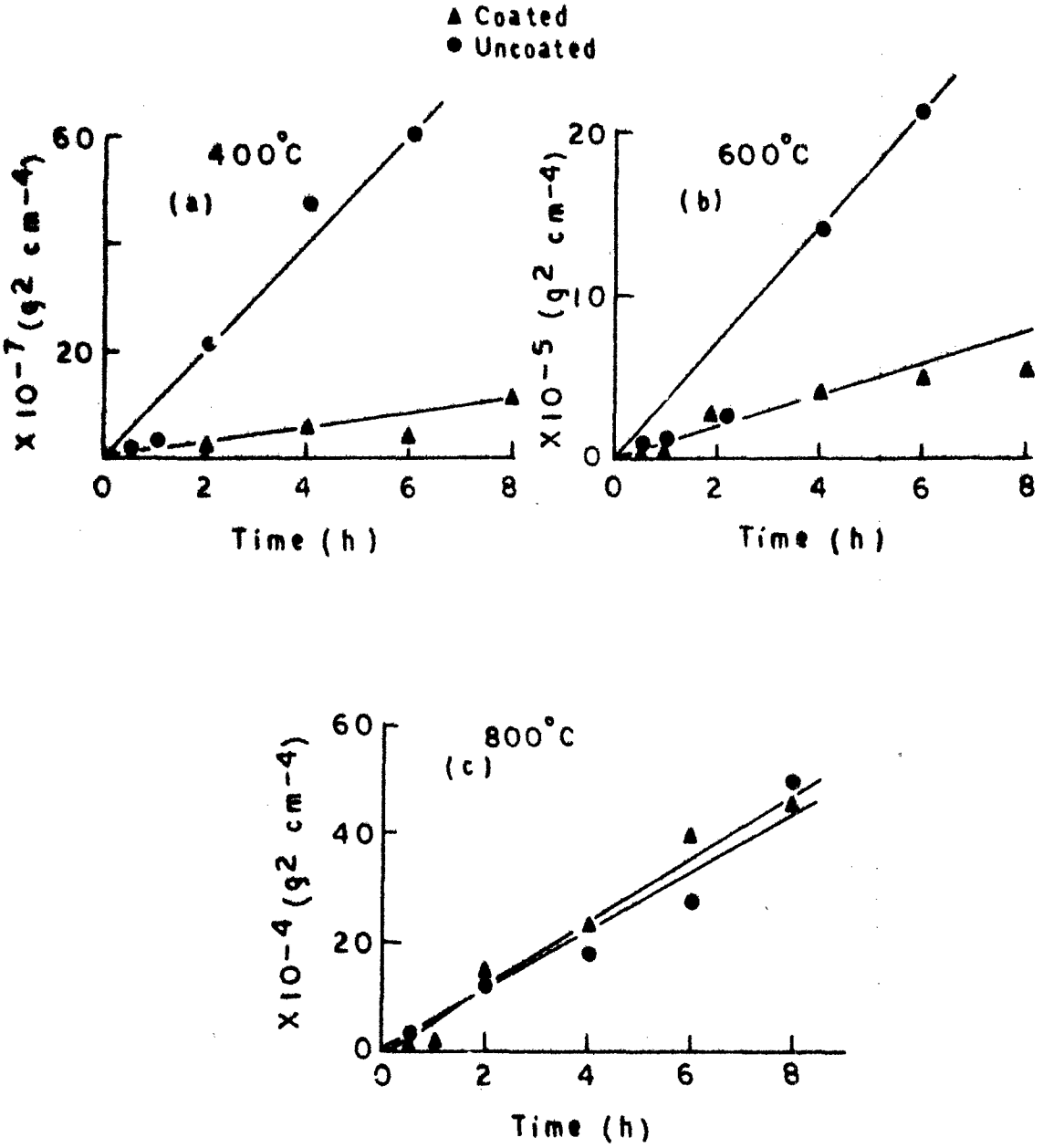

FIG.6.2 WEIGHT GAIN^2 VS. TIME PLOTS OF CHROMATE COATED AND UNCOATED MILD STEEL

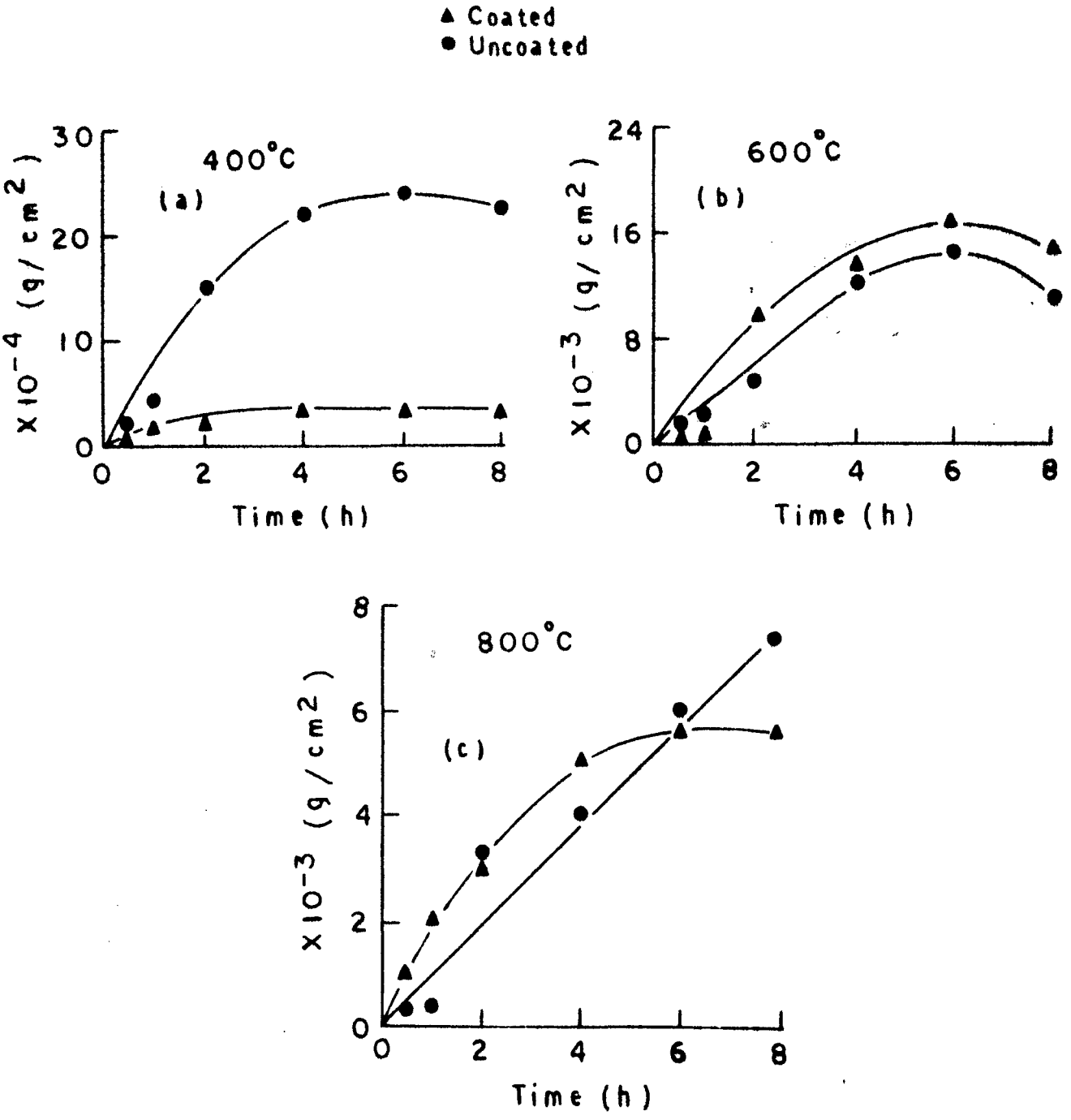

FIG.6.3 WEIGHT GAIN VS. TIME PLOTS OF CARBIDE COATED AND UNCOATED MILD STEEL

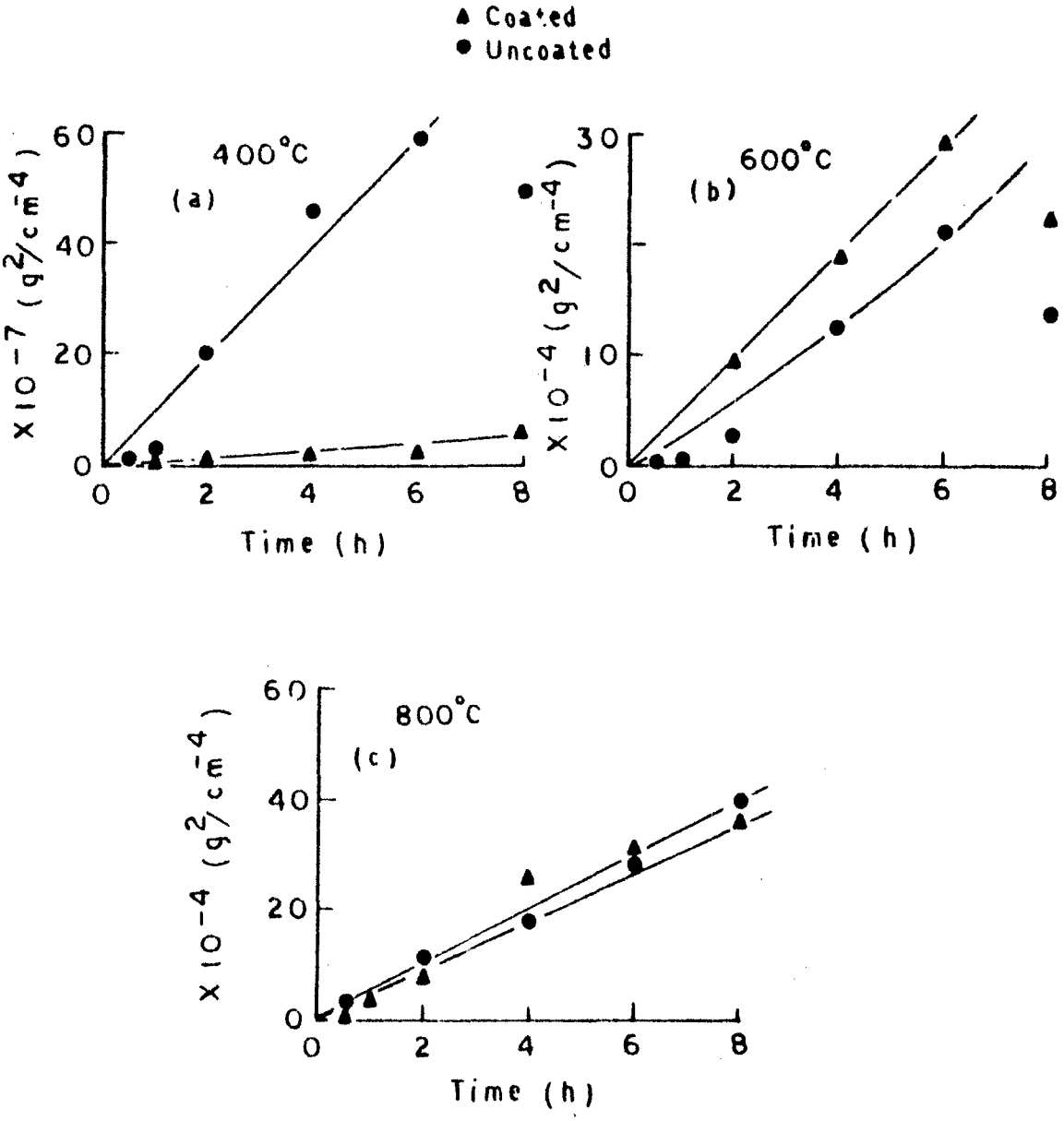

FIG.6.4 WEIGHT GAIN^2 VS. TIME PLOTS OF CARBIDE COATED AND UNCOATED MILD STEEL

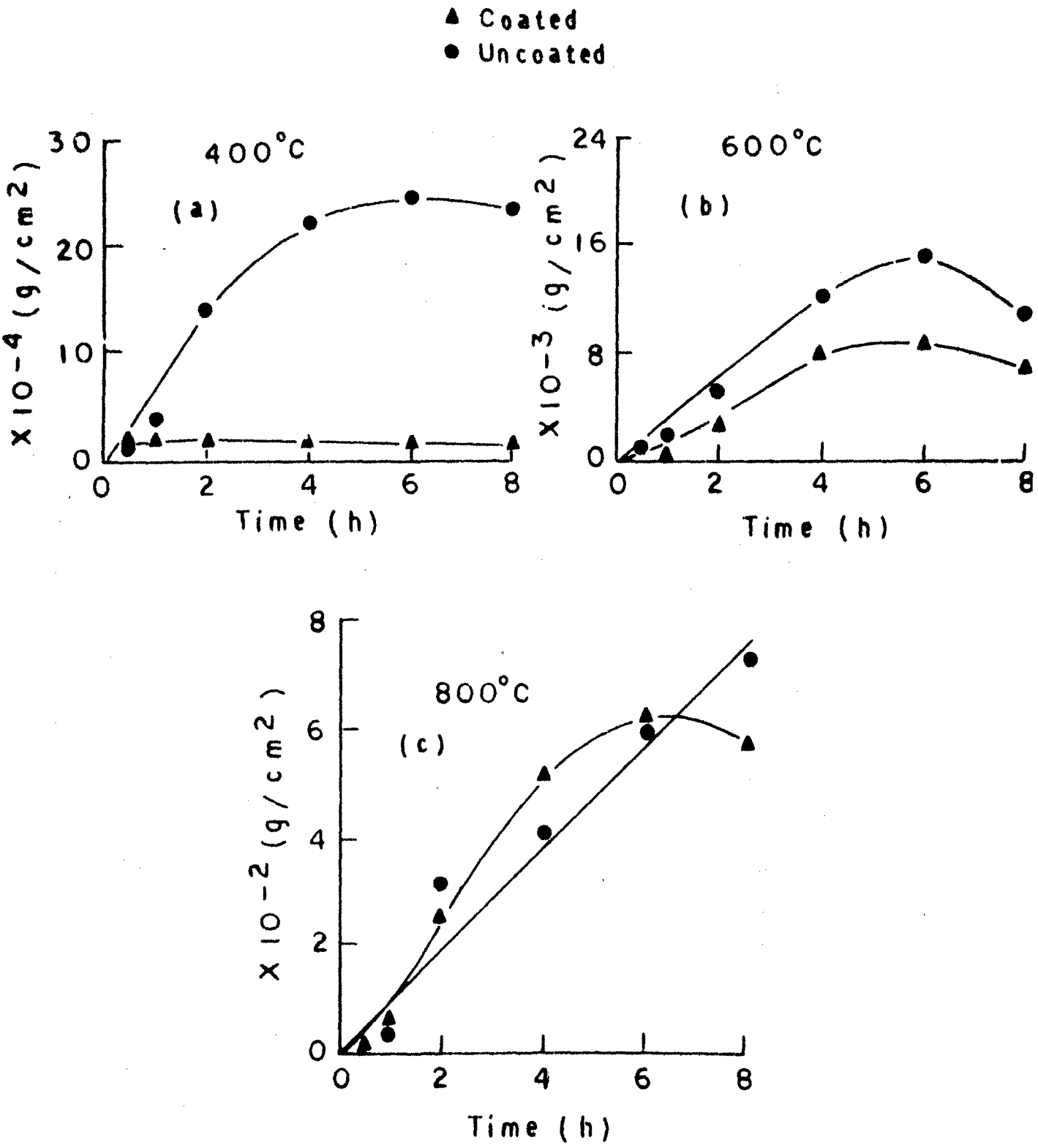

FIG 6.5 WEIGHT GAIN VS. TIME PLOTS OF BORATE COATED AND UNCOATED MILD STEEL

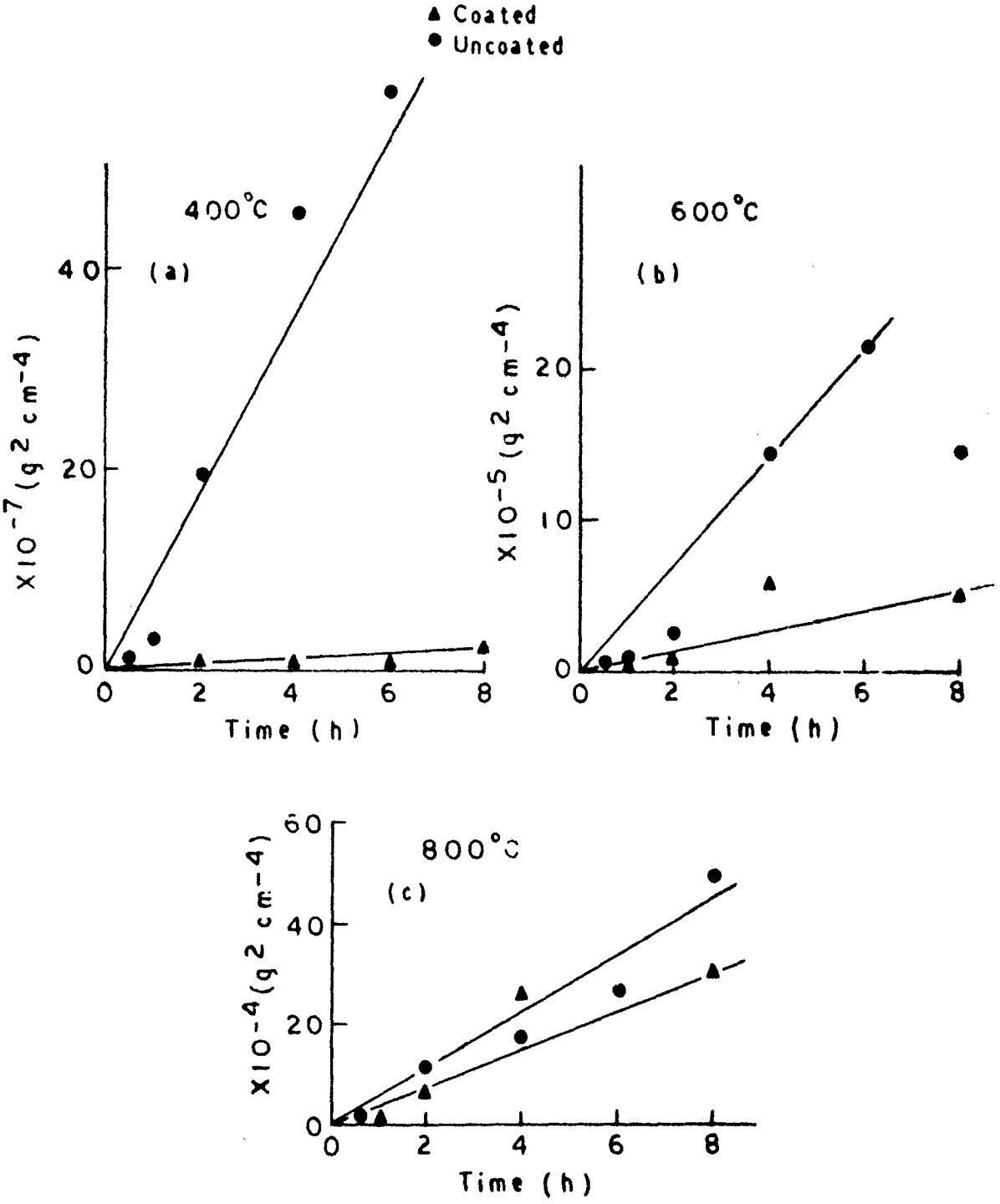

FIG.6.6 WEIGHT GAIN VS. TIME PLOTS OF BORATE COATED AND UNCOATED MILD STEEL

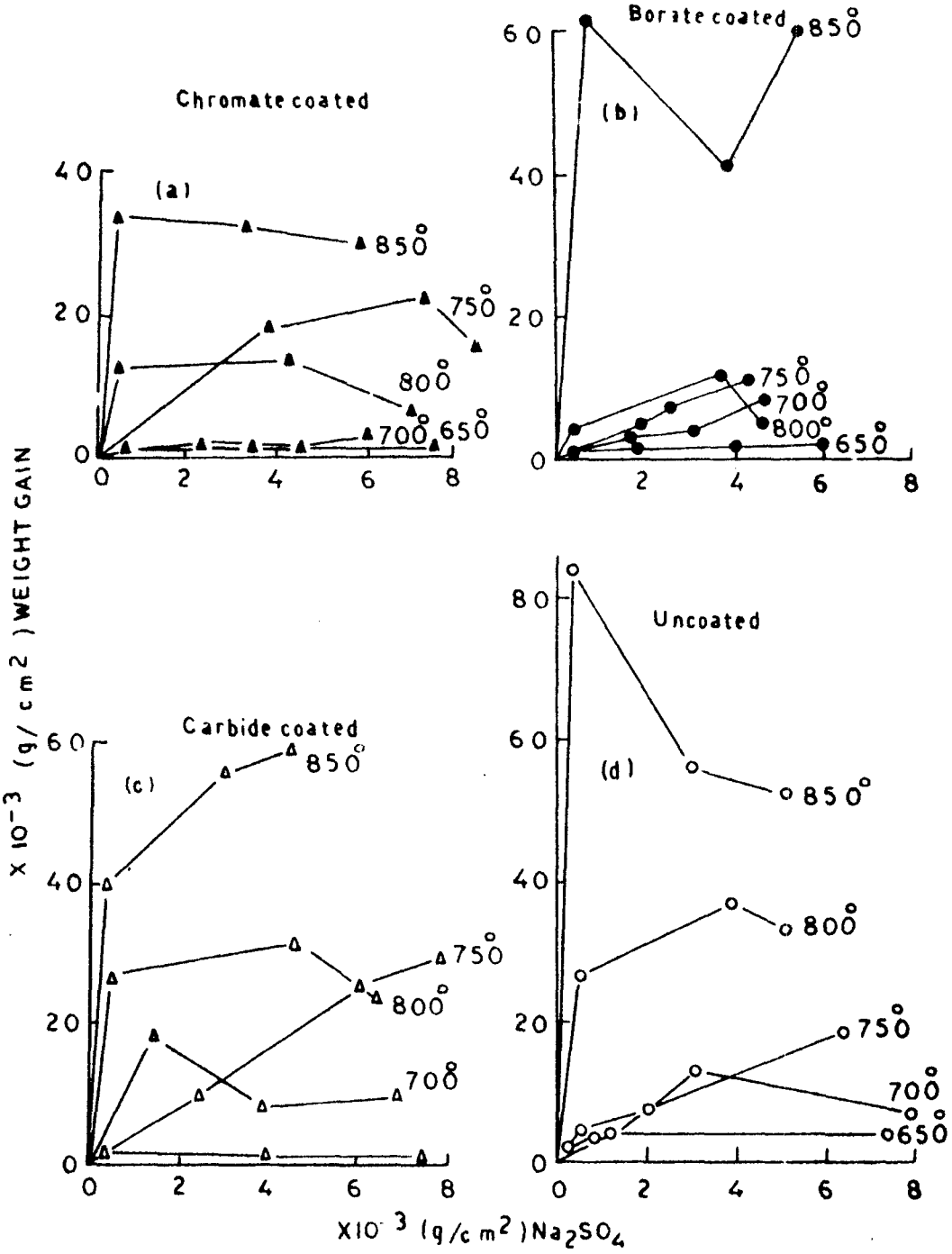

FIG.6.7 WEIGHT GAIN VS. SALT CONCENTRATION PLOTS OF COATED AND UNCOATED MILD STEEL

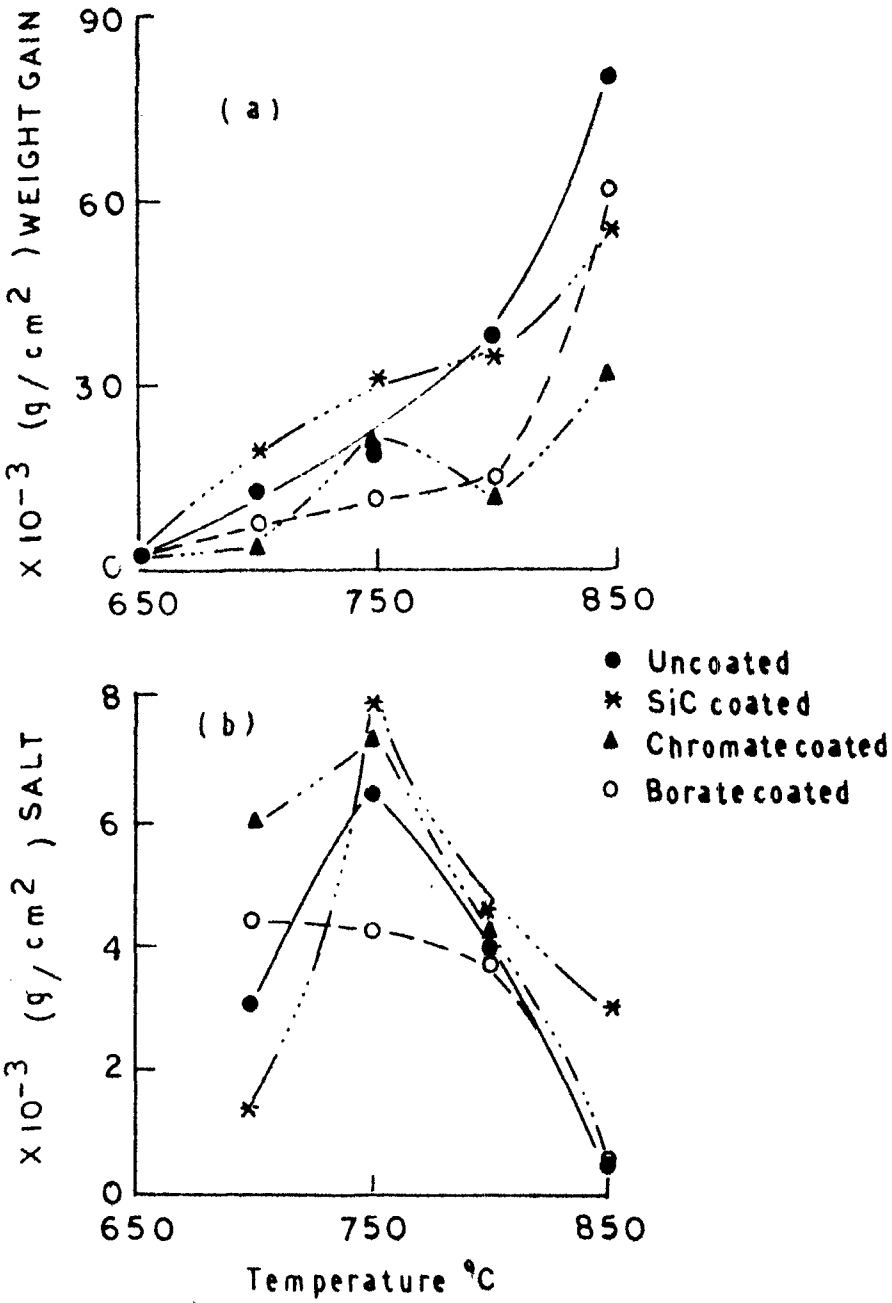

FIG. 6.12 (a) MAXIMUM WEIGHT GAIN VS. TEMPERATURE PLOTS OF COATED AND UNCOATED MILD STEEL
(b) SALT CONCENTRATION AT MAXIMUM WEIGHT GAIN VS. TEMPERATURE PLOTS COATED AND UNCOATED MILD STEEL

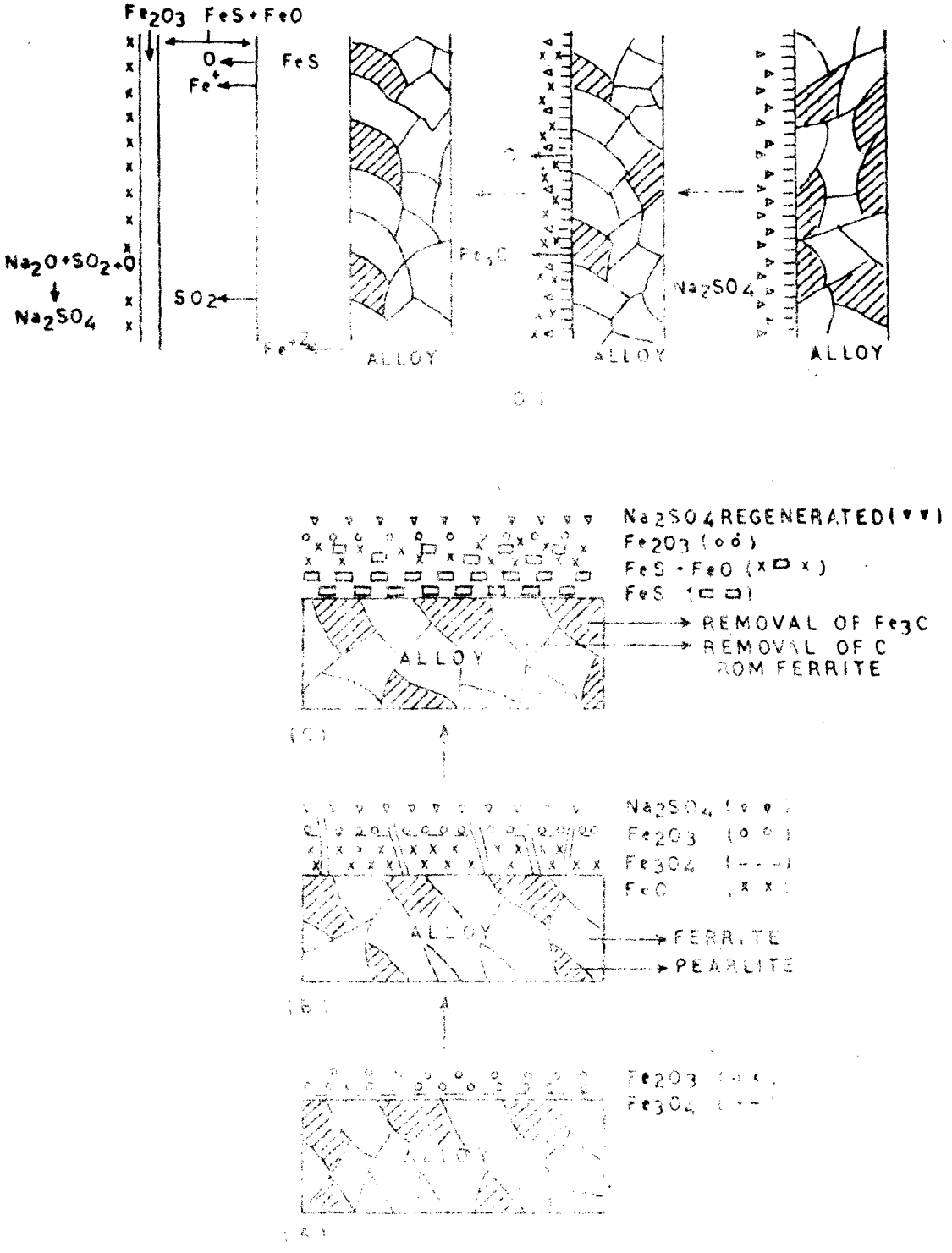

FIG. 6.13 SCHEMATIC DIAGRAMS FOR THE SULFIDATION OF MILD STEEL IN PRESENCE OF Na_2SO_4

A - Mild steel B - Na_2SO_4 Coated mild steel

C - Sulfidation D - Sulfidation mechanism

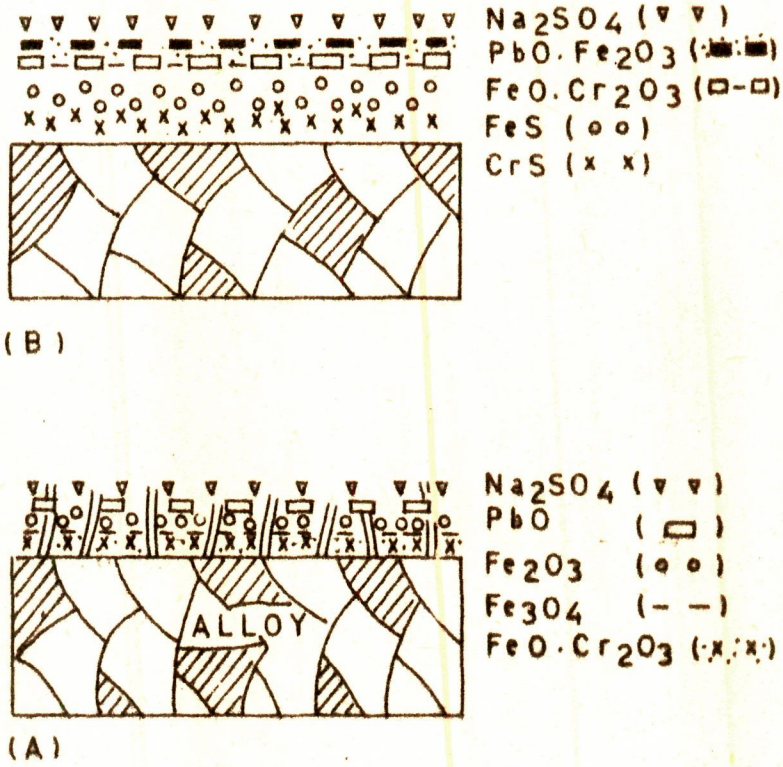

FIG. 6.14 SCHEMATIC DIAGRAMS FOR THE SULFIDATION OF CHROMATE COATED MILD STEEL IN PRESENCE OF Na_2SO_4

A – Na_2SO_4 coated Chromate coating

B – Sulfidation

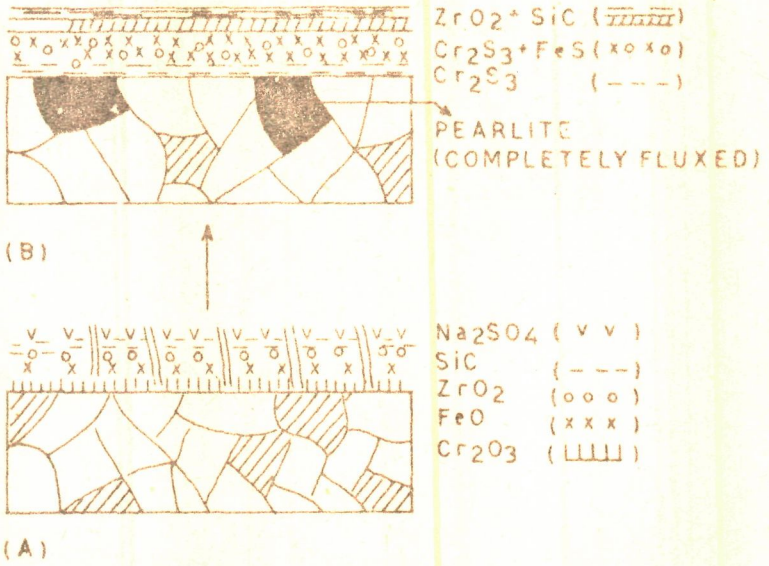

FIG. 6.15 SCHEMATIC DIAGRAMS FOR THE SULFIDATION OF CARBIDE COATED MILD STEEL IN PRESENCE OF Na_2SO_4
A - Na_2SO_4 Coated Carbide coating B - Sulfidation

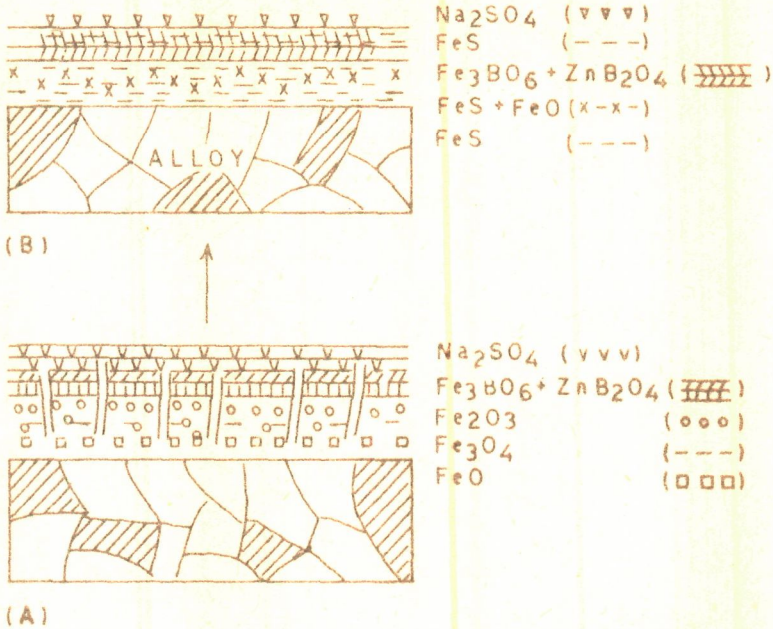

FIG. 6.16 SCHEMATIC DIAGRAMS FOR THE SULFIDATION OF BORATE COATED MILD STEEL IN PRESENCE OF Na_2SO_4
A - Na_2SO_4 Coated Borate coating B - Sulfidation

Fig. 2.1(a) Cross-sectional view of phosphate coating on 303 steel (SEM) 650 x.

Fig. 2.1(b) Surface view of phosphate coating on 303 steel (SEM) 1000 x.

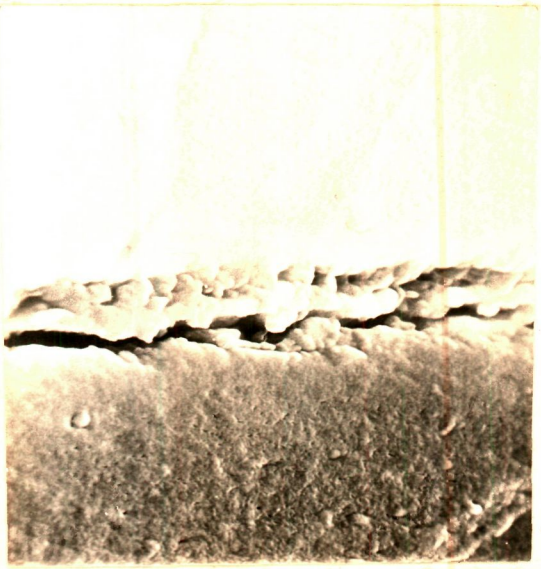

Fig. 2.2 Cross-Sectional view of silicate coating on 303 steel (SEM) 1200 x.

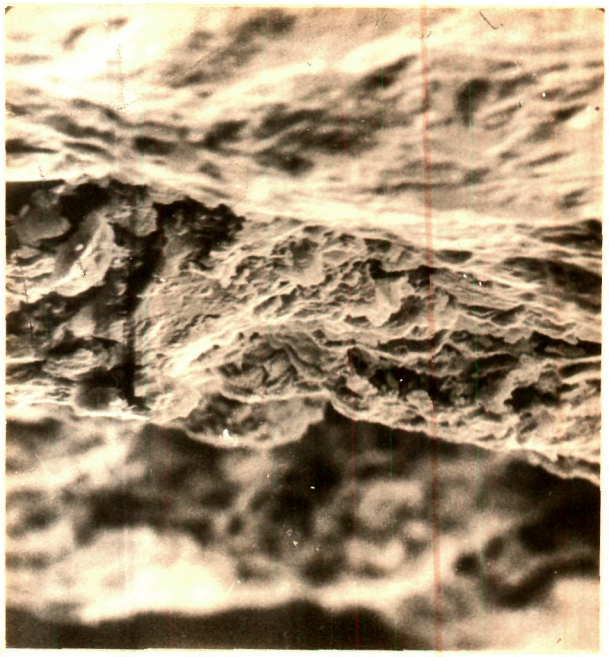

Fig. 2.3(a) Cross-Sectional view of chromate coating on 303 steel (SEM) 2500 x.

Fig. 2.3(b) Surface view of chromate coating on 303 steel (SEM) 1000 x.

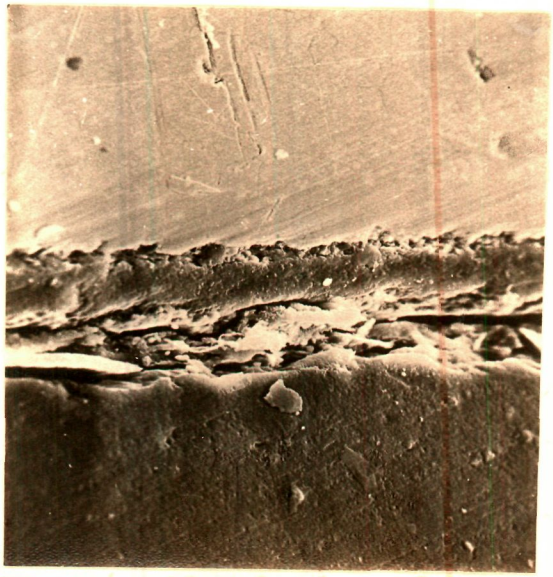

Fig. 2.4(a) Cross-sectional view of borate coating on 303 steel (SEM) 350 x.

Fig. 2.4(b) Surface view of borate coating on 303 steel (SEM) 1000 x.

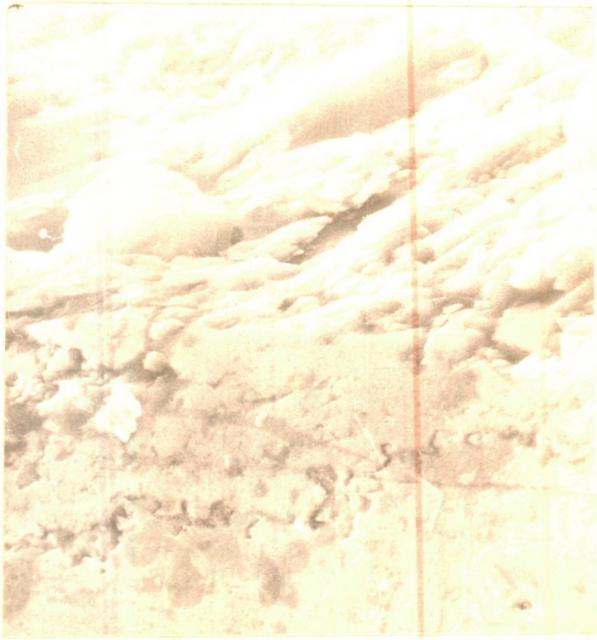

Fig. 2.5(a) Cross-sectional view of oxide coating on 303 steel (SEM) 2200 x.

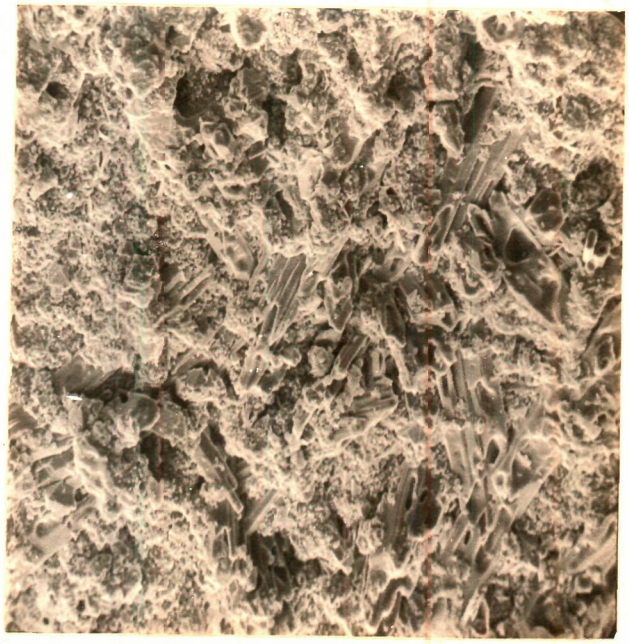

Fig. 2.5(b) Surface view of oxide coating on 303 steel (SEM) 1000 x.

Fig. 2.6(a) Surface view of borate coating on mild steel (SEM) 1000 x.

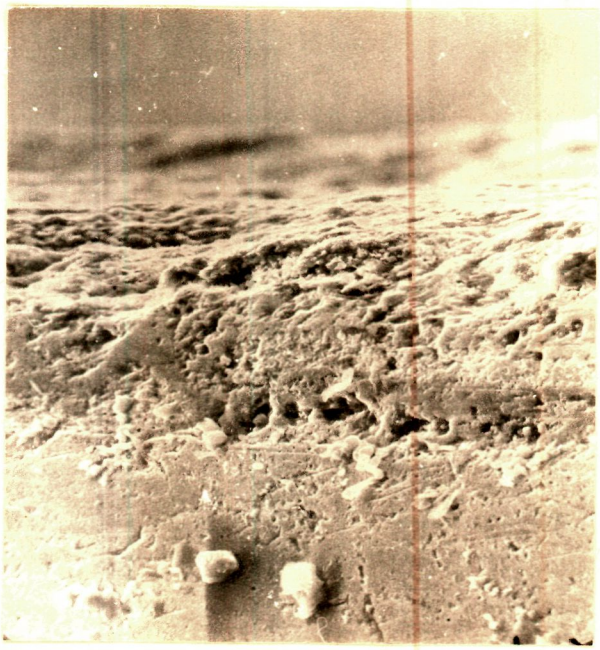

Fig. 2.6(b) Cross-sectional view of borate coating on mild steel (SM) 650 x.

Fig. 2.6(c) Cross-Sectional view of borate coating on mild steel (SM) 160 x.

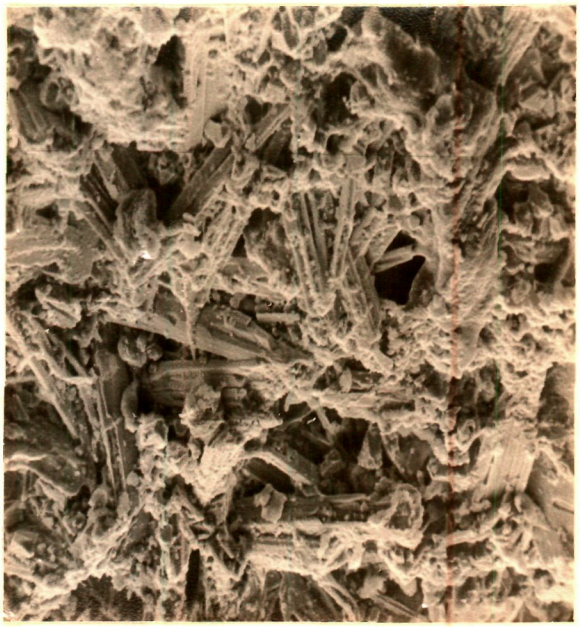

Fig. 2.7(a) Surface view of carbide coating on mild steel (SM) 1100 x.

Fig. 2.7(b) Cross-sectional view of carbide coating on mild steel (SM) 1000 x.

Fig. 2.8(a) Surface view of chromate coating on mild steel (SEM) 1000 x.

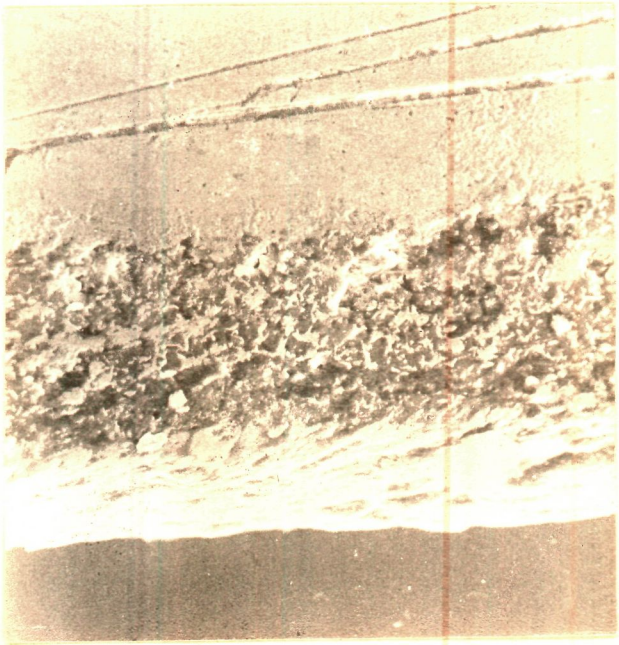

Fig. 2.8(b) Cross-sectional view of chromate coating on mild steel (SEM) 500 x.

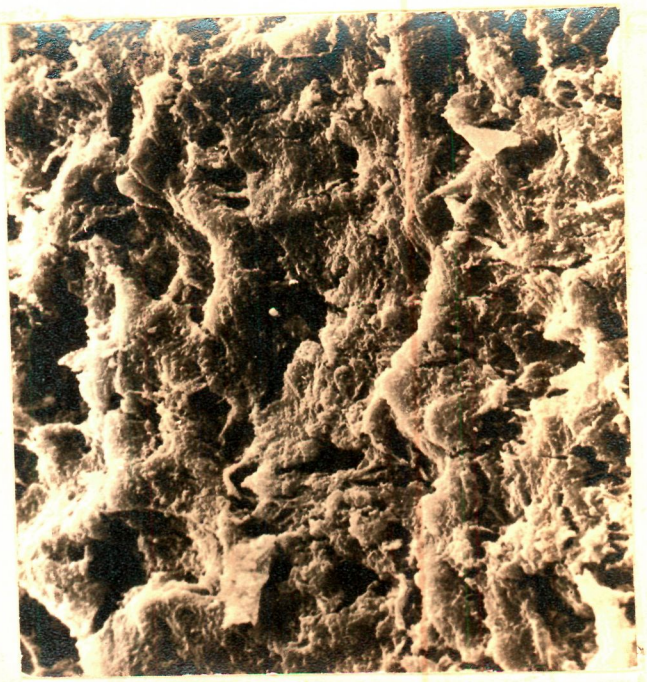

Fig. 3.1(a) SEM picture of 303 steel corroded in 1N HCl showing voids on the surface 900 x.

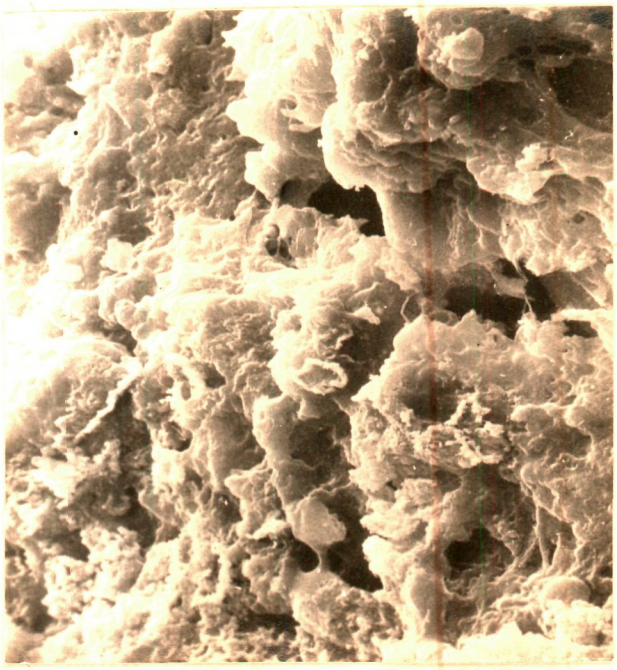

Fig. 3.1(b) SEM picture of phosphate coating corroded in 1N HCl showing pits and microcracks on the surface 600 x.

Fig. 3.1(c) SEM picture of chromate coating corroded in 1N HCl showing pits and voids on the surface 800 x.

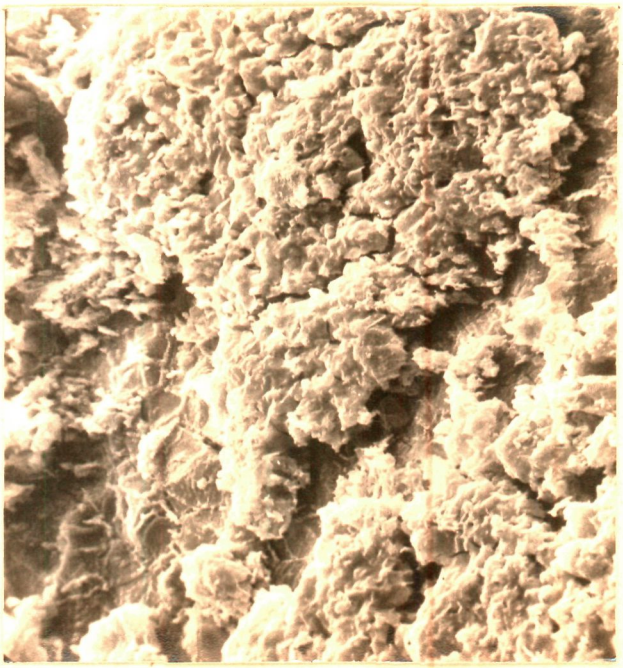

Fig. 3.1(d) SEM picture of oxide coating corroded in 1N HCl showing voids and pits on the surface 400 x.

Fig. 3.2(a) SEM picture of phosphate coating corroded in 1N HNO_3 showing microcracks and pits on the surface 400 x.

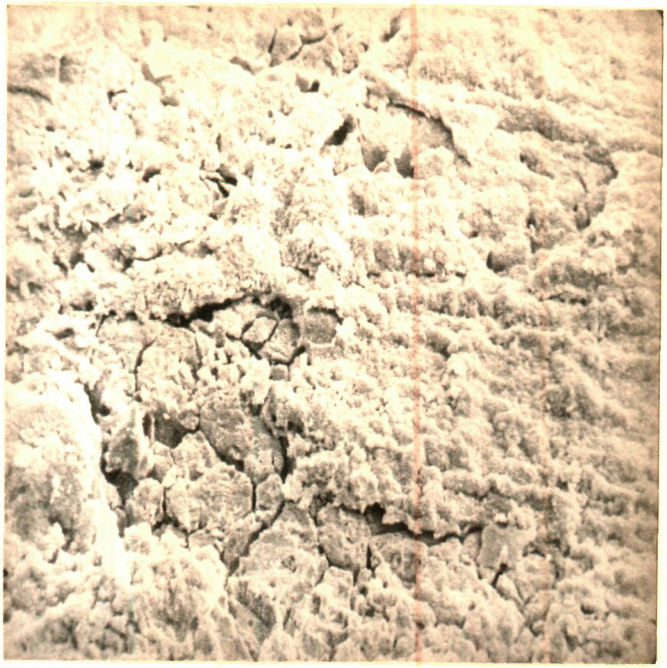

Fig. 3.2(b) SEM picture of phosphate coating corroded in 1N HNO_3 showing microcracks and pits on the surface 1600 x.

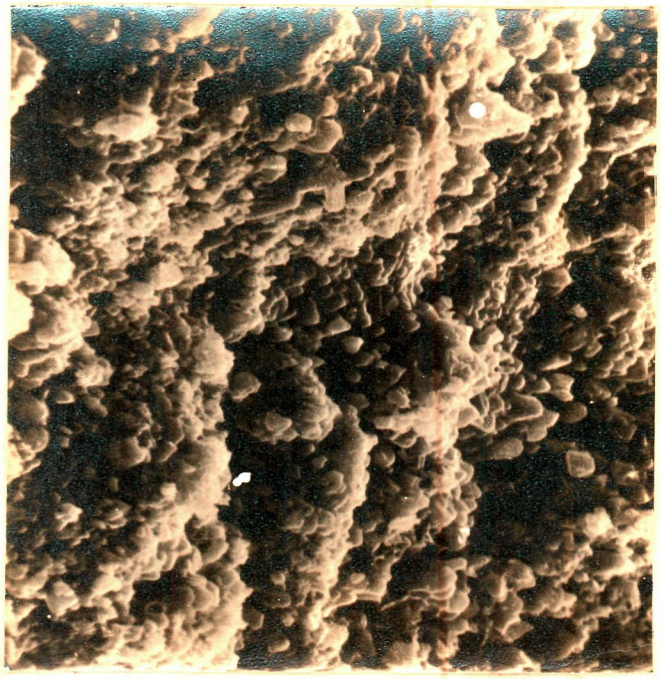

Fig. 3.2(c) SEM picture of chromate coating corroded in 1N HNO_3 showing fine pits and pores on the surface 1600 x.

Fig. 3.2(d) SEM picture of borate coating corroded in 1N HNO_3 showing hexagonal pallets of iron borate along with flecks of Cr_2O_3 on the surface 400 x.

Fig. 3.2(e) SEM picture of borate coating corroded in 1N HNO_3 showing hexagonal pallets of Fe_3BO_6 and flacks of Cr_2O_3 on the surface 1600 x.

Fig. 3.2(f) SEM picture of borate coating corroded in 1N HNO_3 showing hexagonal pallets of Fe_3BO_6 and flacks of Cr_2O_3 on the surface 1600 x.

Fig. 3.2(g) SEM picture of oxide coating corroded in 1N HNO_3 showing micropores and cracks along the grain boundaries 400 x.

Fig. 3.2(h) SEM picture of oxide coating corroded in 1N HNO_3 showing micropores and cracks along the grain boundaries 1600 x

Fig. 3.3(a) SEM picture of 303 steel corroded in 1N H_2SO_4 showing cracks along the grain boundaries 160 x.

Fig. 3.3(b) SEM picture of 303 steel corroded in 1N H_2SO_4 showing cracks along the grain boundaries 1600 x.

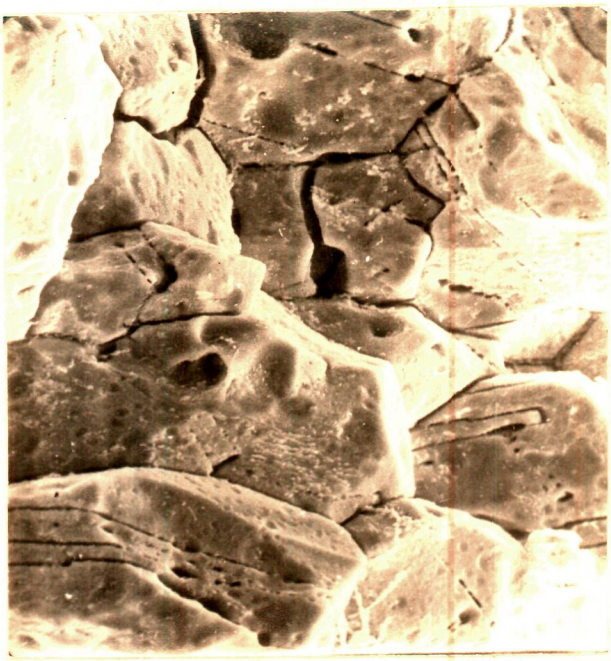

Fig. 3.3(c) SEM picture of borate coating corroded in 1N H_2SO_4 showing crystalloits of metallic borate along with some cracks 900 x.

Fig. 3.3(d) SEM picture of chromate coating corroded in 1N H_2SO_4 showing pores and voids on the surface 400 x.

Fig. 3.3(e) SEM picture of chromate coating corroded in 1N H_2SO_4 showing pores and voids on the surface 1600 x.

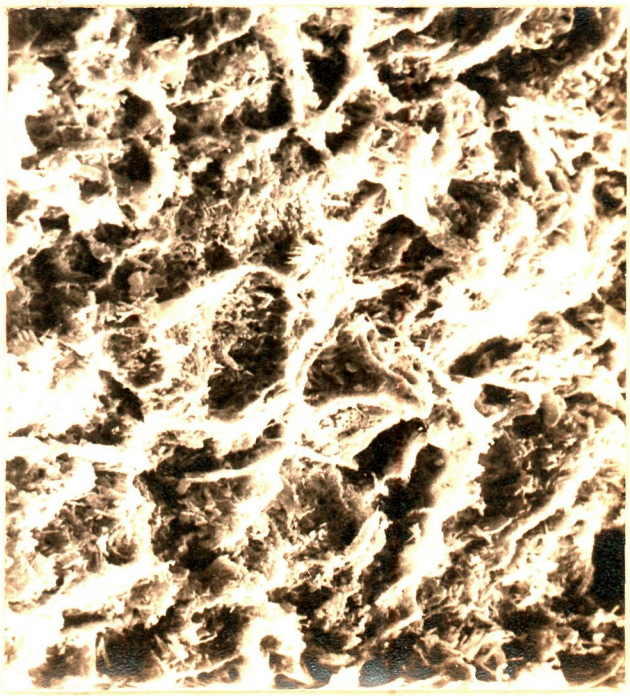

Fig. 3.3(f) SEM picture of oxide coating corroded in 1N H_2SO_4 showing voids and pores on the surface 900 x.

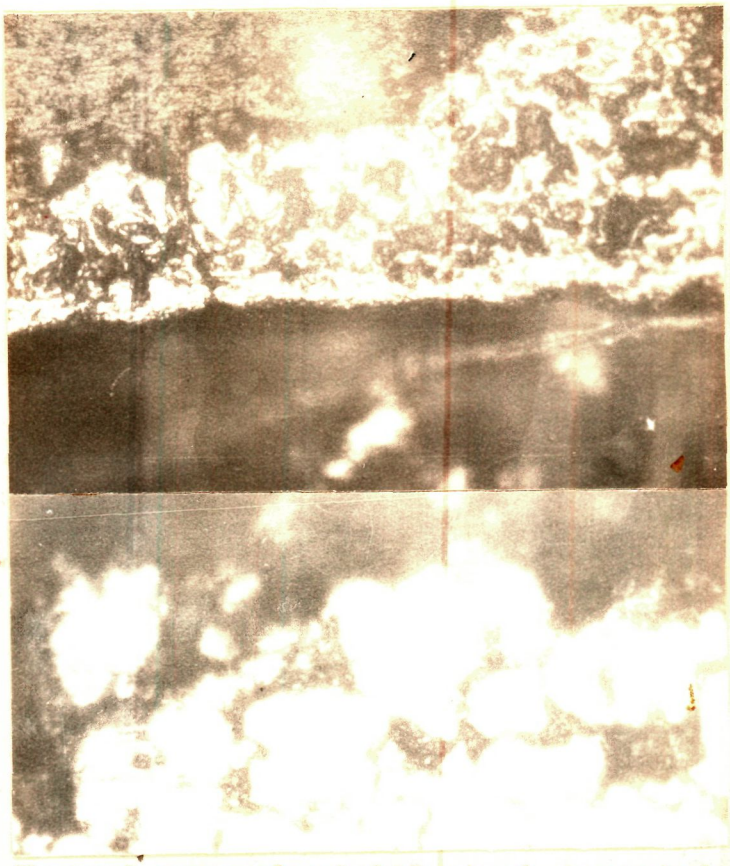

Fig. 5.2(a) Photomicrograph of 303 steel corroded in presence of Na_2SO_4 at 800°C 100 x.

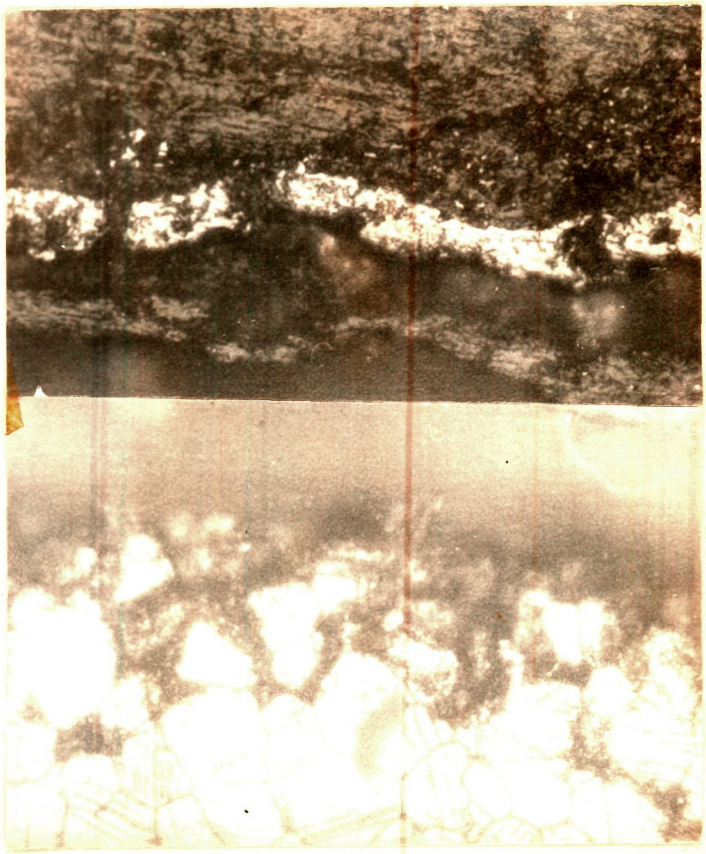

Fig. 5.2(b) Photomicrograph of 303 steel corroded in presence of NaCl at 800°C 100 x.

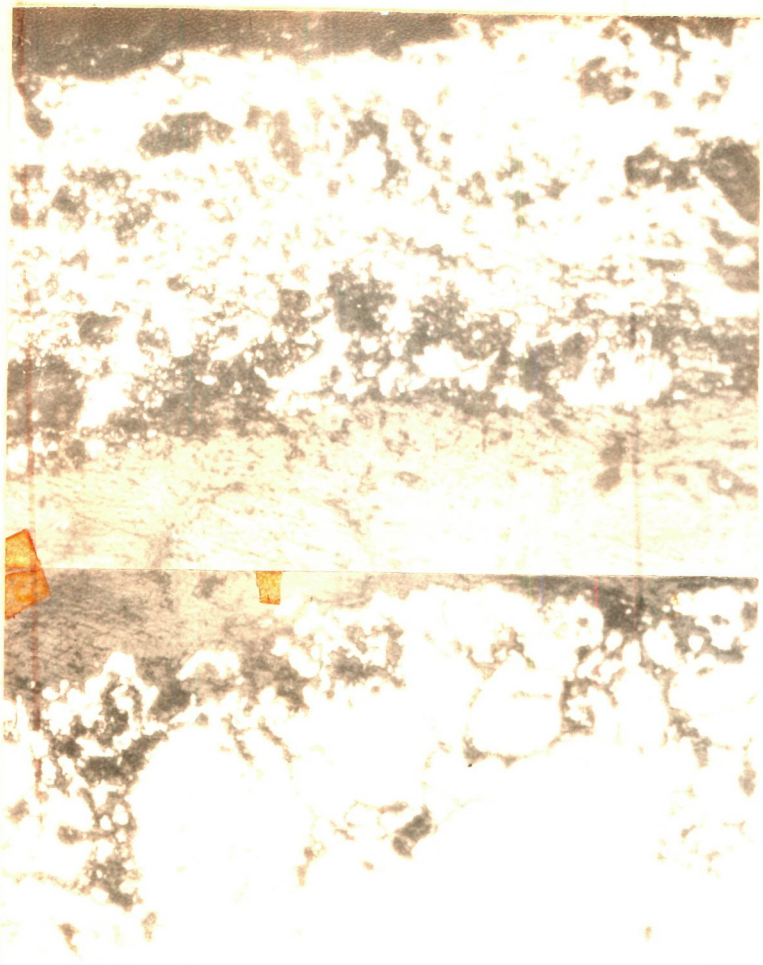

Fig. 5.2(c) Photomicrograph of 303 steel corroded in presence of Na_2SO_4 + NaCl at 800°C 100 x.

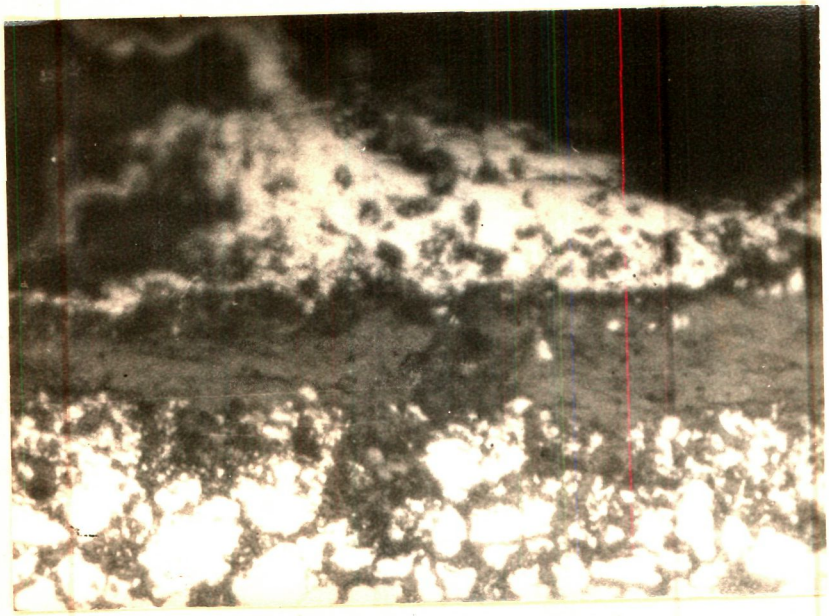

Fig. 5.2(d) Photomicrograph of 303 steel corroded in presence of Na_2SO_4 + NaCl at 800°C 100 x.

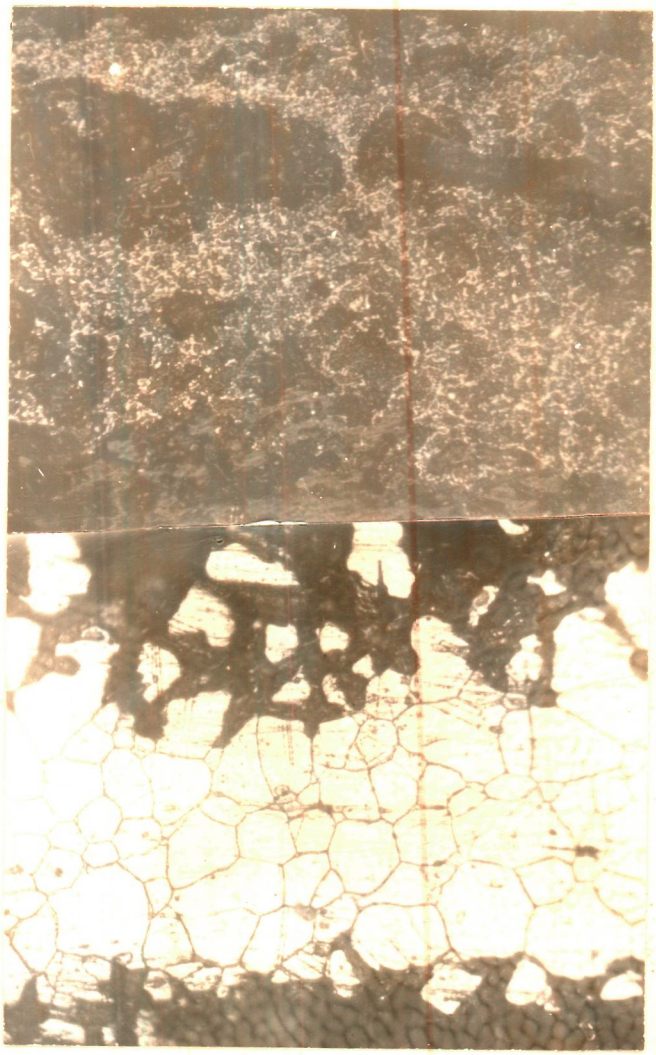

Fig. 5.3(a) Photomicrograph of phosphate coating in presence of Na_2SO_4 at 800°C 100 x

Fig. 5.3(b) SEM picture of phosphate coating in presence of Na_2SO_4 at 800°C 130 x

Fig. 5.3(c) SEM picture at higher magnification of phosphate coating in presence of Na_2SO_4 at 800°C 1300 x.

Fig. 5.4(a) SEM picture of phosphate coating in presence of NaCl at 600°C 130 x.

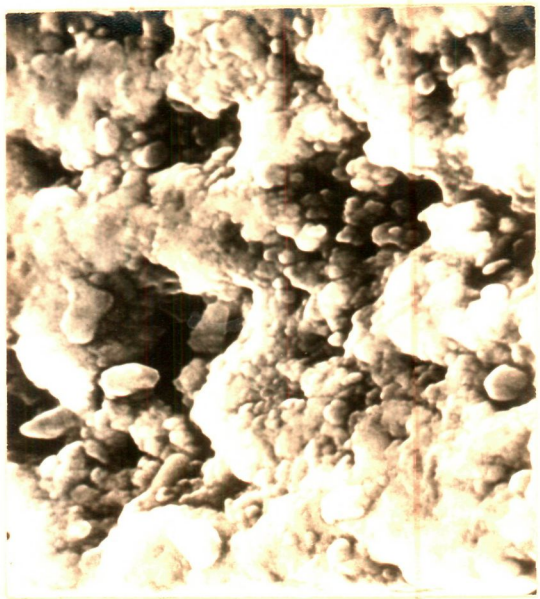

Fig. 5.4(b) SEM picture at higher magnification of phosphate coating in presence of NaCl at 600°C 2600 x.

Fig. 5.4(c) Photomicrograph of phosphate coating in presence of NaCl at 600°C 100 x.

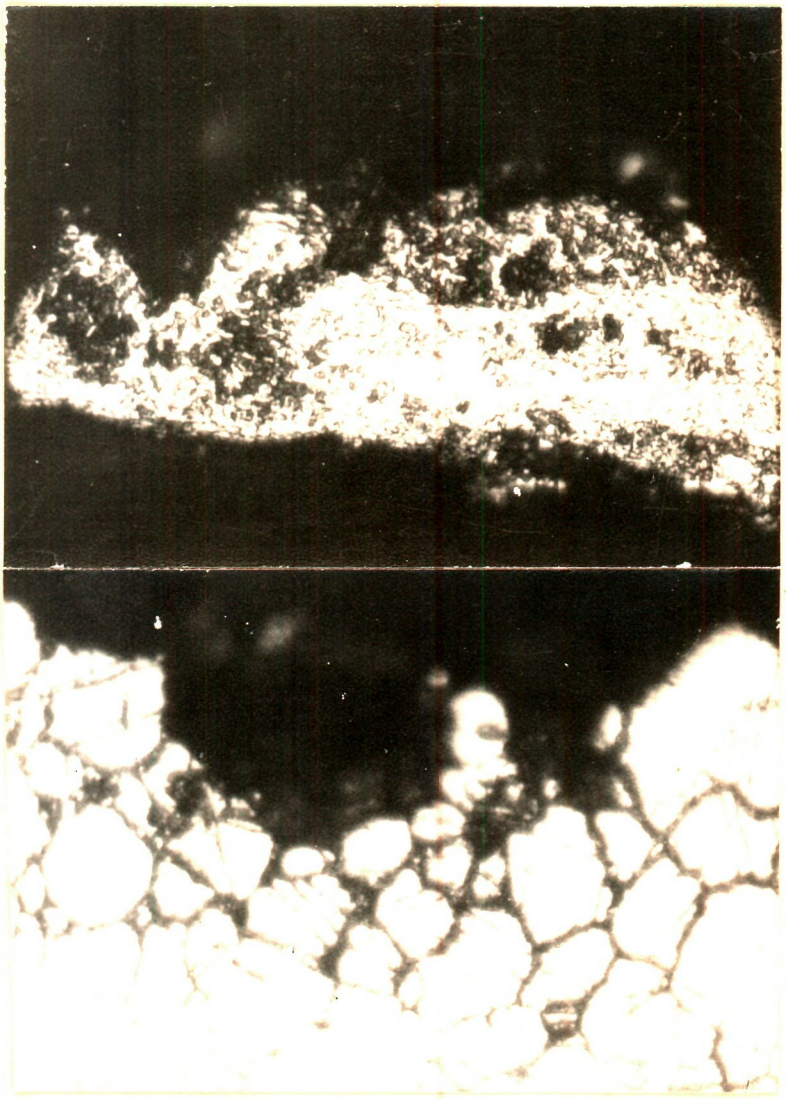

Fig. 5.4(d) Photomicrograph of phosphate coating in presence of NaCl + Na_2SO_4 at 800°C 100 x.

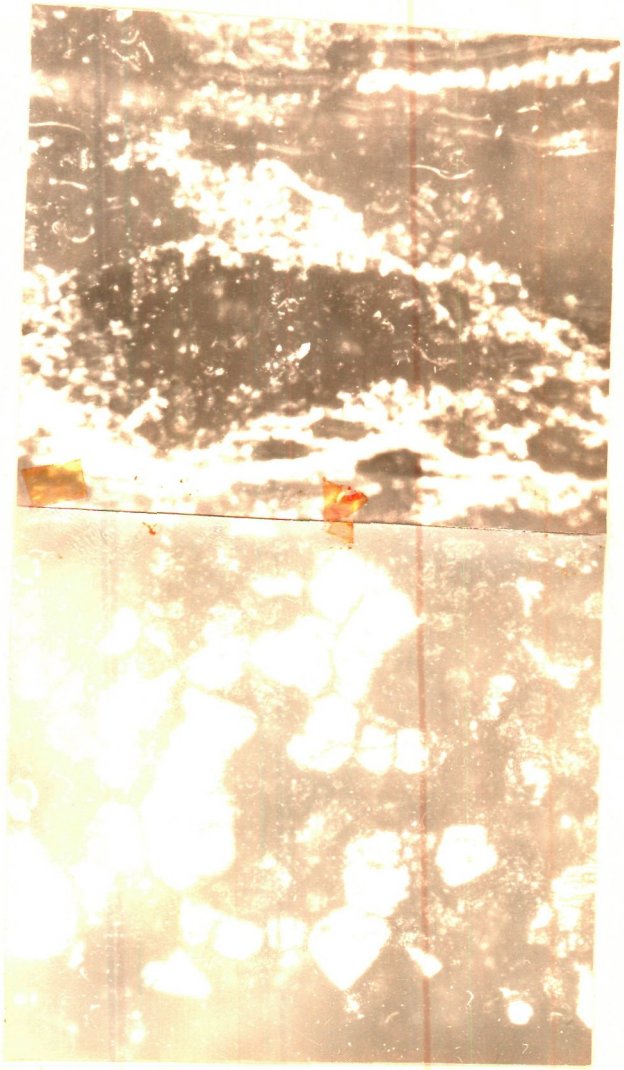

Fig. 5.5(a) Photomicrograph of silicate coating in presence of Na_2SO_4 at 800°C 100 x.

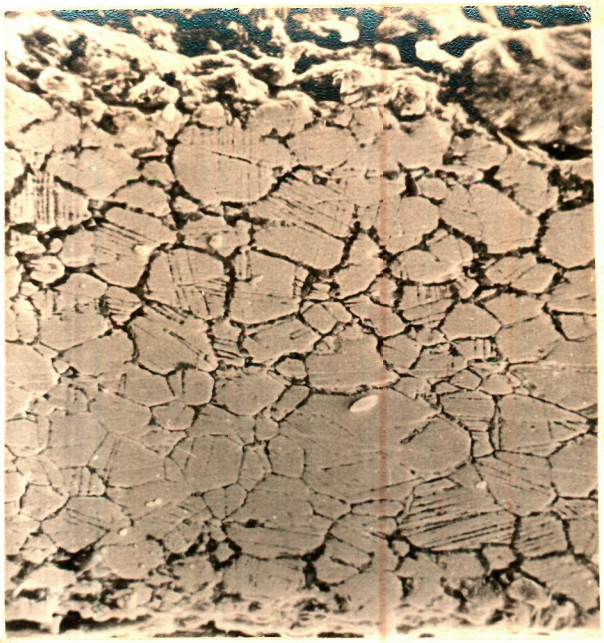

Fig. 5.5(b) SEM picture of silicates coating in presence of Na_2SO_4 at 800°C 240 x.

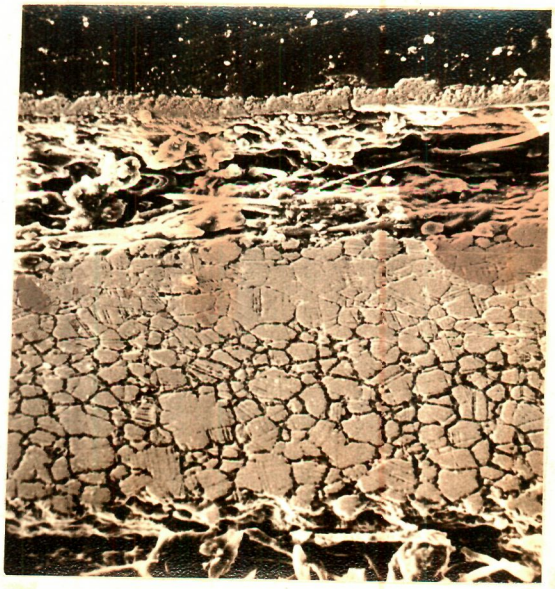

Fig. 5.5(c) SEM picture of silicate coating in presence of NaCl at 800°C 240 x.

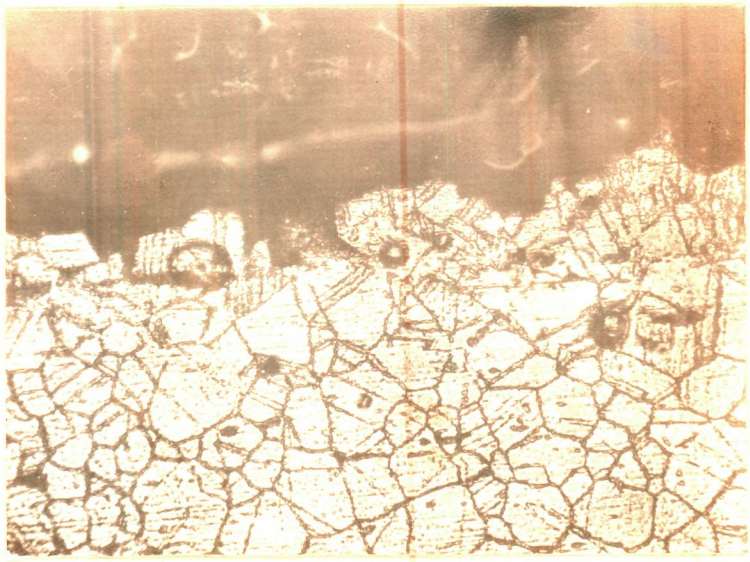

Fig. 5.5(d) Photomicrograph of silicate coating in presence of NaCl at 600°C 100 x.

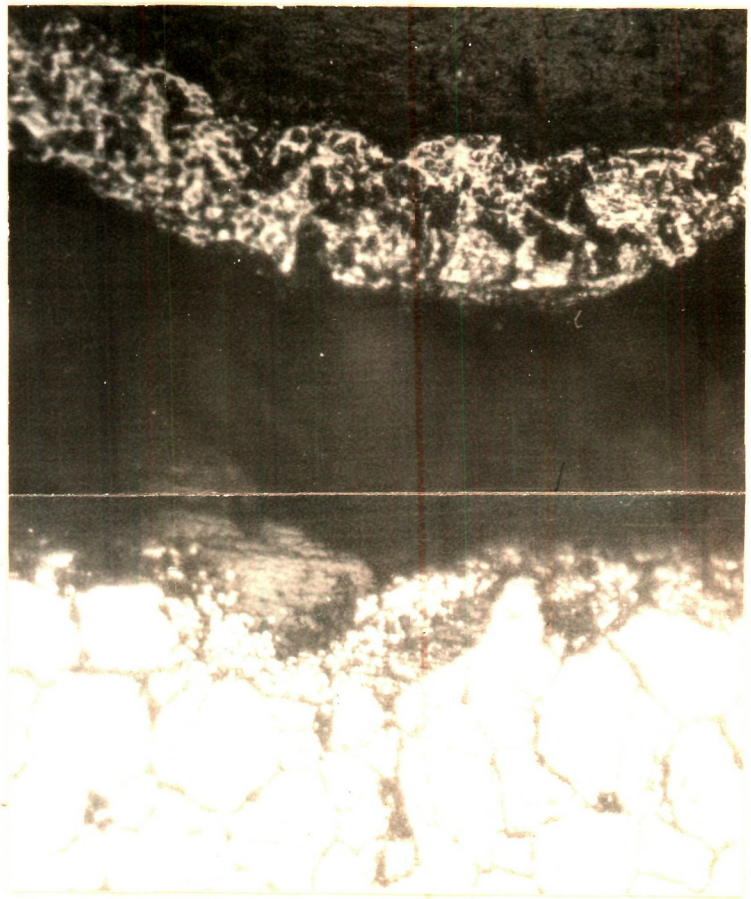

Fig. 5.5(e) Photomicrograph of silicate coating in presence of Na_2SO_4 + NaCl at 600°C 100 x.

Fig. 5.6(a) SEM picture of borate coating in presence of Na_2SO_4 at 800°C 260 x.

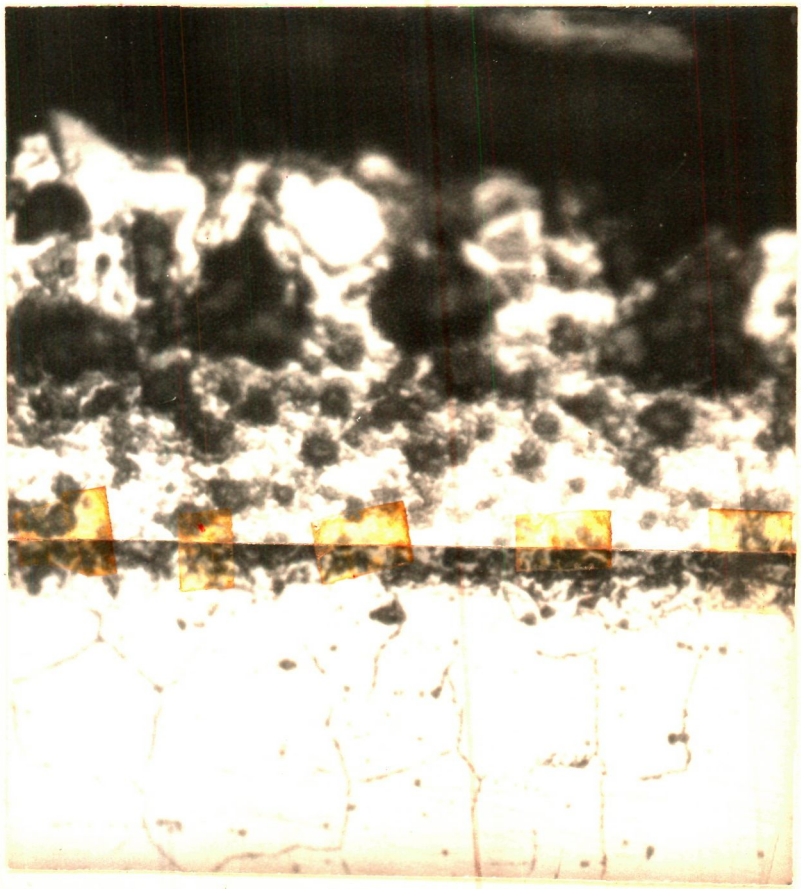

Fig. 5.6(b) Photomicrograph of borate coating in presence of Na_2SO_4 + NaCl at 800°C 100 x.

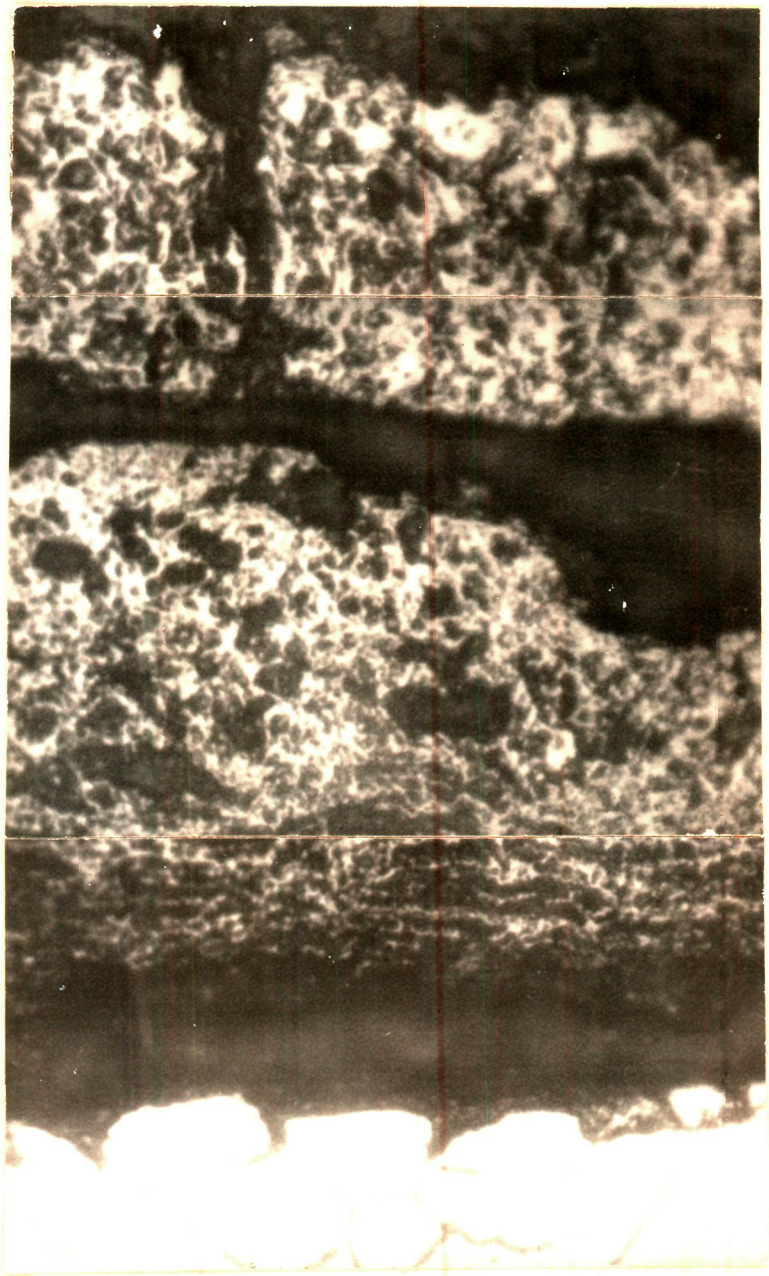

Fig. 5.7(a) Photomicrograph of chromate coating in presence of Na_2SO_4 at 800°C 100 x.

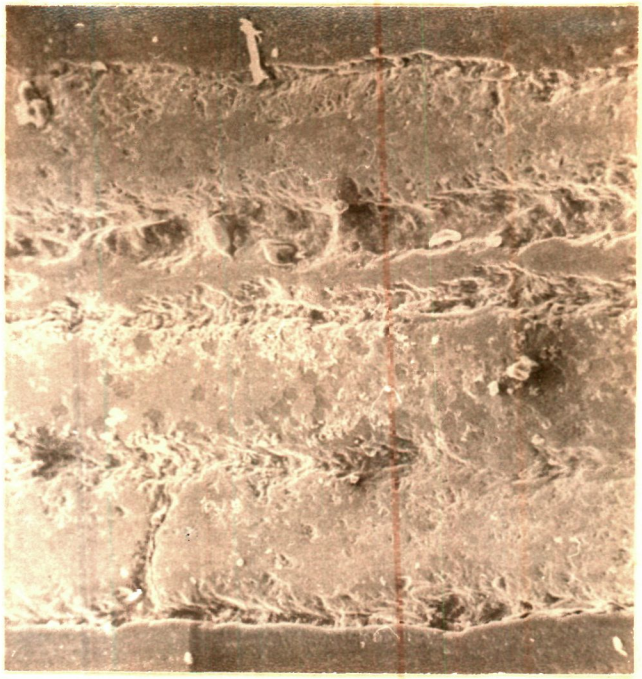

Fig. 5.7(b) SEM picture of chromate coating in presence of Na_2SO_4 at 800°C 100 x.

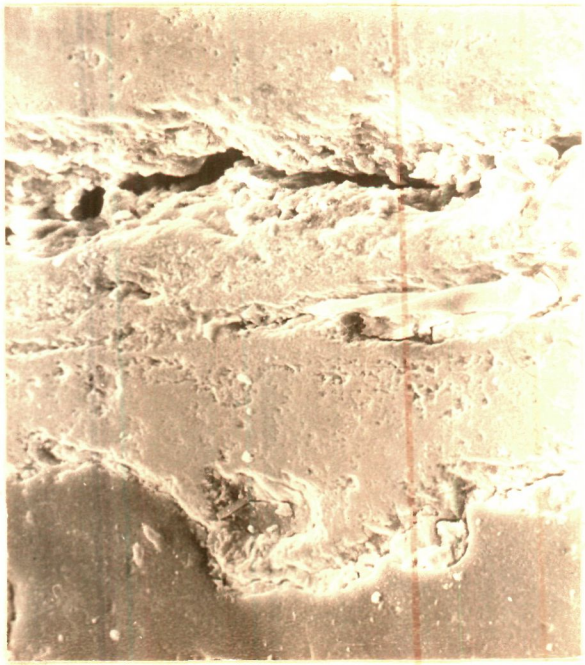

Fig. 5.7(c) SEM picture of chromate coating in presence of NaCl at 850°C 200 x.

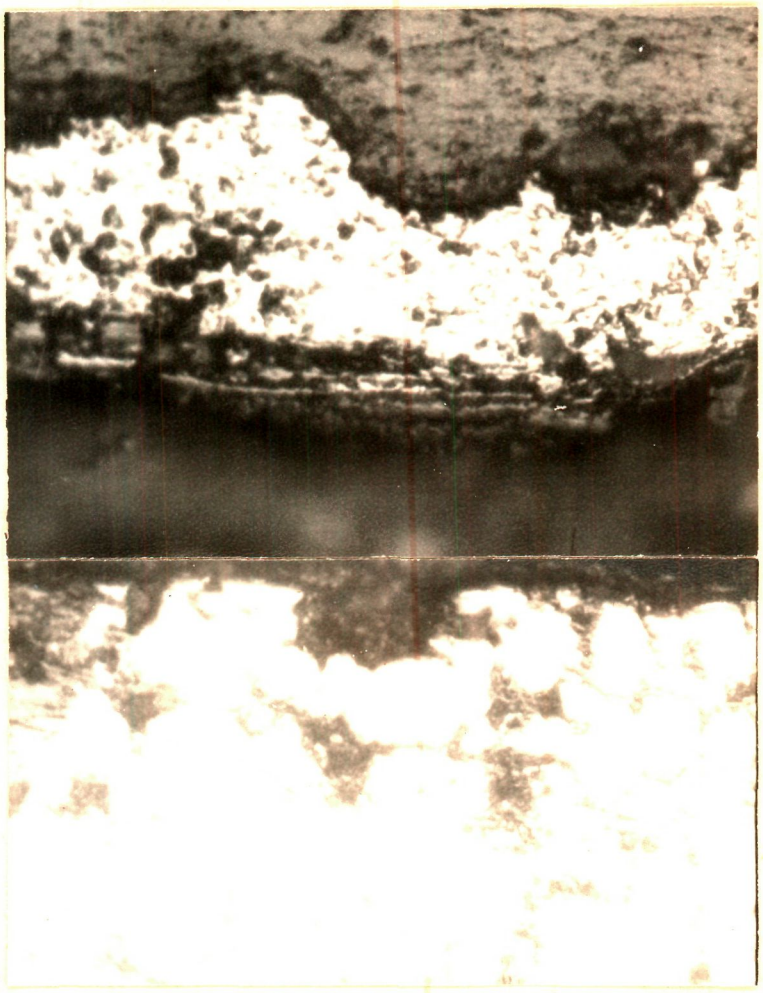

Fig. 5.7(d) Photomicrograph of chromate coating in presence of NaCl at 850°C 100 x.

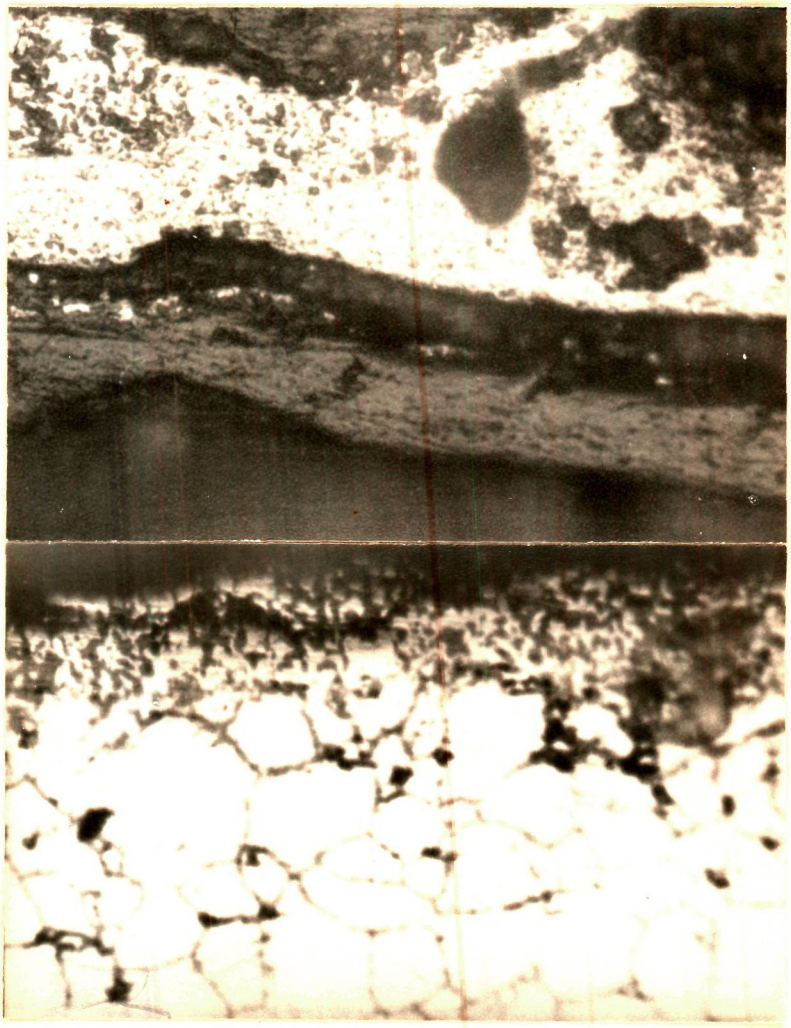

Fig. 5.7(e) Photomicrograph of chromate coating in presence of Na_2SO_4 + NaCl at 850°C 100 x.

Fig. 5.8(a) Photomicrograph of oxide coating in presence of Na_2SO_4 at 800°C 100 x.

Fig. 5.8(b) SEM picture of oxide coating in presence of Na_2SO_4 at 800°C 580 x.

Fig. 5.8(c) Photomicrograph of oxide coating in presence of Na_2SO_4 at 1000°C 100 x.

Fig. 5.8(d) Photomicrograph of oxide coating in presence of NaCl at 800°C 100 x.

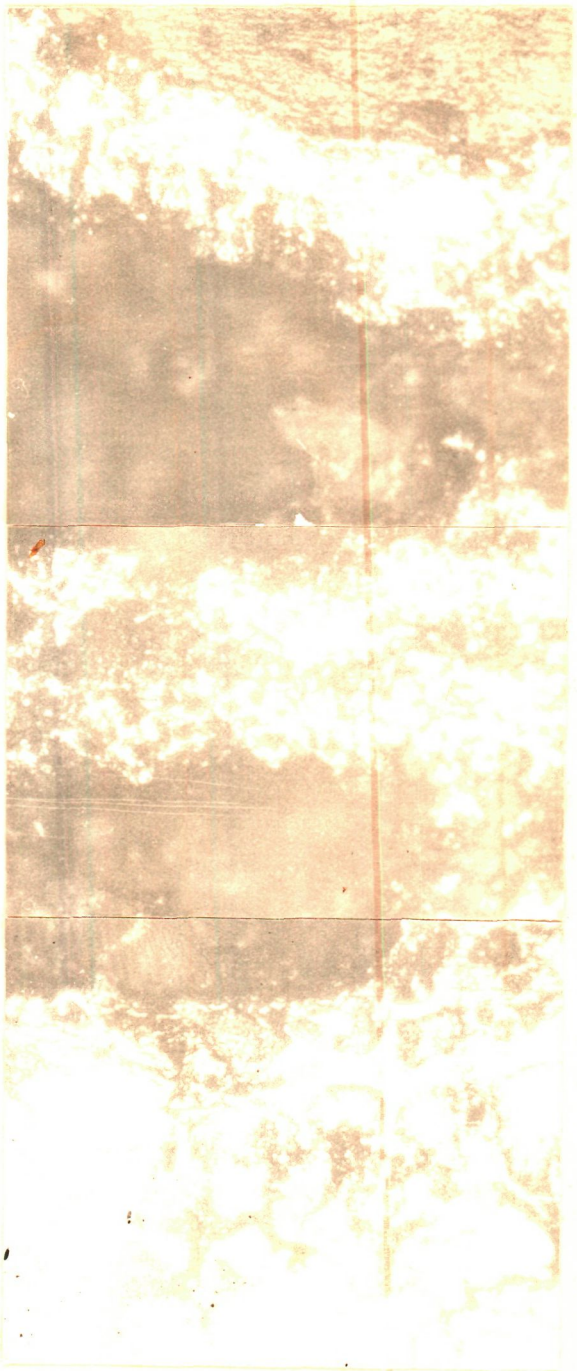

Fig. 5.8(a) Photomicrograph oxide coating in presence of Na_2SO_4 + NaCl at 1000°C 100 x.

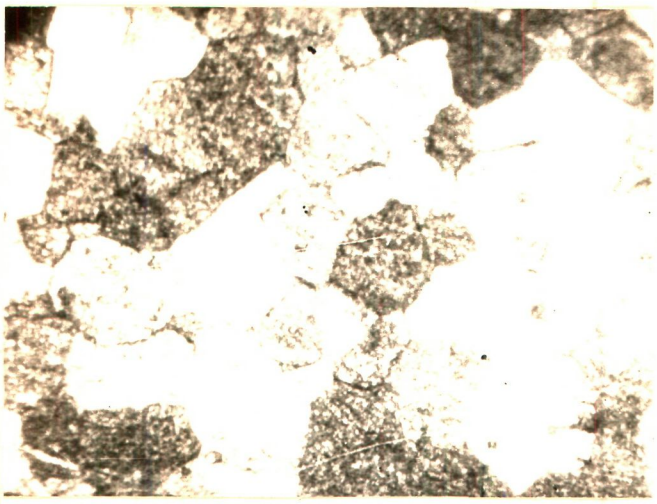

Fig. 6.8(a) Photomicrograph of anealed mild steel showing pearlite and ferrite 100 x.

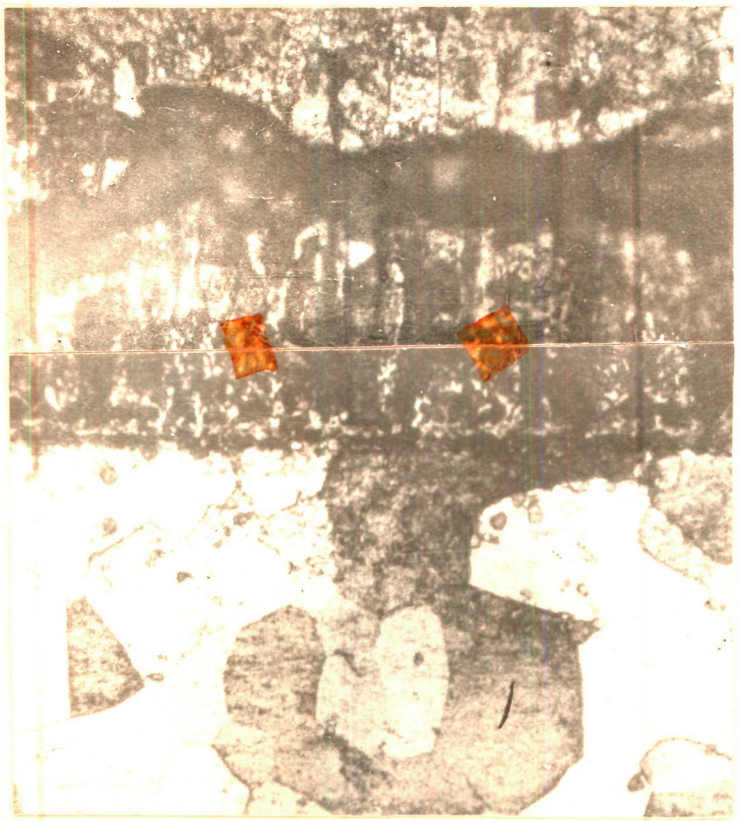

Fig. 6.8(b) Photomicrograph of mild steel in presence of Na_2SO_4 at 750°C 100 x.

Fig. 6.9(a) Photomicrograph of chromate coated mild steel in presence of Na_2SO_4 at 800°C 100 x.

Fig. 6.9(b) Photomicrograph of chromate coated mild steel in presence of Na_2SO_4 at 850°C 100 x.

Fig. 6.9(c) SEM picture of the chromate coated mild steel in presence of Na_2SO_4 at 800°C 1050 x.

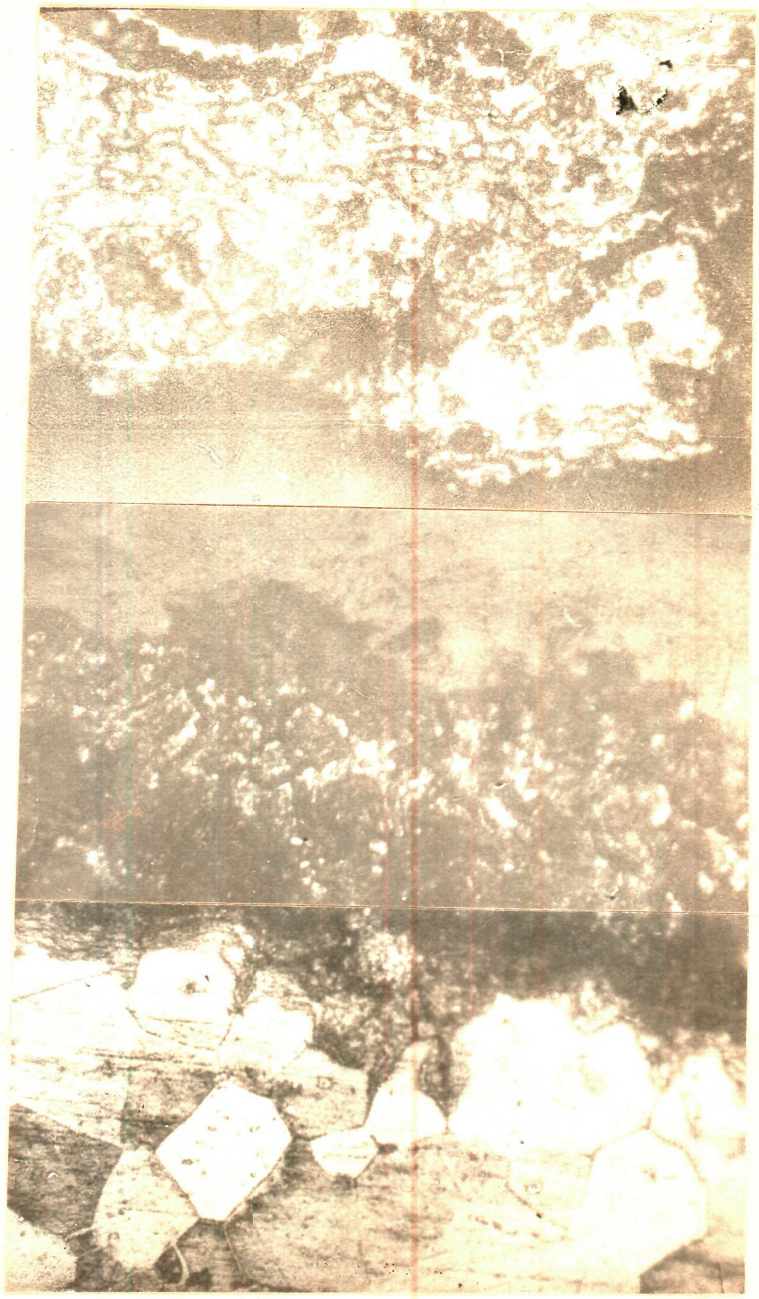

Fig. 6.10(a) Photomicrograph of borate coated mild steel in presence of Na_2SO_4 at 650°C 100 x.

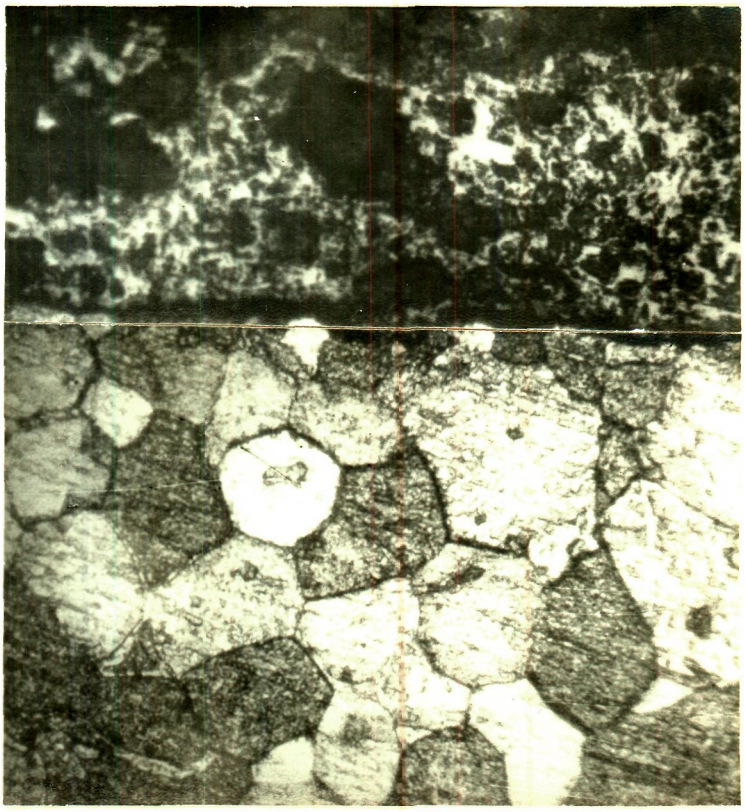

Fig. 6.10(b) Photomicrograph of borate coated mild steel in presence of Na_2SO_4 at 700°C 100 x.

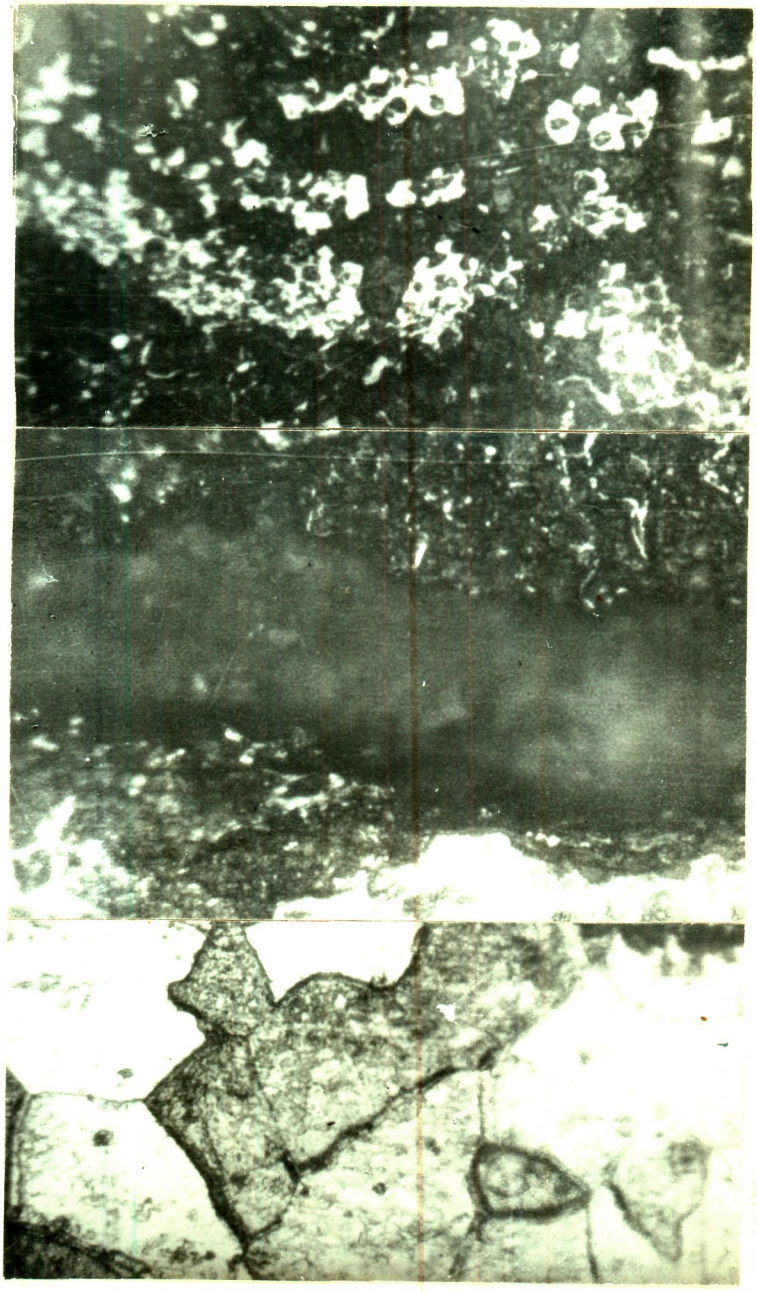

Fig. 6.10(c) Photomicrograph of borate coated mild steel in presence of Na_2SO_4 at 800°C 100 x.

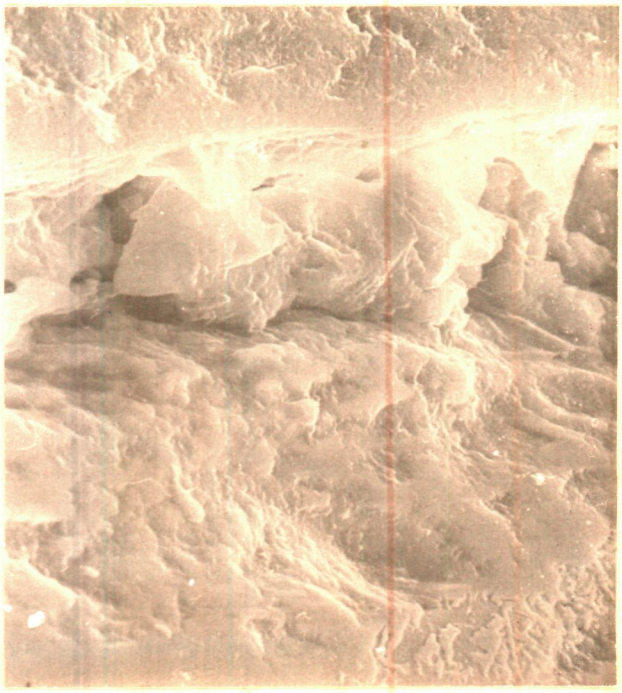

Fig. 6.10(d) SEM picture of the borate coated mild steel in presence of Na_2SO_4 at 600°C 1300 x.

Fig. 6.11(a) Photomicrograph of carbide coated mild steel in presence of Na_2SO_4 at 600°C 100 x.

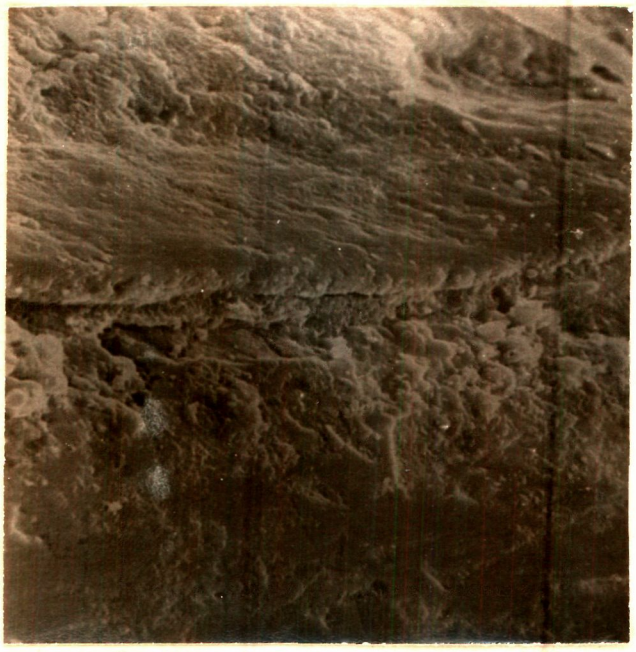

Fig. 6.11(b) SEM picture of carbide coated mid steel in presence of Na_2SO_4 at 600°C 1200 x.